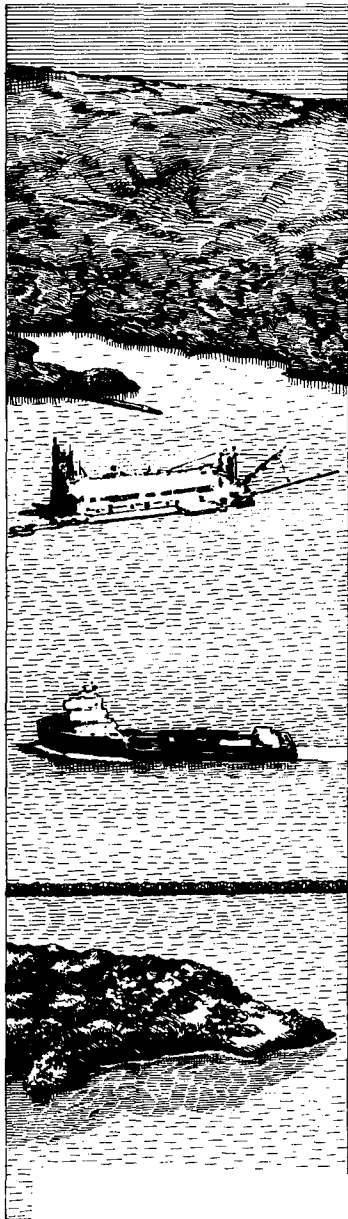US Army Corps
of Engineers

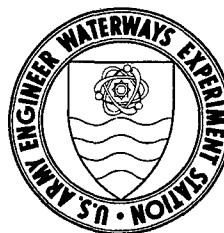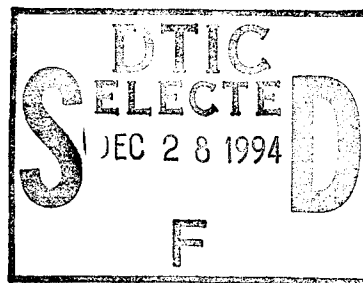**DREDGING RESEARCH PROGRAM**

CONTRACT REPORT DRP-94-7

CALCULATION OF SUSPENDED SEDIMENT TRANSPORT BY COMBINED WAVE-CURRENT FLOWS

by

Palitha Nalin Wikramanayake, Ole Secher Madsen

Ralph M. Parsons Laboratory
Massachusetts Institute of Technology
Cambridge, Massachusetts   02139

DTIC
SELECTE
JEC 2 8 1994
F

November 1994

Final Report

Approved For Public Release; Distribution Is Unlimited

19941223 029

Prepared for DEPARTMENT OF THE ARMY
U.S. Army Corps of Engineers
Washington, DC   20314-1000

Monitored by U.S. Army Engineer Waterways Experiment Station
3909 Halls Ferry Road, Vicksburg, Mississippi   39180-6199

Under Work Unit No. 32463

DTIC QUALITY INSPECTED 1

The contents of this report are not to be used for advertising, publication, or promotional purposes. Citation of trade names does not constitute an official endorsement or approval of the use of such commercial products.

Calculation of Suspended Sediment Transport by Combined Wave-Current Flows (CR DRP-94-7)

ISSUE:

Much of the difficulty in obtaining accurate estimates in simulating the movement of dredged material disposed in open water results from limited understanding of water-sediment interaction at the bed. Waves and currents, nearly always present in coastal waters, transport loose bottom sediment in most coastal regions. Ability to quantify sediment-fluid interaction is required to model this aspect of dredged material disposal.

RESEARCH:

This study was designed to extend turbulent eddy viscosity models, which dealt with purely hydrodynamic aspects of wave-current interaction, to the case of suspended sediment under wave and current flows (limited to nonbreaking waves over a horizontal bottom).

SUMMARY:

The objective of the study was to investigate the application of simple eddy viscosity models, developed for wave-current interaction, to the problem of sediment suspension and transport. A review of existing models is given; however, it is pointed out that all models compute suspended sediment transport by integrating the product of mean concentration and mean velocity. Because recent field experiments indicate that time-varying quantities may dominate the sediment flux due to mean components, the model described in this report calculates the time-varying components of the concentration along with the mean flow component.

The report describes the governing equations and boundary conditions, the process used to select an eddy viscosity model for hydrodynamics of wave-current interaction, and the determination of a resuspension coefficient. A detailed summary of the model development and solution scheme is provided in this documentation, and example calculations using the computer program WCSTRANS are reported. A source listing of the computer model is included.

AVAILABILITY OF REPORT:

The report is available through the Interlibrary Loan Service from the U.S. Army Engineer Waterways Experiment Station (WES) Library, telephone number (601) 634-2355. National Technical Information Service (NTIS) report numbers may be requested from WES Librarians. To purchase a copy of this report, call NTIS at (703) 487-4780.

About the Authors: The report was prepared and the associated research performed by Palitha Nalin Wikramanayake and Ole Secher Madsen, Ralph M. Parsons Laboratory, Massachusetts Institute of Technology, Cambridge, MA. Point of Contact: Dr. Norman W. Scheffner, Coastal Engineering Research Center, WES, was the Principal Investigator for the DRP work unit. For further information about the DRP, contact Mr. E. Clark McNair, Jr., Manager, DRP, at (601) 634-2070.
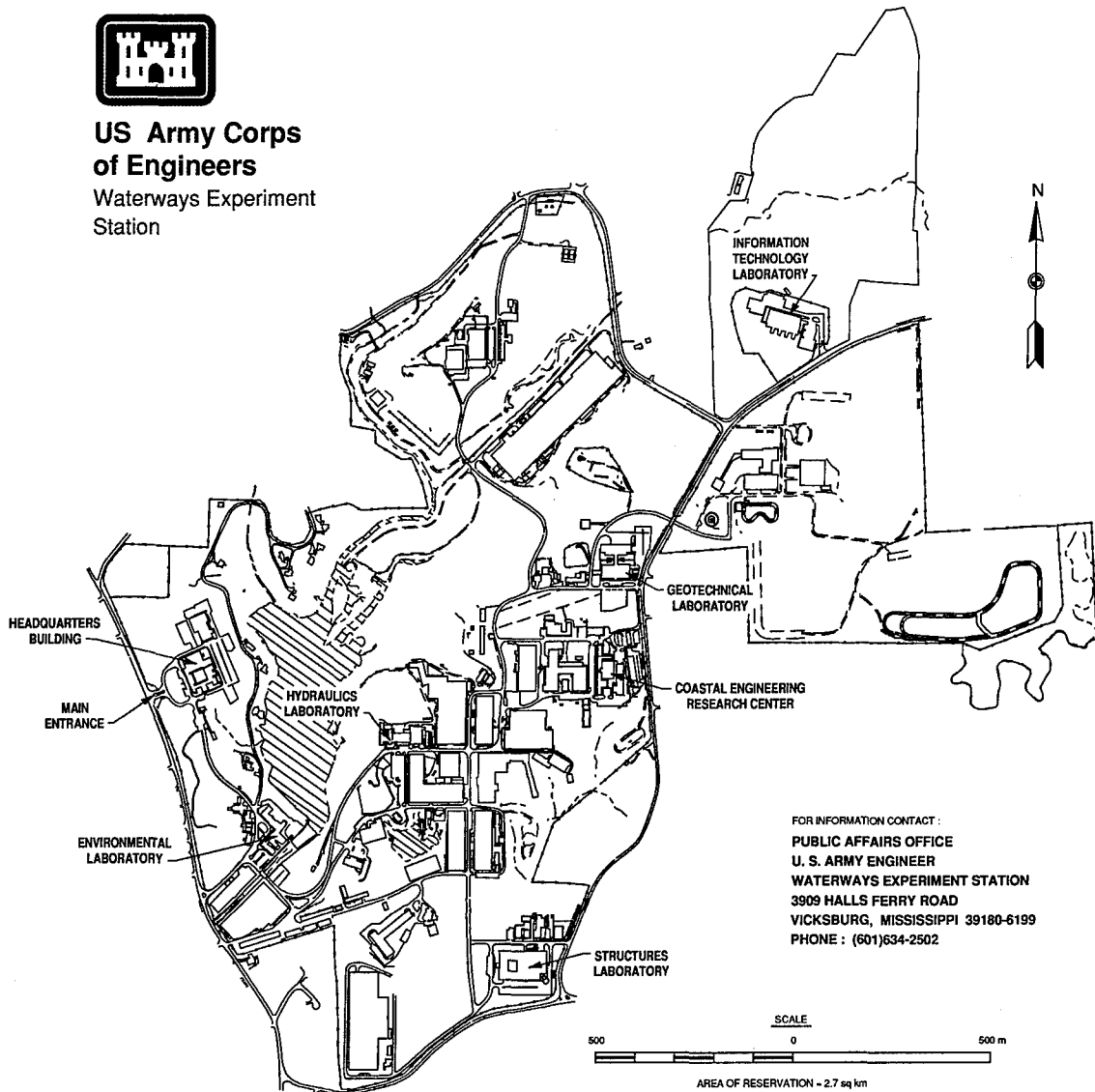
Calculation of Suspended Sediment Transport by Combined Wave-Current Flows

by   Palitha Nalin Wikramanayake, Ole Secher Madsen

Ralph M. Parsons Laboratory
Massachusetts Institute of Technology
Cambridge, MA   02139

Final report

Prepared for   U.S. Army Corps of Engineers
               Washington, DC   20314-1000

**US Army Corps
of Engineers**
Waterways Experiment
Station

INFORMATION
TECHNOLOGY
LABORATORY

N

GEOTECHNICAL
LABORATORY

HEADQUARTERS
BUILDING

COASTAL ENGINEERING
RESEARCH CENTER

MAIN
ENTRANCE

HYDRAULICS
LABORATORY

ENVIRONMENTAL
LABORATORY

FOR INFORMATION CONTACT :
**PUBLIC AFFAIRS OFFICE
U. S. ARMY ENGINEER
WATERWAYS EXPERIMENT STATION
3909 HALLS FERRY ROAD
VICKSBURG, MISSISSIPPI 39180-6199
PHONE : (601)634-2502**

STRUCTURES
LABORATORY

SCALE

500   0   500 m

AREA OF RESERVATION = 2.7 sq km

CONTENTS

LIST OF TABLES

LIST OF FIGURES

2

Preface

This study was conducted at the Ralph M. Parsons Laboratory, Department of Civil Engineering (DCE), Massachusetts Institute of Technology (MIT), under contract with the Coastal Engineering Research Center (CERC), U.S. Army Engineer Waterways Experiment Station (WES). The work described herein was authorized as part of the Dredging Research Program (DRP), of Headquarters, U.S. Army Corps of Engineers (HQUSACE) and was performed under the Calculation of Boundary Layer Properties (Noncohesive Sediments) Work Unit 32463 of DRP Technical Area 1 (TA1). Messrs. Robert H. Campbell and John H. Lockhart, Jr., were the Chief HQUSACE and TA1 Technical Monitors, respectively, for the DRP. Mr. E.Clark McNair, Jr., CERC, was DRP Program Manager (PM), and Dr. Lyndell Z. Hales, CERC, was Assistant PM. Dr. Nicholas C. Kraus, Senior Scientist, CERC, was Technical Manager for DRP TA1 and Principal Investigator of Work Unit 32463 during the investigation. Dr. Kraus was succeeded as Technical Manager of TA1 by Dr. Billy H. Johnson, WES Hydraulics Laboratory, and as Principal Investigator for Work Unit 32463 by Dr. Norman W. Scheffner, CERC Coastal Oceanography Branch.

This study was performed and the report prepared over the period 1 October 1991 through 30 September 1992 by Mr. Palitha Nalin Wikramanayake, Research Assistant, and Dr. Ole Secher Madsen, Professor, both of DCE, MIT. Drs. Kraus and Scheffner were under the supervision of Dr. James R. Houston and Mr. Charles C. Calhoun, Jr., Director and Assistant Director, CERC, respectively.

At the time of publication of this report, Director of WES was Dr. Robert W. Whalin. Commander was COL Bruce K. Howard, EN.

Additional information can be obtained from
Mr. E. Clark McNair, Jr., DRP Program
Manager, at (601)634-2070.

SUMMARY

     The objective of the study was to investigate the
application of simple eddy viscosity models, developed for wave-
current interaction, to the problem of sediment suspension and
transport. A review of existing models is given in this report,
however, it is pointed out that all models compute suspended
sediment transport by integrating the product of mean
concentration and mean velocity. Because recent field
experiments indicate that time-varying quantities may dominate
the sediment flux due to mean components, the model described in
this report calculates the time-varying components of the
concentration along with the mean flow component.
     The report describes the governing equations and boundary
conditions, the process used to select an eddy viscosity model
for hydrodynamics of wave-current interaction, and the
determination of a resuspension coefficient. A detailed summary
of the model development and solution scheme is provided in this
documantation and example calculations using the computer program
WCSTRANS are reported. The report contains a source listing of
the computer model.

CALCULATION OF SUSPENDED SEDIMENT TRANSPORT BY COMBINED WAVE-CURRENT FLOWS

PART I: INTRODUCTION

1. When undertaking engineering projects in the coastal zone it is necessary to consider the effect of the waves and currents that are nearly always present in coastal waters. Waves and currents affect structures directly by the action of fluid forces and indirectly by their ability to transport the loose bottom sediment found in most coastal regions.

2. Sediment grains on the bottom will move when the shear stress exerted on the bottom by the flow exceeds a critical value. This shear stress is caused by the no-slip condition imposed by the bottom on the flow above it, thereby creating a rotational boundary layer near the bottom. Due to the wave flow reversing in direction twice every wave period the wave boundary layer is limited to the near-bottom region while the current boundary layer grows until it reaches the free surface. The limited height of the wave boundary layer means that the shear stress due to a wave motion is much greater than the shear stress due to a current of a comparable magnitude. Therefore the motion of sediment on the bottom in coastal regions is nearly always governed by the wave motion.

3. The mobility of the sediment affects the bottom boundary layer processes in several ways. First, after the critical shear stress for initiation of motion is exceeded ripples will be formed on the bed. These ripples will increase the effective roughness felt by the fluid motion from a value scaled by the grain diameter to a value scaled by the ripple height. An increase in the roughness results in increased shear stress and energy dissipation in the boundary layer. Further increase in the wave motion will lead to the disappearance of the ripples and to sheet flow where a layer of grains moves to and fro on the bed. This hydrodynamic effect of a movable bed was studied by Wikramanayake and Madsen (1990).

4. A second effect of the movable bed is that the sediment grains will be transported by the flow. The transport is usually divided into two modes—bedload and suspended load transport. Bed load transport is defined as taking place in the region of high concentration near the bed where

transport is due primarily to grains rolling and jumping along the bottom. Suspended load transport is defined as taking place in the main body of the flow where grain-grain collision is negligible and the grains are carried in suspension by the fluid turbulence.

5. The bed load flux can be thought of as being a function of the bottom shear stress, while the suspended load flux is a function of both the bottom shear stress, which controls the quantity of entrained sediment, and the fluid velocity. The shear stress and velocity are in turn a function of the fluid forcing and the bedforms. This demonstrates the complicated nature of the interaction between the fluid motion and the movable bed. A further complication is that stable stratification associated with the gradient of suspended sediment concentration could dampen the turbulence in the wave boundary layer. All these possible interactions should be kept in mind when modeling the sediment transport by waves and currents.

6. Despite the fact that sediment is usually mobilized by the wave motion it is apparent that a purely linear symmetric wave motion would not result in a net flux of sediment. However, the sediment thus mobilized could be transported by any factor—such as wave non-linearity, a superimposed current, or wave-induced mass transport—that causes an asymmetry in the wave motion. For example consider the case of a weak current acting together with a strong wave motion. While the net bed load flux due to the asymmetric bed shear stress may be small, the current may be able to transport significant quantities of the sediment that is brought into suspension by the wave motion.

7. This mechanism of sediment mobilization by the wave motion and transportation by the mean current velocity was commonly accepted in previous treatments of the transport of suspended sediment by waves and currents. The time variation of the suspended sediment concentration and the net flux due to the product of the time-varying concentration and the time-varying fluid velocity were not considered. A possible reason may have been that sufficiently detailed data was not available to validate this concept.

8. However, recent field experiments, such as those reported by Vincent and Green (1990) and Hanes and Huntley (1986), have shown that the

flux due to the time-varying components of velocity and concentration potentially can be of the same order of magnitude as, and in some cases dominates, the flux due to the product of the mean velocity and the mean concentration. Thus a model for the transport of sediment should include these components.

Scope of This Report

9. The scope of this report is to extend the turbulent eddy viscosity models developed by Madsen and Wikramanayake (1991), which dealt with purely hydrodynamic aspects of wave-current interaction, to the case of suspended sediment under wave and current flows. The treatment is limited to the case of non-breaking waves over a horizontal bottom. The objective is to formulate a theoretical framework for the problem that together with recent field measurements of the instantaneous suspended sediment concentration can be used to develop a predictive model for sediment transport in the coastal zone.

10. In Part II the governing equation for the suspended sediment profile is presented along with its assumptions and limitations. Some previous models that have been put forward to solve this equation for the suspended sediment concentration and flux profiles are then discussed. Recent laboratory and field measurements that indicate the importance of the time-varying components of the suspended sediment concentration are presented. The two eddy viscosity models proposed by Madsen and Wikramanayake (1991) are discussed and the time-invariant eddy viscosity model is selected for application to sediment in suspension. This model is extended to include the case where the wave motion is specified by many periodic wave components. A brief outline of the solution of the wave current problem is given. The empirical relations of Wikramanayake and Madsen (1990) are proposed to calculate the equivalent roughness of a movable sand bed.

11. The solution of the governing equation using the selected eddy viscosity model is presented in Part III. The solution for the periodic components of the velocity is found to be a special case of the solution for the periodic components of the concentration. The mean and time-

varying components of the concentrations are found to be scaled by the reference concentration specified near the bottom. Most researchers have linked this reference concentration to the concentration in the bed load layer. Therefore the conceptual model of Madsen (1991) for bed load transport in the coastal environment is discussed along with the implications for the reference concentration. Some reference concentration models proposed in the literature are reviewed and a simple formulation is chosen for use in this report.

12. The reference values for the periodic components of concentration are derived for the case where the wave motion is represented by two components, one at twice the frequency of the other. The method by which the sediment fluxes due to the mean and the wave components are calculated is outlined.

13. It is observed that the model developed in Parts II and III is completely deterministic except for the constant in the reference concentration model known as the resuspension coefficient. Therefore, Part IV is devoted to the determination of this coefficient by comparing the model predictions to available field data. Appropriate values of the coefficient for both rippled and flat beds were determined. The factors that affect the accuracy of these determinations are discussed and additional measurements that would improve the reliability of field experiments are proposed.

14. The program WCSTRANS, which performs the model calculation, is outlined in detail in Part V along with two example calculations. The model predictions of mean concentration and suspended sediment fluxes are compared to the observed values. The effect of non-uniform sediment size is investigated by a simple extension of the model. The model development and results are summarized in Part VI along with proposed work for its further development.

PART II: GOVERNING EQUATION AND SELECTION OF AN EDDY VISCOSITY MODEL

15. The equation governing the distribution of suspended sediment is
stated and discussed in this part. Some previous models put forward to
solve this equation under wave and wave and current flow conditions are
reviewed. It is found that none of the previous models considered the
sediment flux due to the time varying components of velocity and
concentration. Results from recent laboratory and field experiments that
show the importance of these components are presented. It is concluded
that a successful transport model should include the flux caused by these
components. The models of Madsen and Wikramanayake (1991) are discussed
and the time-invariant eddy viscosity model selected for application to the
sediment problem. The use of this model in wave-current flows is outlined
briefly. The model is then extended to include the case of many linearly
superposed wave components.

The Governing Equation

16. Sediment is considered to be in suspension when the grains are
supported entirely by fluid forces. In this case the profile of the
suspended sediment concentration is governed by the diffusion equation.
With the assumption of negligible horizontal concentration gradients this
equation can be written as

$$\frac{\partial c}{\partial t} = w_f \frac{\partial c}{\partial z} + \frac{\partial}{\partial z}(F_d) \qquad\qquad (1)$$

where

      c = instantaneous sediment concentration

      w_f = fall velocity of the sediment grains

      F_d = diffusive sediment flux

      t = time

      z = height above the bottom

17. It should be noted that Equation 1 is valid only in the region
where the concentration is small enough to make intergranular collisions

negligible, i.e., it is not valid very near the bottom where the sediment moves mostly as bed load. The neglect of horizontal gradients would seem to be inapplicable in the case of a rippled bed which could have large horizontal variations caused by the entrainment of sediment by vortices. In this case c is understood to be the concentration averaged over a distance that is large compared to the ripple wavelength but small compared to the wavelength of the wave motion.

18. Equation 1 requires two boundary conditions, one each at the top and bottom boundaries of the flow. The upper boundary condition is generally specified as zero sediment flux through the free surface. For the case of non-breaking waves in fairly deep water this condition is equivalent to the requirement that c approach zero for large values of z. The bottom boundary condition is specified as a prescribed value of either the concentration or the sediment flux at some level near the bed. The relative merits of these two methods are discussed in Part III and the reference concentration method selected for this study.

19. These boundary conditions show an important difference between the suspended sediment problem and the fluid velocity problem, which is governed by an equation similar to Equation 1. The fluid velocity in the boundary layer is forced by, and therefore scaled by, the near-bottom wave velocity while the suspended sediment concentration is forced and scaled by the prescribed reference value near the bottom. Therefore this reference concentration is a critical component of any suspended sediment model. Possible formulations of the reference concentration component of the model will be discussed in Part III.

20. Under conditions of turbulent flow, which is nearly always the case in coastal wave boundary layers, the diffusive flux, F_d can be written as

$$F_d = -\overline{c'w'} \tag{2}$$

where c' and w' are the turbulent fluctuations in the concentration and vertical velocity, respectively, and the overbar denotes averaging in time.

21. In order to solve Equation 1 and obtain c as a function of z and t it is necessary to express the diffusive flux F_d in terms of the

mean flow characteristics. Since this flux arises due to turbulent mixing along a concentration gradient it is usually expressed, analogous to molecular diffusion, as

$$F_d = -\overline{c'w'} = \nu_t \frac{\partial c}{\partial z} \tag{3}$$

where ν_t is referred to as the turbulent eddy diffusivity. It will be assumed in this report that the turbulent diffusivities for mass and momentum are the same, i.e., turbulent eddy diffusivity and eddy viscosity are assumed identical and the terms are used interchangeably from here on. Another assumption made in the present model is that the suspended-sediment-induced stratification is negligible. The solution of Equation 1 depends on the formulation of the eddy diffusivity. Some of the turbulence models used to derive the eddy viscosity are discussed by Madsen and Wikramanayake (1991). The models proposed for the suspended sediment problem will be discussed in the next section.

Review of Previous Models for the Suspended Sediment Problem

22. In contrast to the plethora of models developed for wave and wave-current boundary layer flows there are relatively few models proposed in the literature for the suspension and subsequent transport of sediment by waves and currents. One of the reasons for this situation is the difficulty of making experimental measurements of the suspended sediment concentration, particularly under field conditions, and especially near the bottom where the concentrations are the highest. As a result, approaches to this problem tend to be qualitative rather than quantitative and the models are more empirical than those used for the velocity.

23. One of the first models for the distribution of suspended sediment under waves was the mixing length model of Homma, Horikawa, and Kajima (1965) which used the potential wave velocity to derive the mixing length. Another mixing length model was proposed by Bakker (1974). Other models that do not use the eddy viscosity approach are the empirical model of Vongvisessomjai (1986) and the k-ϵ model of Hagatun and Eidsvik (1986).

24. Kennedy and Locher (1972) reviewed various formulations of the problem and attempted to fit measured profiles of the mean concentration using different eddy viscosity models. They concluded that the form of the profiles was well described by all three models considered. Nielsen (1979) used an eddy viscosity that was constant over the depth to analyze the mean concentration profiles measured in the laboratory. He derived an eddy viscosity and a mean bottom concentration from these profiles and then attempted to obtain an empirical relationship for these values in terms of the wave, sediment and ripple parameters. Nielsen (1986) obtained an empirical relation for the mean bottom concentration that was valid for both a rippled and a flat bed.

25. Skafel and Krishnappan (1984) proposed an eddy viscosity model that had a velocity scale proportional to the shear velocity and a length scale proportional to the wave orbital amplitude at the bottom. The bottom concentration was obtained by considering the bed load transport. Fredsoe, Anderson, and Silberg (1985) presented a model that had an eddy viscosity and boundary layer thickness that varied in time. The reference concentration was obtained by extending the steady flow formulation of Engelund and Fredsoe (1976) to the case of unsteady flow.

26. Glenn and Grant (1987) extended the wave-current model of Grant and Madsen (1979) to include the stratification effect of sediment in suspension resulting in a combined wave-current-sediment model. This model, along with that of Fredsoe, Anderson, and Silberg (1985), are the only two models that account for both the sediment and the velocity profiles.

27. The net transport predicted by the Glenn and Grant (1987) model was analyzed by Goud (1987). She calculated the suspended sediment transport by integrating the product of the mean velocity and the mean concentration. This method of calculating the suspended load transport ignores any correlation between the periodic components of the velocity and the concentration. Even in the model of Fredsoe, Anderson, and Silberg (1985), which calculated the time-varying concentration, the transport was calculated considering only the mean values. The results of recent laboratory and field measurements of the instantaneous suspended sediment

13

concentration under waves will be discussed in the next section in order to show the importance of the time-varying components.

Evidence for the Importance of the Time-varying Components

The neglect of the time-varying concentration would imply that the mean concentration is more important. However, laboratory experiments have shown that the instantaneous sediment concentration under a wave motion is strongly time dependent. Entrainment and suspension from rippled beds have been observed by Homma, Horikawa, and Kajima (1965), Nakato et al. (1977), and Sleath (1982). Measurement of the instantaneous concentration shows from two to five peaks for each wave cycle. Visual observation indicates that these peaks correspond to the passage of vortices shed from the ripple crest carrying entrained sand past the measurement point. The variation from the mean has been observed to be as much as 100 percent of the mean value.

28. Sleath (1982) has observed that the lee vortices entrain sand by trapping sediment carried over the ripple crest and by active erosion from the lee slope of the ripple. The quantity of sand entrained in a vortex is proportional to the strength of the flow over the ripple. The vortex is then thrown outwards in a direction opposite to the flow that created it. In the case of a wave and current flow the vortex formed when the wave velocity is in the current direction will contain more sand and be thrown back against the current. Nielsen (1988) suggested that this mechanism could explain the observation by Inman and Bowen (1963) that the transport caused by waves and a current over a rippled bed was against the current.

29. For example, some of the measurements of Nakato et al. (1977) are shown in Figure 1. The figure shows the instantaneous sediment concentrations measured over a ripple crest and a ripple trough under a pure wave motion. The level of measurement is 3 mm above the level of the ripple crest. The grain diameter is 0.14 mm, the wave period T is 1.8 sec, and the near-bottom excursion amplitude is 76 mm. The origin of the time axis corresponds to the maximum horizontal velocity in the shoreward direction.
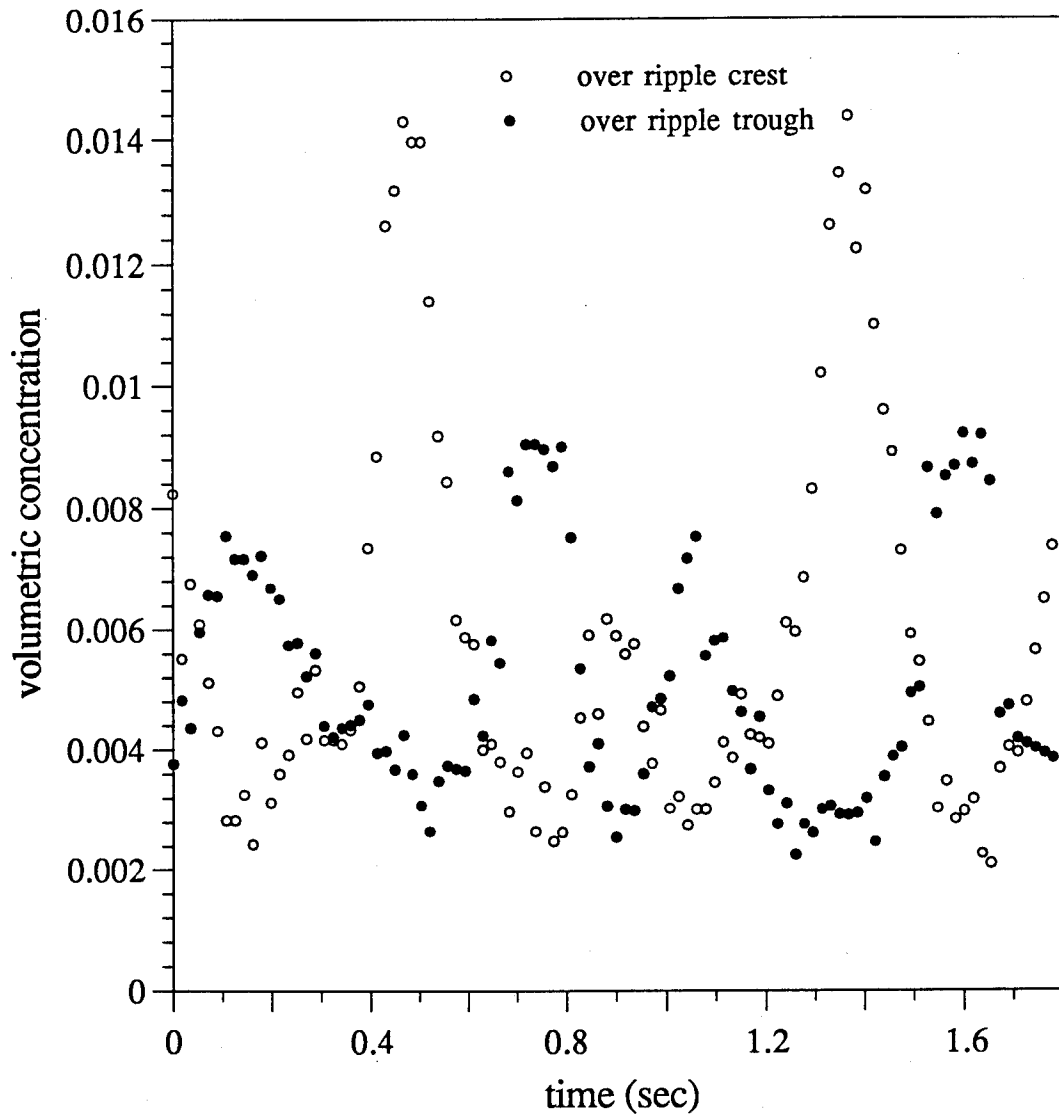
Figure 1. Measured instantaneous suspended sediment concentration over a
wave period above a rippled bed from Test 2 of Nakato et al. (1977).

30. The figure shows that there are four peaks in each record for a wave period. Nakato et al. explain these peaks using the vortex shedding mechanisms described above. In the record over the ripple crest, the large peaks at around $T/4$ and $3T/4$ correspond to the shedding of the vortex after the flow reverses direction. Since the ripple wavelength, which was 85 mm, is less than the magnitude of the near-bottom excursion, which is 152 mm, the vortex shed by a certain ripple will be carried beyond the adjacent ripple. It is the arrival of the vortex from the adjacent ripple that causes the peak at around $T/2$ and T over the ripple crest.

31. Similarly for the record over the trough, the peaks at around $3T/8$ and $7T/8$ are caused by the vortices shed at times $T/4$ and $3T/4$ from the shoreward and seaward crest, respectively. The peaks at $T/8$ and $5T/8$ were caused by the sediment-entraining vortex prior to being shed at $T/4$ and $3T/4$. For the record over the crest the peak volumetric concentration is 1.4×10^{-2} while the mean value is 5.7×10^{-3}. For the record over the trough the corresponding values are 9.2×10^{-3} and 5.1×10^{-3}, respectively. These comparisons demonstrate the strongly time-varying nature of the suspended sediment concentration.

32. The instantaneous concentration over a flat bed, i.e., sheet flow conditions, has been measured by Horikawa, Watanabe, and Katori (1982) and Staub, Jonsson, and Svendsen (1984). The data show two peaks in the concentration for each wave cycle. The measurements very close to the bottom indicate that the concentration peaks there correspond to the maximum flow velocity. The variation from the mean is as much as 60 percent of the mean concentration.

33. Therefore laboratory data indicate that the time-varying component of the concentration under waves is of the same order of magnitude as the mean concentration. The concentrations must be multiplied by the velocities in order to calculate the fluxes. The common situation in coastal sediment transport is for waves to be accompanied by a weak current motion, i.e., the wave or time-varying velocity is stronger than the current or mean velocity. Under these conditions the only way in which the time-averaged product of the periodic components could be much smaller than the product of the mean values is if the phase difference between velocity and concentration is close to 90 degrees.

16

34. However, as observed in the laboratory experiments the peaks in the concentration are caused by, and therefore correlated with, the times of high wave velocity. This correlation would lead us to expect that the time-averaged product of the periodic components of the concentration and velocity is at least of the same order of magnitude as the product of the mean concentration and the mean velocity. Such a possibility has been ignored by all models proposed for the transport of suspended sediment by waves and currents.

35. As mentioned above, a probable reason for the very few models that have considered the time-varying component of the concentration is the paucity of data against which such a model can be compared. Recent developments in instrumentation, however, have permitted detailed measurements of the instantaneous velocity and suspended sediment concentration under waves and currents. Such measurements have been reported by Hanes and Huntley (1986), Huntley and Hanes (1987), Doering and Bowen (1988), Vincent and Green (1990), Kim (1990), Hanes (1991), and Greenwood, Osborne, and Bowen (1991), among others.

36. In these experiments the instantaneous sediment concentration was measured at frequencies from 1 to 4 Hertz—either by using optical backscatter sensors at several points near the bottom or by using an acoustic concentration meter to obtain the profile of suspended sediment in the bottom region. Simultaneous measurements of the horizontal velocities were made at one or more points on the same vertical line. Using these measurements estimates of the instantaneous and time-averaged fluxes could be made over the near-bottom region.

37. A portion of the measurements reported by Hanes (1991) is shown in Figure 2. The figure shows the instantaneous suspended sediment concentration averaged over the region 0.5—4.5 cm above the bed, along with the instantaneous velocity in the wave direction measured at a point 15 cm above the bed. The concentration was measured by an acoustic concentration meter and the velocity by an electromagnetic current meter. The instruments were sampled simultaneously at a rate of 4 Hz.

38. The figure shows the strongly time-varying nature of the near-bottom concentration. There is a definite correlation between the peaks in the velocity record and the peaks in the concentration record. Another
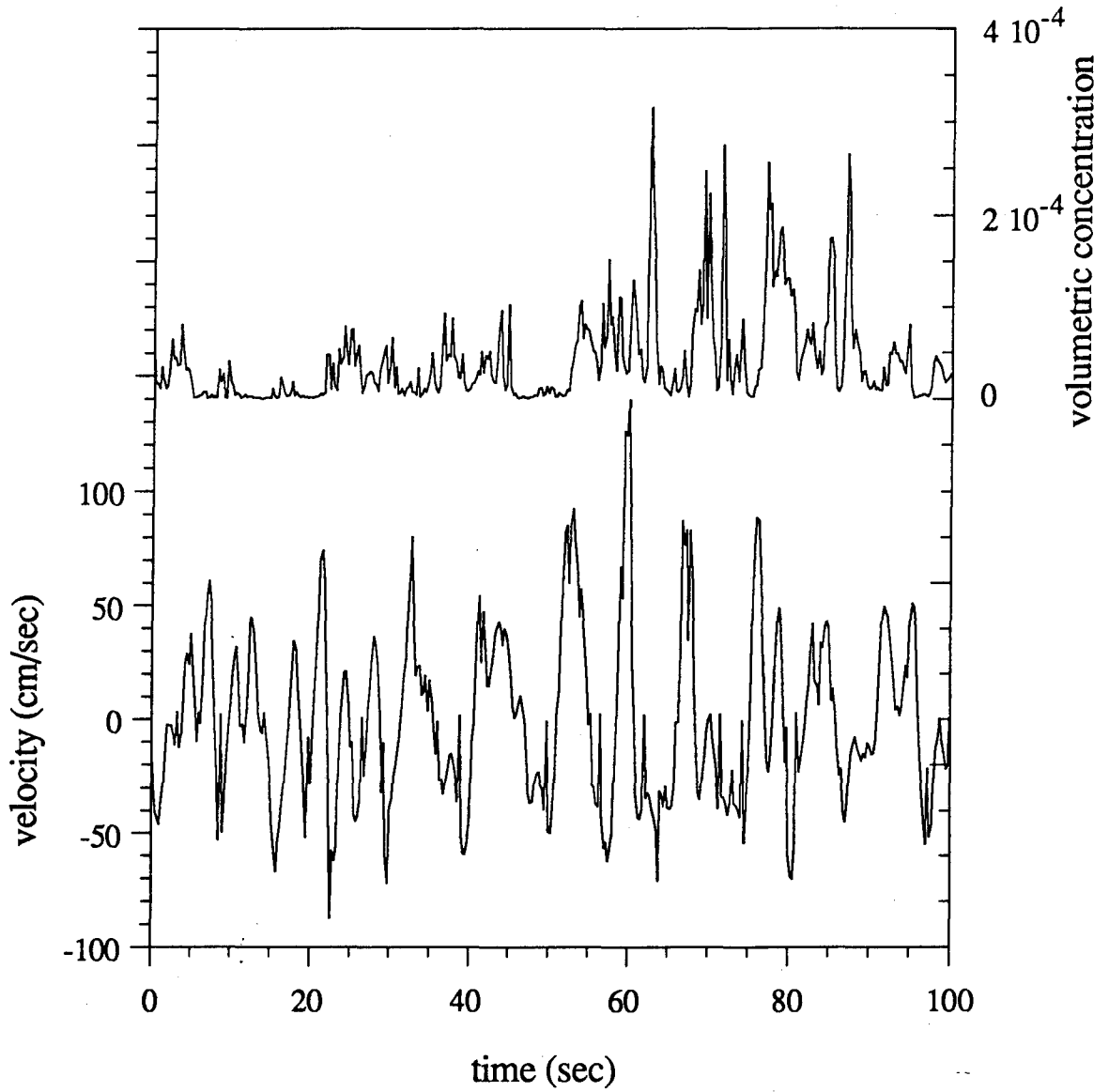
Figure 2. 100-second time series of near-bottom suspended sediment concentration and velocity in the wave direction from Hanes (1991).

feature of the data is the effect of a few large waves in suspending large amounts of sediment. It is obvious that a model that considers only the mean velocity and concentration would not be able to represent the field observations.

39. Vincent and Green (1990) found that the transport very close to the bed was dominated by the periodic components and not by the mean values. Huntley and Hanes (1987) estimated that while the transport due to the mean components was offshore the transport due to the time-varying components was about twice as large in the opposite direction and resulted in a net onshore transport. Similar results have been reported by other researchers.

40. The effect of wave groups on the suspension and transport of sediment in the field was analyzed by Osborne and Greenwood (1992). They investigated the frequency dependence of the suspended sediment flux by calculating the co-spectrum of the velocity and the concentration. The co-spectrum showed that while flux at frequencies close to the incident short wave frequency of around 0.2 Hz was onshore, flux at frequencies around 0.04 Hz was offshore. Osborne and Greenwood (1992) showed that this offshore flux was caused by the increased concentration due to the passage of the wave group coinciding with the offshore phase (trough) of the forced long wave associated with the wave group. A similar effect of wave groupiness is shown by the data of Sato (1992).

41. The preceding discussion indicates that any model for the transport of suspended sediment by waves and currents should include the time-varying components of the concentration and calculate the flux as the time-averaged product of instantaneous velocity and concentration. If only the mean components are considered it is possible that the result obtained for the transport will be incorrect in direction as well as in magnitude.

Selection of an Eddy Viscosity Model

42. This report attempts to rectify the deficiency in the calculation of the suspended sediment transport models discussed above by using a single eddy viscosity model to calculate the mean and time-varying profiles of fluid velocity and suspended sediment concentration. The flux is then

calculated using the contributions from both the mean and the time-varying components. Before the development of the suspended sediment model it is necessary to select an eddy viscosity model.

43. Madsen and Wikramanayake (1991) proposed two eddy viscosity models for wave-current interaction. Though these models have a similar variation of the eddy viscosity in the vertical, they differ in that one model uses a time-invariant eddy viscosity, while the other model allows the eddy viscosity to vary over a wave period. The time-invariant model allows an analytic solution to be obtained for the full range of wave-current interaction. The solution to the time-varying model was much more complicated and only an approximate solution, which involved numerical integration, for the case of a current that was weak with respect to the waves was obtained.

44. The results of these models were compared with experimental data and with the results of the numerical model of Davies, Soulsby, and King (1988). Both models were successful in reproducing the data for the cases where the waves and the current were in the same direction. The comparison with the results of the numerical model for the case of waves at an angle to the current showed that the time-invariant model did not show the changes in the magnitude and direction of the mean velocity caused by a change in the angle between the waves and the current. The time-varying model did show these features but the results were not in complete agreement with those of the numerical model. As there is no experimental verification for the case of waves at an angle between 0° and 90° to the current, which is the range in which the deflection of the mean velocity is predicted, it is not possible to say whether the time-varying eddy viscosity model or the numerical turbulence model gives the better result in this case.

45. Comparing the results of the two eddy viscosity models shows that for the case of waves at an angle to the current, the difference in the mean velocity profiles outside the wave boundary layer is less than 10 percent, a difference that is fairy small compared to the uncertainty in the specification of parameters such as the bottom roughness. The deflection of the mean velocity from the direction of the current shear stress, for the case of waves at 45° to the current, shown by the time-

varying model, decrease from a value of about 15° very near the bottom to about 5° near the top of the wave boundary layer. Again this value is not very significant compared to uncertainties in specifying the wave and current directions. The two models predict nearly identical values of the maximum bottom shear stress, a factor that is important in the suspended sediment model.

46. As far as the application of the model to the suspended sediment problem is concerned the most important aspect is the calculation of the time-varying concentration profiles. Time variation in the suspended sediment profile can arise due to a time-varying reference concentration as well as due to a time-varying eddy viscosity. However, an inspection of the results of the laboratory experiments discussed above shows that the time-variation in the concentration is greatest very near the bottom. This observation implies that the time-varying reference concentration is the important mechanism in the forcing of a time-variation in the suspended sediment concentration.

47. In summary it can be concluded that the time-varying eddy viscosity brings out aspects of the wave-current interaction that are not shown by the time-invariant model. However, in the context of suspended sediment transport computations it appears that these effects are not very significant when compared to other possible uncertainties. These uncertainties include the specification of the wave and current conditions, the bottom roughness, the grain diameter, and the resuspension coefficient. The time-invariant model has the advantages of a relatively simple solution and validity over the full range of wave-current interaction. Therefore it is decided to use the time-invariant eddy viscosity model to calculate the fluid velocities and sediment concentrations that are needed to obtain the suspended sediment transport.

Review of Time-Invariant Eddy Viscosity Model for the Hydrodynamics of Wave-Current Interaction

48. The solution of the wave-current problem using the time-invariant eddy viscosity profile is reviewed in this section. Additional details of the solution procedure can be found in Madsen and Wikramanayake (1991). As derived in Part II of that report the horizontal velocity is written as

$$u = u_W + u_C \tag{4}$$

where u_C is the time-invariant (current) component and u_W the periodic (wave) component.

49. The governing equation for u_W is

$$\frac{\partial u_W}{\partial t} = -\frac{1}{\rho}\frac{\partial p_W}{\partial x} + \frac{\partial}{\partial z}\left[\nu_t\frac{\partial u_W}{\partial z}\right] \tag{5}$$

where

ρ = density of water

p_W = time-varying component of pressure

x = direction of wave motion

50. The equation for u_C is

$$\nu_t\frac{du_C}{dz} = \frac{\tau_C}{\rho} \tag{6}$$

where τ_C is the mean (current) shear stress. In the general case τ_C is at an angle ϕ_{CW} to the wave direction.

51. Equations 5 and 6 must be solved for the velocities u_W and u_C using the time-invariant eddy viscosity model proposed by Madsen and Wikramanayake (1991). This model is given by

$$\nu_t = \begin{cases} \kappa u_{*CW}z & z \le a\delta \\ \kappa u_{*CW}a\delta & a\delta \le z \le a\delta/\epsilon \\ \kappa u_{*C}z & a\delta/\epsilon \le z \end{cases} \tag{7}$$

where

ν_t = turbulent eddy viscosity

κ = 0.4 = von Karman's constant

u_{*CW} = shear velocity based on the maximum combined bottom shear stress

u_{*C} = shear velocity based on mean (current) shear stress

Here

$$\delta = \frac{\kappa u_{*cw}}{\omega} \tag{8}$$

is the boundary layer length scale with ω the radian wave frequency while ϵ , given by

$$\epsilon = \frac{u_{*c}}{u_{*cw}} \tag{9}$$

is a parameter that expresses the relative strength of the current motion.

52. A sketch of the variation of eddy viscosity with the vertical coordinate z is given in Figure 3. The model is based on the two-layer model put forward by Grant and Madsen (1979) with the bottom layer scaled by the shear velocity based on the maximum shear stress and the upper layer scaled by the current shear velocity. The intermediate region ensures a smooth transition between the layers. Comparison of the results of this model with laboratory and numerical results led to the adoption of 0.5 as a suitable value for the parameter a .

53. Madsen and Wikramanayake (1991) used the eddy viscosity model of Equation 7 to solve Equations 5 and 6. The current velocity, u_c , was obtained in terms of the non-dimensional vertical coordinate, ζ , as

$$\begin{aligned}
u_c &= \epsilon \frac{u_{*c}}{\kappa} \ln\left[\frac{\zeta}{\zeta_0}\right] & \zeta < a \\
&= \epsilon \frac{u_{*c}}{\kappa}\left[\frac{\zeta}{a} - 1 + \ln\left[\frac{a}{\zeta_0}\right]\right] & a < \zeta < a/\epsilon \\
&= \frac{u_{*c}}{\kappa}\left\{\ln\left[\frac{\zeta}{a/\epsilon}\right] + 1 + \epsilon\left[\ln\left[\frac{a}{\zeta_0}\right] - 1\right]\right\} & \zeta > a/\epsilon
\end{aligned} \tag{10}$$

54. Here ζ is defined by

$$\zeta = \frac{z}{\delta} \tag{11}$$

and ζ_0 by

$$\zeta_0 = \frac{z_0}{\delta} = \frac{k_n/30}{\delta} \tag{12}$$

23
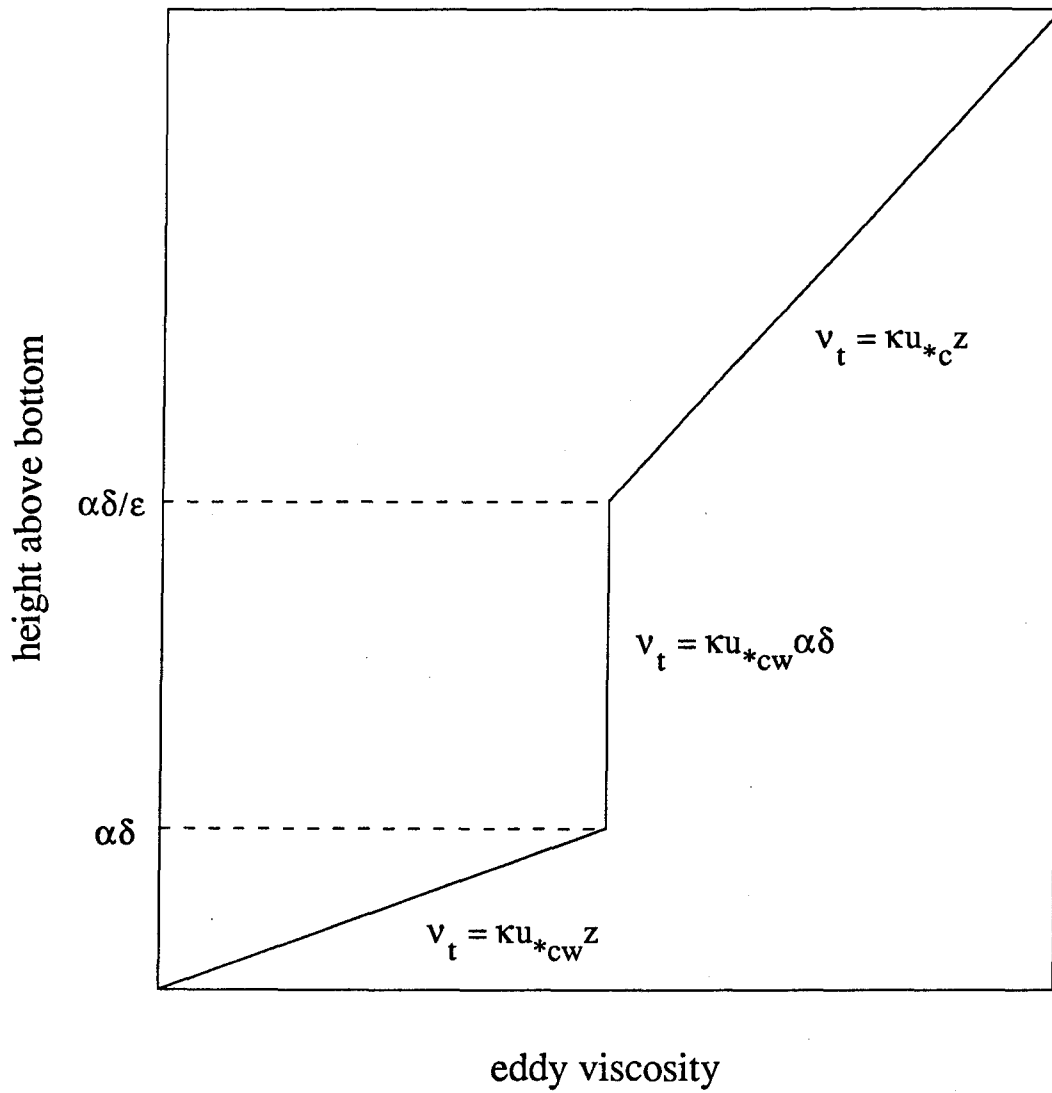
Figure 3. Variation of the eddy viscosity with height above the bottom.

where k_n is the equivalent Nikuradse roughness of the bottom

55. A typical current velocity profile is shown in Figure 4a. The profile has three regions that correspond to the three layers in the eddy viscosity model of Equation 7. The upper and lower layers are logarithmic and the dotted line extending the upper logarithmic section to the line $u_c = 0$ shows that the effective roughness (z_{0c}) caused by the wave boundary layer is much larger than the real value of z_0.

56. Equation 5, for the wave velocity, is solved by noting that

$$\frac{\partial u_\infty}{\partial t} = -\frac{1}{\rho}\frac{\partial p_w}{\partial x} \tag{13}$$

where u_∞ is the near-bottom potential wave velocity given by

$$u_\infty = u_b \cos \omega t \tag{14}$$

with ω being the wave radian frequency.

57. Introducing Equation 13 into Equation 5 gives

$$\frac{\partial(u_w - u_\infty)}{\partial t} = \frac{\partial}{\partial z}\left[\nu_t\frac{\partial}{\partial z}(u_w - u_\infty)\right] \tag{15}$$

58. The solution of Equation 15 can be simplified by writing

$$\frac{u_w - u_\infty}{u_b} = \mathrm{Re}\{u_d e^{i\omega t}\} \tag{16}$$

where $\mathrm{Re}\{\ \}$ means the real part of the bracketed quantity and u_d is a complex function of z. Substitution of Equation 16 into Equation 15 leads to

$$\frac{d}{dz}\left[\nu_t\frac{du_d}{dz}\right] - i\omega u_d = 0 \tag{17}$$

59. The boundary conditions for this equation will be

$$u_d = -1 \quad \text{at} \quad z = z_0 \tag{18}$$

and
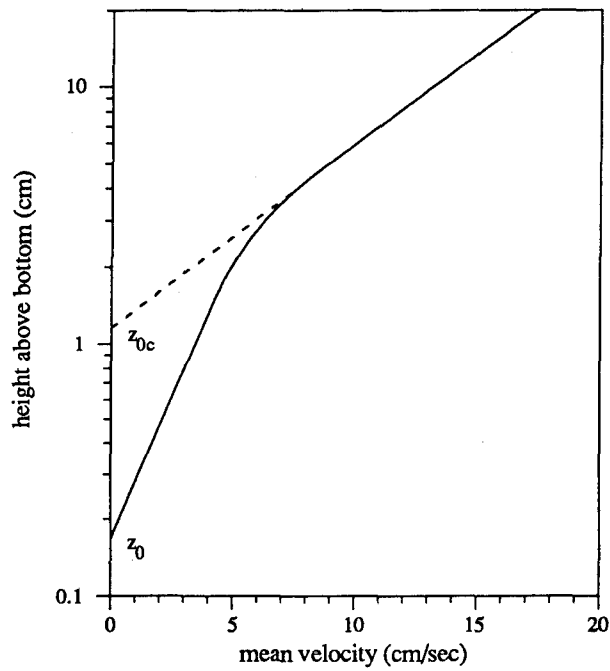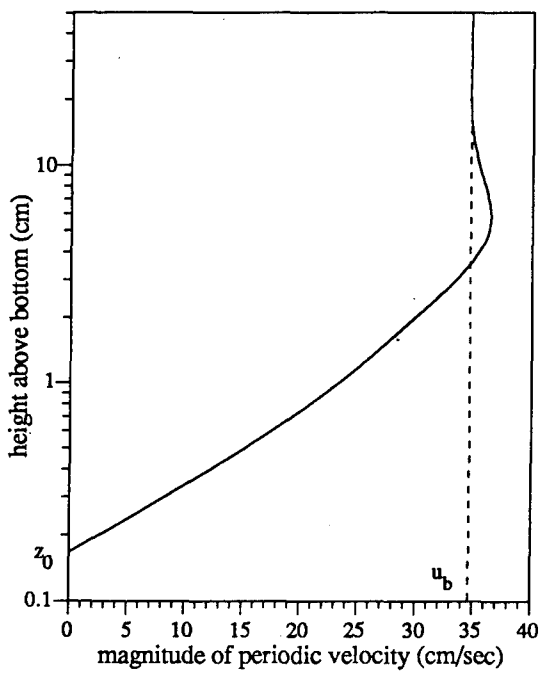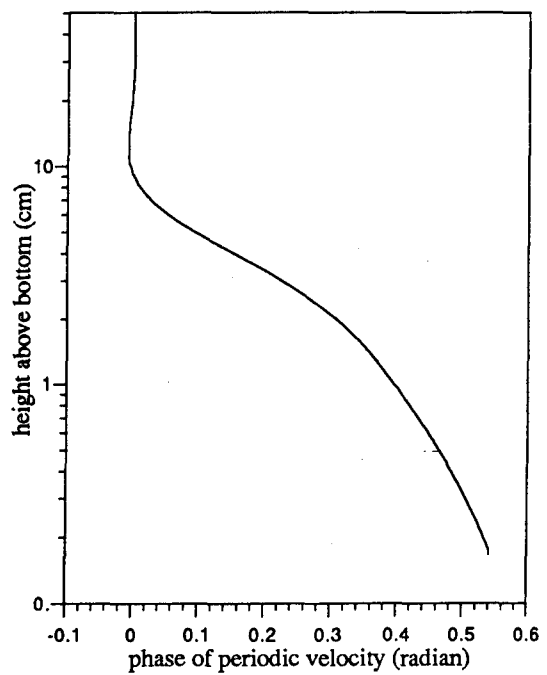
Figure 4. Profiles of a) current (mean) velocity, b) magnitude of the periodic velocity, and c) phase of the periodic velocity

$$u_d \to 0 \quad \text{as} \quad z \to \infty \tag{19}$$

60. The solution of Equation 17 using the eddy viscosity distribution of Equation 7 is given in detail in Madsen and Wikramanayake (1991). It will not be given here because, as will be shown in Part III, Equation 17 is a special case of the equation governing the suspended sediment concentration. Therefore, the solution for u_d can be obtained from the solution for the time-varying concentration in Part III.

61. A typical wave velocity profile is shown in Figure 4b. The profile is close to logarithmic in the lower region and then overshoots the near bottom value u_b before returning to that value for larger values of z. The corresponding profile of the phase of the velocity with respect to the phase of the near bottom velocity is shown in Figure 4c.

62. The solution for u_c and u_w so far has been developed in terms of the shear velocities u_{*c} and u_{*cw}, which are also unknowns that must be determined as part of the solution. The combined wave-current shear velocity u_{*cw} is related to the wave and current shear stresses by

$$\rho u_{*cw}{}^2 = \tau_{cw} = \max\{(\tau_w{}^2 + 2\tau_w \tau_c \cos\phi_{cw} + \tau_c{}^2)^{1/2}\} \tag{20}$$

where

τ_{cw} = combined shear stress

τ_w = wave shear stress

τ_c = current shear stress

ϕ_{cw} = angle between the waves and the current

63. The wave problem is closed by defining the wave shear stress, τ_w, as

$$\frac{\tau_w}{\rho} = \left[\nu_t \frac{\partial u_w}{\partial z}\right]_{z=z_0} \tag{21}$$

while the current shear stress is either specified or determined iteratively by using the specified current velocity. The details of the iterative solution can be found in Madsen and Wikramanayake (1991).

27

64. The solution of the wave-current problem requires the input of the wave, current, and bottom parameters. The wave is specified by the near-bottom wave velocity u_b and the radian wave frequency ω. The bottom parameter is the bottom roughness, specified by k_n, the equivalent Nikuradse sand roughness, which is scaled by the grain diameter for flat beds and the ripple height for rippled beds. The current is given by a specified current shear stress, a specified value of the mean (current) velocity at a certain height above the bottom, or by a specified depth-averaged mean velocity. The angle between the current and the wave direction, ϕ_{cw}, must also be specified.

65. Once the hydrodynamic problem is solved the wave and current velocities, u_c and u_w, are determined as a function of the height above the bottom. The representation of u_w in Equation 16 as a complex number means that once u_w is determined as a complex number both its magnitude and its phase with respect to the near-bottom wave motion will be known.

66. Similarly, the wave shear stress defined in Equation 21 using the complex quantity u_w, is also determined as a complex number. This allows the phase of τ_w, with respect to the near bottom velocity, to be determined as well as its magnitude. The phase of the bottom shear stress is important in determining the phase of the time-varying components of concentration.

Extension of the Wave-Current Model to Include Many Wave Components

67. The wave-current model, developed by Madsen and Wikramanayake (1991), and outlined in the preceding section, represents the wave motion by a single sinusoidal component. This representation is a simplification of the irregular wave motion observed in the field, which generally has wave components of many different frequencies. Some features of the irregular wave motion seen in the field indicate that using a single sinusoidal component for the wave conditions will result in an incorrect assessment of the sediment transport. Two such features are wave asymmetry and wave groups.

68. It is possible to simulate these effects by considering the wave motion to consist of two or more linearly superposed sinusoidal waves. For example, wave asymmetry can be accounted for by considering two sinusoidal

components, one with twice the frequency of the other, that are in phase with each other. The wave-current model outlined previously must be extended to allow more than one sinusoidal wave component. It should be noted that even though some of the irregular motion observed in the field may be due to the effects of non-linearity, the representation here is taken to be a linear superposition of sinusoidal components such that the required feature in the observed wave record is reproduced.

69. When many wave components are considered the near bottom wave motion can be written as

$$u_b(t) = u_{b1}\cos(\omega_1 t + \phi_1) + u_{b2}\cos(\omega_2 t + \phi_2) + \cdots \tag{22}$$

where u_{b1}, ω_1, and ϕ_1 are the magnitude, frequency, and phase of the first component, respectively. Similarly, the wave velocity u_w can be written as

$$u_w = u_{w1} + u_{w2} + \cdots \tag{23}$$

where u_{w1} has a frequency ω_1, and u_{w2} has a frequency ω_2.

70. Since the equation governing u_w, Equation 5, is linear, Equation 23 can be substituted into Equation 5 and components of the same frequency grouped to obtain different equations for each component of the wave motion. For example, the equation for the first component would be

$$\frac{\partial u_{w1}}{\partial t} = -\frac{1}{\rho}\frac{\partial p_{w1}}{\partial x} + \frac{\partial}{\partial z}\left[\nu_t\frac{\partial u_{w1}}{\partial z}\right] \tag{24}$$

71. As before the pressure gradient term is related to the external wave motion by

$$\frac{\partial u_{\infty 1}}{\partial t} = -\frac{1}{\rho}\frac{\partial p_{w1}}{\partial x} \tag{25}$$

where in this case

$$u_{\infty 1} = u_{b1}\cos(\omega_1 t + \phi_1) \tag{26}$$

72. Defining

$$\frac{u_{w1} - u_{\infty 1}}{u_{b1}} = \mathrm{Re}\left\{u_{d1}e^{i(\omega_1 t + \phi_1)}\right\} \tag{27}$$

and using Equations 25, 26, and 27 in Equation 24 the governing equation for u_{w1} is obtained as

$$\frac{d}{dz}\left[\nu_t \frac{du_{d1}}{dz}\right] - i\omega_1 u_{d1} = 0 \tag{28}$$

with boundary conditions

$$u_{d1} = -1 \quad \text{at} \quad z = z_0 \tag{29}$$

and

$$u_{d1} \to 0 \quad \text{as} \quad z \to \infty \tag{30}$$

73. Equation 28 is very similar to Equation 17 so that once ν_t is known the solution of each component u_{w1} , u_{w2} , etc., will be very similar to the solution for u_w in the original wave current model. However, the question that arises in the case of many wave components is which value to use for the combined shear velocity, u_{*cw} .

74. In the case of a single wave component u_{*cw} was given by Equation 20, which relates u_{*cw} to the wave and current shear stresses, τ_w and τ_c . Equation 20 can also be used for the case of many wave components if τ_w is defined as the shear stress due to an equivalent periodic wave that is representative of the sum of the many individual components.

75. Madsen (1992) shows that the near bottom orbital velocity amplitude of this representative wave, u_{br} , should be taken as

$$u_{br} = \sqrt{\Sigma u_{bi}^2} \tag{31}$$

where u_{bi} are the amplitudes of the individual components. The frequency, ω_r , of this representative wave is derived by Madsen (1992) as

$$w_r = \frac{\sum \omega_i u_{bi}^2}{\sum u_{bi}^2} \qquad (32)$$

where ω_i are the frequencies of the individual components.

Another quantity that must be defined newly for the case of many waves is the boundary layer length scale, δ, defined by Equation 8 for the case of one wave. δ is present in Equation 7 which gives the distribution of the eddy viscosity. For the case of many wave components δ can be defined using the representative wave frequency as

$$\delta = \frac{\kappa u_{*cw}}{\omega_r} \qquad (33)$$

76. Once u_{*cw} and δ are defined as above the velocity problem associated with each component can be solved just as in the case of a single wave component. The detailed solution is shown in Part III to be included in the solution of the concentration equation. The individual bottom shear stresses, τ_{w1}, τ_{w2}, etc., and their phases with respect to the phases of the corresponding near bottom wave component can be found from the relation

$$\frac{\tau_{wi}}{\rho} = \left[\nu_t \frac{\partial u_{wi}}{\partial z} \right]_{z=z_0} \qquad (34)$$

Movable Bed Roughness

77. The hydrodynamic model outlined in this part requires the equivalent Nikuradse roughness of the bottom, k_n, as an input value. However, for a movable sand bed this value is itself a function of the wave and sediment parameter. The roughness of a movable sand bed was investigated by Wikramanayake and Madsen (1990) using laboratory and field data.

78. They concluded that for a rippled sand bed the equivalent roughness was given by

$$k_n = 4\eta \qquad (35)$$

where η is the ripple height. The ripple height can be calculated from the empirical equation

$$\frac{\eta}{A_{br}} = \begin{cases} 0.0181Z^{-0.5} & 0.0016 < Z < 0.012 \\ 0.0007Z^{-1.23} & 0.012 < Z < 0.18 \end{cases} \tag{36}$$

where

$$Z = \frac{\psi_w{}'}{S_*} \tag{37}$$

and A_{br} is the near-bottom excursion amplitude given by

$$A_{br} = \frac{u_{br}}{\omega_r} \tag{38}$$

with u_{br} the near-bottom wave velocity and ω_r the wave frequency of the representative periodic wave.

79. In Equation 37 $\psi_w{}'$ is the Shields parameter based on the wave skin friction shear stress, $\tau_w{}'$, and is defined by

$$\psi_w{}' = \frac{\tau_w{}'}{\rho(s-1)gd} \tag{39}$$

and S_* is defined by

$$S_* = \frac{d}{4\nu}\sqrt{(s-1)gd} \tag{40}$$

where

    d = grain diameter

    s = specific gravity of sediment

    ν = kinematic viscosity

    g = acceleration due to gravity

80. Equation 36, which is a slight modification of the relation proposed by Wikramanayake and Madsen (1990), is based entirely on ripple measurements in the field. For $Z \geq 0.18$ the bed will be flat while no

32

ripples have been observed for $Z < 0.0016$. For flat bed (sheet flow) conditions, Wikramanayake and Madsen (1990) showed that the relations for the equivalent roughness due to sheet flow proposed by Grant and Madsen (1982) and Nielsen (1983) were not validated by the available data. Therefore for the model proposed in this report the equivalent roughness due to sheet flow will be calculated by

$$k_n = 10d \tag{41}$$

81. Some recent measuremens of the current velocity profile in the field under sheet flow conditions (Madsen et al. (in review)) indicate a roughness of $k_n = 12\ d$. This shows that Equation 109 is a reasonable assumption. However, it must be emphasized that the equivalent roughness for sheet flow conditions is an area where much research is needed.

82. It should be noted that the parameter Z in Equation 36 is based on the root-mean-square wave velocity and the average period. Therefore when the wave condition is specified as the sum of many components the equivalent periodic wave defined in the previous section must be used to calculate Z . The empirical relation of Equation 36 was based on field measurements of ripples on beds that had mean grain diameters ranging from 0.01 cm to 0.062 cm. Flat bed conditions were observed on beds with mean grain size ranging from 0.012 cm to 0.025 cm. These ranges should be kept in mind when using Equation 36 for grain sizes finer than 0.01 cm.

PART III: SOLUTION OF THE GOVERNING EQUATION AND THE DEVELOPMENT OF AN APPROPRIATE BOUNDARY CONDITION

83. The time-invariant eddy viscosity model of Madsen and Wikramanayake (1991) was reviewed in Part II and extended to the case of many wave components. Given the wave velocities and frequencies, the current specification, and the bottom roughness, the model allows the calculation of the velocity field, the bottom shear stress, and the eddy viscosity distribution. The solution of the governing equation for the distribution of suspended sediment using this eddy viscosity will be outlined in this part.

84. The concentration distributions are found to be scaled by the reference concentration near the bottom. As the reference concentration is closely linked to the bed load transport a simple conceptual formulation for the bed load is discussed. The development of reference concentration models is reviewed and some models applicable to wave-current flows are suggested. Since the concept of skin friction shear stress is used in many of these models a method to obtain this component of the shear stress is outlined. Finally, a procedure to derive the reference values for the mean and time-varying components of the concentration using the selected reference concentration formulation is outlined.

Solution of the Governing Equation

85. The diffusive flux F_d in Equation 1 can be expressed in terms of the eddy viscosity and concentration gradient as in Equation 3. After this is done the governing equation can be written as

$$\frac{\partial c}{\partial t} = w_f \frac{\partial c}{\partial z} + \frac{\partial}{\partial z}\left[\nu_t \frac{\partial c}{\partial z}\right] \tag{42}$$

86. Since both the mean and time-varying components of the concentration are of interest, separate equations for each component of the suspended sediment concentration, c , can be derived by writing c as

$$c = \bar{c} + \tilde{c}_1 + \tilde{c}_2 + \cdots \tag{43}$$

34

where $\bar{c}$ is the mean concentration and $\tilde{c}_1$ and $\tilde{c}_2$ are periodic components with frequencies ω_1 and ω_2 respectively. As the time variation of the concentration is forced by the wave motion, it can be expected that the frequencies of the periodic components of the concentration will be first and higher harmonics of the frequencies of the wave motion defined in Equation 22.

87.   The definition of Equation 43 can be substituted into Equation 42. Since the fall velocity w_f and the eddy viscosity ν_t are time-invariant and Equation 42 is linear in c , separate equations for each component can be obtained. The mean and the time-varying components will be considered separately in the next two sections.

Solution for the mean concentration

88.   Substituting the definition of Equation 43 into Equation 42 and taking the time-average results in an equation for the mean concentration of the form

$$0 = w_f\frac{\partial \bar{c}}{\partial z} + \frac{\partial}{\partial z}\left[\nu_t\frac{\partial \bar{c}}{\partial z}\right]$$

(44)

89.   Integrating once with respect to z and using the boundary condition of no sediment flux through the free surface we obtain

$$0 = w_f\bar{c} + \nu_t\frac{\partial \bar{c}}{\partial z}$$

(45)

90.   The solution of Equation 45 using the eddy viscosity distribution in Equation 7 is facilitated by the introduction of a non-dimensional vertical coordinate ζ that is defined by

$$\zeta = \frac{z}{\delta}$$

(46)

where δ is defined in Equation 33.

91.   The use of this definition in Equation 45 along with the eddy viscosity model of Equation 7 results in the equation for $\bar{c}$ being obtained as

$$0 = \begin{cases} a\dfrac{\partial \bar{c}}{\partial \zeta} + \dfrac{\partial}{\partial \zeta}\left[\zeta\dfrac{\partial \bar{c}}{\partial \zeta}\right] & \zeta < \alpha \\[12pt] a\dfrac{\partial \bar{c}}{\partial \zeta} + \alpha\dfrac{\partial^2 \bar{c}}{\partial \zeta^2} & \alpha < \zeta < \alpha/\epsilon \\[12pt] a\dfrac{\partial \bar{c}}{\partial \zeta} + \epsilon\dfrac{\partial}{\partial \zeta}\left[\zeta\dfrac{\partial \bar{c}}{\partial \zeta}\right] & \alpha/\epsilon < \zeta \end{cases} \tag{47}$$

where

$$a = \frac{w_f}{\kappa u_{*cw}} \tag{48}$$

is the non-dimensional fall velocity.

92. The boundary condition for the mean concentration $\bar{c}$ is that

$$\bar{c} = \bar{c}_r \quad \text{at} \quad \zeta = \zeta_r = \frac{z_r}{\delta} \tag{49}$$

where

$\bar{c}_r$ = mean reference concentration

z_r = reference level

and ζ_r is usually smaller than α .

93. For $\zeta < \alpha$ the solution is obtained as

$$\bar{c} = \bar{c}_r\left[\frac{\zeta}{\zeta_r}\right]^{-a} \qquad \zeta < \alpha \tag{50}$$

94. For the region $\alpha < \zeta < \alpha/\epsilon$ the solution to Equation 41 is

$$\bar{c} = A_1 e^{-a\zeta/\alpha} \tag{51}$$

where A_1 is a constant. After matching with Equation 50 at the level of $\zeta = \alpha$ to obtain A_1 , the solution is found to be

$$\bar{c} = \bar{c}_r\left[\frac{\alpha}{\zeta_r e}\right]^{-a} e^{-a\zeta/\alpha} \qquad \alpha < \zeta < \alpha/\epsilon \tag{52}$$

95. For $\zeta > a/\epsilon$ the solution is

$$\bar{c} = A_2(\zeta)^{-a/\epsilon} \tag{53}$$

where A_2 is a constant to be determined by matching with Equation 52 at the level $\zeta = a/\epsilon$. The solution is obtained as

$$\bar{c} = \bar{c}_r\left[\frac{a}{\zeta_r e}\right]^{-a}\left[\frac{e\epsilon}{a}\right]^{-a/\epsilon}(\zeta)^{-a/\epsilon} \qquad a/\epsilon < \zeta \tag{54}$$

96. A typical mean concentration profile is shown in Figure 5a. As with the current profile this profile has three regions. For a pure wave flow field only the two lower sections of the profiles would be seen, i.e., according to the theory presented here the second section would extend from the level $z = a\delta$ upward.

Solution for the time varying components of the concentration

97. The solution of the governing equation for a time-varying component, $\tilde{c}_1$, with frequency ω_1 , will be derived in this section. In order to keep the solution as general as possible ω_1 is allowed to be different from the representative frequency, ω_r , that was used to define the length scale δ in Equation 33.

98. The equation for $\tilde{c}_1$ is found to be

$$\frac{\partial \tilde{c}_1}{\partial t} = w_f\frac{\partial \tilde{c}_1}{\partial z} + \frac{\partial}{\partial z}\left[\nu_t\frac{\partial \tilde{c}_1}{\partial z}\right] \tag{55}$$

99. The boundary conditions for this equation are

$$\tilde{c}_1 = \tilde{c}_{1r} = \mathrm{Re}\{c_{1r}e^{i\omega_1 t}\} \tag{56}$$

and the condition of no sediment flux through the free surface. In practice this second condition is equivalent to requiring that $\tilde{c}_1$ go to zero as z becomes very large.

100. As $\tilde{c}_1$ is a periodic quantity the solution of Equation 55 is facilitated by defining $\tilde{c}_1$ as
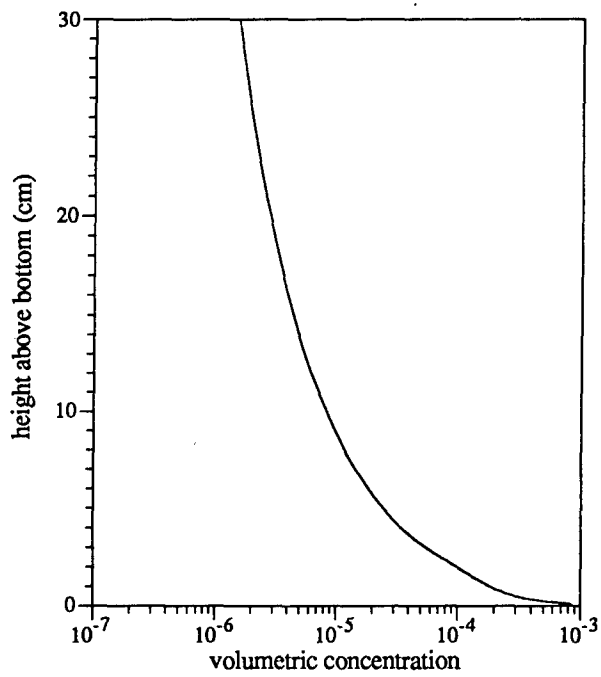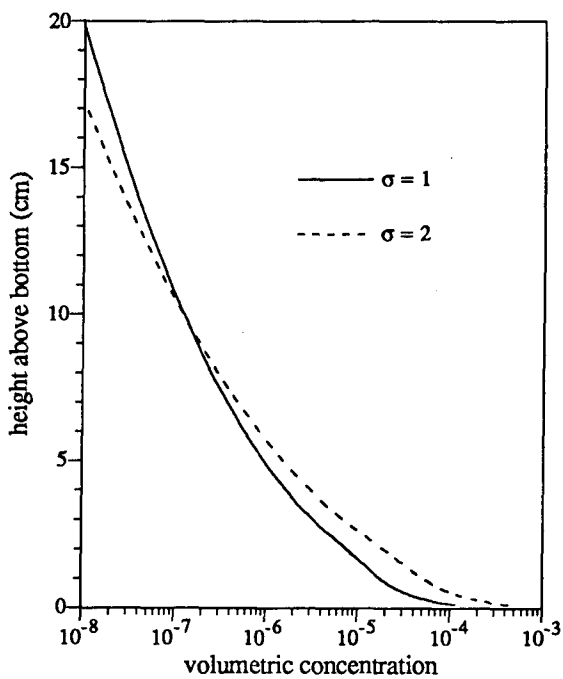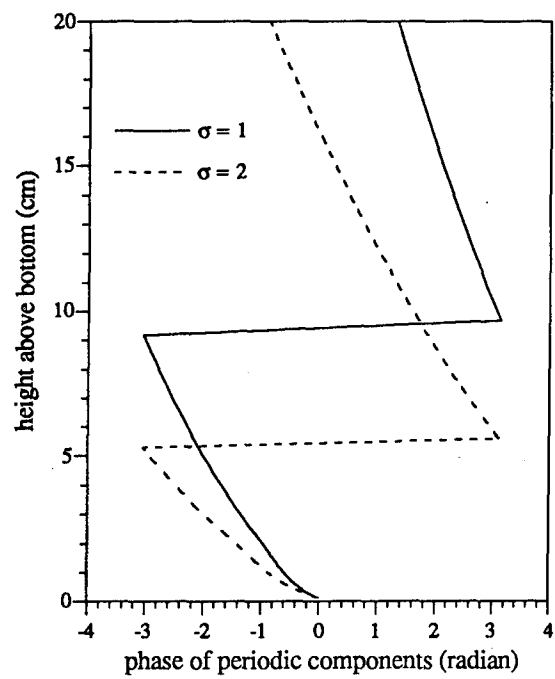
Figure 5. Profiles of a) mean concentration, b) magnitude of periodic concentration components with $\sigma = 1$ and $\sigma = 2$, and c) phase of periodic components

$$\frac{\tilde{c}_1}{c_{1r}} = \text{Re}[c_1(z)e^{iw_1t}] \tag{57}$$

where c_1 is a complex function of z. Using this definition in Equation 55 the governing equation for c_1 is found to be

$$i\omega_1 c_1 = w_f\frac{\partial c_1}{\partial z} + \frac{\partial}{\partial z}\left[\nu_t\frac{\partial c_1}{\partial z}\right] \tag{58}$$

with boundary conditions

$$c_1 = 1 \quad \text{at} \quad z = z_r \tag{59}$$

and

$$c_1 \to 0 \quad \text{as} \quad z \to \infty \tag{60}$$

101. The definition of c_1 in Equation 57 means that the phase of c_1 is the phase with respect to the phase of $\tilde{c}_{1r}$, the reference value for this component.

102. Using the eddy viscosity distribution of Equation 7 and the non-dimensional vertical coordinate ζ given in Equation 46 the equations governing c_1 are found to be

$$i\sigma c_1 = \begin{cases} a\dfrac{\partial c_1}{\partial \zeta} + \dfrac{\partial}{\partial \zeta}\left[\zeta\dfrac{\partial c_1}{\partial \zeta}\right] & \zeta < a \\[2ex] a\dfrac{\partial c_1}{\partial \zeta} + a\dfrac{\partial^2 c_1}{\partial \zeta^2} & a < \zeta < a/\epsilon \\[2ex] a\dfrac{\partial c_1}{\partial \zeta} + \epsilon\dfrac{\partial}{\partial \zeta}\left[\zeta\dfrac{\partial c_1}{\partial \zeta}\right] & a/\epsilon < \zeta \end{cases} \tag{61}$$

where

$$\sigma = \frac{\omega_1}{\omega_r} \tag{62}$$

and the boundary conditions are

$$c_1 = 1 \quad \text{at} \quad \zeta = \zeta_r = \frac{z_r}{\delta} \tag{63}$$

39

and

$$c_1 \rightarrow 0 \quad \text{as} \quad \zeta \rightarrow \infty \tag{64}$$

103. Equation 61 must be solved in each region and the solutions matched at the levels $\zeta = a$ and $\zeta = a/\epsilon$. For the region $\zeta < a$ the equation is

$$\zeta^2 \frac{\partial^2 c_1}{\partial \zeta^2} + \zeta(1+a)\frac{\partial c_1}{\partial \zeta} - i\sigma\zeta c_1 = 0 \tag{65}$$

104. Comparing this equation with Equation 127 on page 152 of Hildebrand (1976) we see that the solution can be written as

$$c_1 = \zeta^{-a/2} Z_a(i^{3/2} 2\sqrt{\sigma\zeta}) \tag{66}$$

where Z_a is the generalized Bessel function of order a. The solution can be expressed conveniently in terms of Kelvin functions as

$$c_1 = A\zeta^{-a/2}[\text{ker}_a(2\sqrt{\sigma\zeta}) + i\text{kei}_a(2\sqrt{\sigma\zeta})] + B\zeta^{-a/2}[\text{ber}_a(2\sqrt{\sigma\zeta}) + i\text{bei}_a(2\sqrt{\sigma\zeta})] \tag{67}$$

where A and B are constants.

105. For the region $a < \zeta < a/\epsilon$ the equation is

$$a\frac{\partial^2 c_1}{\partial \zeta^2} + a\frac{\partial c_1}{\partial \zeta} - i\sigma c_1 = 0 \tag{68}$$

and the solution can be written as

$$c_1 = Ce^{r_+\zeta} + De^{r_-\zeta} \tag{69}$$

where C and D are constants and r_+ and r_- are found from

$$r_\pm = \frac{-a \pm \sqrt{a^2 + 4i\sigma a}}{2a} \tag{70}$$

106. For $\zeta > a/\epsilon$ the equation is

$$\zeta^2\frac{\partial^2 c_1}{\partial\zeta^2} + \zeta\left[1+\frac{a}{\epsilon}\right]\frac{\partial c_1}{\partial\zeta} - \frac{i}{\epsilon}\sigma\zeta c_1 = 0 \tag{71}$$

and the solution can be written in terms of Kelvin functions as

$$c_1 = E\zeta^{-a/2\epsilon}[ker_{a/\epsilon}(2\sqrt{\sigma\zeta/\epsilon}) + ikei_{a/\epsilon}(2\sqrt{\sigma\zeta/\epsilon})]$$
$$+ F\zeta^{-a/2\epsilon}[ber_{a/\epsilon}(2\sqrt{\sigma\zeta/\epsilon}) + ibei_{a/\epsilon}(2\sqrt{\sigma\zeta/\epsilon})] \tag{72}$$

where E and F are constants.

107. Using the boundary condition that c_1 should vanish as z
becomes very large and noting that the functions ber and bei blow up at
large arguments (Abramowitz and Stegun, 1971) we obtain

$$F = 0 \tag{73}$$

108. The remaining constants A , B , C , D , and E must be
obtained by using the boundary condition at $\zeta = \zeta_r$ and matching the
concentrations and concentration gradients at the levels $\zeta = a$ and
$\zeta = a/\epsilon$.

109. Using the boundary condition of Equation 63 we have

$$A\zeta_r^{-a/2}[ker_a(2\sqrt{\sigma\zeta_r}) + ikei_a(2\sqrt{\sigma\zeta_r})]$$
$$+ B\zeta_r^{-a/2}[ber_a(2\sqrt{\sigma\zeta_r}) + ibei_a(2\sqrt{\sigma\zeta_r})] = 1 \tag{74}$$

The solution of Equation 67, valid for the region $\zeta < a$, is used for the
application of the boundary condition to obtain Equation 74 because it is
assumed that $\zeta_r < a$. If $\zeta_r > a$ Equation 74 should be replaced by a
similar equation obtained by applying the boundary condition of Equation 63
together with the appropriate solution for c_1.

110. Matching the concentrations at $\zeta = a$ from Equations 67 and 69 we
have

$$A(a)^{-a/2}[ker_a(2\sqrt{\sigma a}) + ikei_a(2\sqrt{\sigma a})]$$
$$+ B(a)^{-a/2}[ber_a(2\sqrt{\sigma a}) + ibei_a(2\sqrt{\sigma a})] - Ce^{r+a} - De^{r-a} = 0 \tag{75}$$

41

111. Matching the concentration gradients at $\zeta = a$ from Equations 67 and 69 we have

$$A a^{-a/2-1}\left\{a^{1/2}\sqrt{\sigma}[\ker_a'(2\sqrt{\sigma a}) + i\kei_a'(2\sqrt{\sigma a})] - \frac{a}{2}[\ker_a(2\sqrt{\sigma a}) + i\kei_a(2\sqrt{\sigma a})]\right\}$$
$$+ B a^{-a/2-1}\left\{a^{1/2}\sqrt{\sigma}[\ber_a'(2\sqrt{\sigma a}) + i\bei_a'(2\sqrt{\sigma a})] - \frac{a}{2}[\ber_a(2\sqrt{\sigma a})\right.$$
$$\left. + i\bei_a(2\sqrt{\sigma a})]\right\}$$
$$- r_+ C e^{r_+ a} - r_- D e^{r_- a} = 0 \qquad (76)$$

where the primes, i.e., $\ker'$, denote the derivatives of the functions with respect to their arguments.

112. Equating the concentrations from Equations 63 and 66 at the level $\zeta = a/\epsilon$

$$C e^{r_+ a/\epsilon} + D e^{r_- a/\epsilon} - E\left[\frac{a}{\epsilon}\right]^{-a/2\epsilon}\left[\ker_{a/\epsilon}\left[\frac{2\sqrt{\sigma a}}{\epsilon}\right] + i\kei_{a/\epsilon}\left[\frac{2\sqrt{\sigma a}}{\epsilon}\right]\right] = 0 \qquad (77)$$

113. Equating the concentration gradients at this level we have

$$C r_+ e^{r_+ a/\epsilon} + D r_- e^{r_- a/\epsilon} - E\left\{\frac{\sqrt{\sigma}(a/\epsilon)^{-a/2\epsilon}}{\sqrt{a}}\left[\ker_{a/\epsilon}'\left[\frac{2\sqrt{\sigma a}}{\epsilon}\right] + i\kei_{a/\epsilon}'\left[\frac{2\sqrt{\sigma a}}{\epsilon}\right]\right]\right.$$
$$\left. - \frac{a}{2\epsilon}\left[\frac{a}{\epsilon}\right]^{-a/2\epsilon-1}\left[\ker_{a/\epsilon}\left[\frac{2\sqrt{\sigma a}}{\epsilon}\right] + i\kei_{a/\epsilon}\left[\frac{2\sqrt{\sigma a}}{\epsilon}\right]\right]\right\} = 0 \qquad (78)$$

114. Equations 74 through 78 form five simultaneous equations for the five complex coefficient A , B , C , D , and E. Once these are solved the distribution of c_1 can be found in each region using Equations 67, 69, or 72. The five coefficients are functions of the parameters ζ_r , a , σ , a , and ϵ . Of these a is a fixed model parameter while ζ_r , a , and ϵ can be calculated using the results of the wave current model. σ is the ratio of the frequency of the concentration components ω_1 to the frequency ω_r that was used to define the length scale δ in Equation 33.

115. Figure 5b shows two profiles of the magnitude of the periodic component of concentration with $\sigma = 1$ and $\sigma = 2$. The figure shows that the periodic components decrease more rapidly with increasing z than the

mean concentration. The rate of decrease also increases with increase in the parameter σ (i.e., higher frequency). Figure 5c shows the phase of the two components with respect to the phase of the reference value for each component.

Relationship between the solutions for
the velocity and the concentration

116. As derived in Equation 28 of Part II, the governing equation for a periodic velocity component, u_{w1}, with frequency ω_1 is

$$\frac{d}{dz}\left[\nu_t \frac{du_{d1}}{dz}\right] - i\omega_1 u_{d1} = 0 \tag{79}$$

where u_{d1} is related to u_{w1} by Equation 27.

117. Using the eddy viscosity distribution of Equation 7 and the non-dimensional vertical coordinate ζ defined by Equation 46 the equations for u_{d1} are found to be

$$i\sigma u_{d1} = \begin{cases} \dfrac{\partial}{\partial\zeta}\left[\zeta\dfrac{\partial u_{d1}}{\partial\zeta}\right] & \zeta < a \\[2mm] a\dfrac{\partial^2 u_{d1}}{\partial\zeta} & a < \zeta < a/\epsilon \\[2mm] \epsilon\dfrac{\partial}{\partial\zeta}\left[\zeta\dfrac{\partial u_{d1}}{\partial\zeta}\right] & a/\epsilon < \zeta \end{cases} \tag{80}$$

118. Comparing Equations 80 and 61 shows that Equation 80 can be obtained by setting $a = 0$ in Equation 61. Therefore the solution for u_{d1} in the three regions can be obtained from the solution for c_1 in Equations 67, 69, and 72 by setting $a = 0$ in those three equations. The resulting equations will be the solution for u_{d1} in terms of five unknown coefficients. These coefficients must be found by using the boundary conditions and matching the solution at $\zeta = a$ and $\zeta = a/\epsilon$ just as for c_1.

119. The boundary conditions for u_{d1} are given by

$$u_{d1} = -1 \quad \text{at} \quad \zeta = \zeta_0 = \frac{z_0}{\delta} \tag{81}$$

and

$$u_{d1} \to 0 \quad \text{as} \quad \zeta \to \infty \tag{82}$$

43

120. Equations 81 and 82 are very similar to Equations 63 and 64, which are the boundary conditions for the equation governing c_1 . The only difference is that u_{d1} is set to -1 at $\zeta = \zeta_0$ while c_1 is set to 1 at $\zeta = \zeta_r$. Thus the five simultaneous equations that must be solved to find the coefficients in the solution for u_{d1} will be Equations 74, 75, 76, 77, and 78 with $a = 0$ and the right-hand side of Equation 68 set to -1 instead of 1 , with ζ_0 replacing ζ_r in Equation 68.

121. This similarity between the solutions for the velocity and concentration is useful in writing the program for the wave-current-sediment problem. If the solution for the velocity is required the only changes to the input are that $a = 0$, the reference level is given as ζ_0 instead of ζ_r , and a flag that sets the right-hand side to the correct value.

The Reference Concentration for Sediment in Suspension

122. The boundary conditions of Equations 49 and 63, along with the condition that the concentration should vanish at large z , mean that all the components of the concentration are scaled by the specified reference value near the bottom. This reference value reflects the complicated interaction of the fluid motion with the movable bed——a process that is not well understood. Therefore some of the equations proposed for the reference concentration will be reviewed in this section.

123. Equations 49 and 63 are based on the specification of the bottom boundary condition as a given value of the concentration at some reference level near the bottom. As mentioned in Part II, another condition that has been used is a given upward sediment flux at the reference level. The first type of condition is referred to as the reference concentration condition and is expressed as

$$ c = f_1(T, d) \quad \text{at} \quad z = z_r \tag{83} $$

while the second type is referred to as the pickup or entrainment condition, is expressed as

$$-\nu_t \frac{\partial c}{\partial z} = f_2(\mathcal{T}, d) \quad \text{at} \quad z = z_r \tag{84}$$

124. In Equations 83 and 84 the functions f_1 and f_2 indicate that the specified concentration or flux is a function of the shear stress, $\mathcal{T}$, and the grain diameter, d. The choice of a formulation for the bottom boundary condition has been the subject of discussion in the recent literature. Simple models of bed load processes, such as that of Madsen (1991) outlined later in in this section, indicate that Equation 83 should be used.

125. However, Equation 83 has been criticized because it implies that the reference concentration will vanish if the function on the right-hand side vanishes. This implication is not physically realistic as there will be a continual supply of sediment falling from above, thus ensuring a non-zero value of concentration at the reference level.

126. Soulsby (1991) has examined the difference in the solution for the concentration when these two formulations are applied by using a simple constant-in-depth eddy viscosity model. He showed that the mean concentration profile in steady flow does not depend on which formulation is used.

127. For wave-current flow Soulsby (1991) assumed a simple linear relation with the shear stress for the functions f_1 and f_2 in Equation 83 and 84. He obtained solutions for the mean and time-varying concentration using each of these equations as a boundary condition, for the case of a non-reversing shear stress. By matching the solution for the mean concentration Soulsby (1991) obtained a relation between these two equations.

128. However, when this relation was used for the time-varying concentration it was found that the concentration obtained using the reference concentration formulation was always greater than the concentration obtained using the pick-up condition by a constant factor. This factor was found to increase with increasing frequency and eddy viscosity and decrease with increasing sediment fall velocity.

129. The difference in the solution for the periodic components can be explained by considering the physical meaning of Equations 83 and 84. Equation 83 implies that the concentration at $z = z_r$ changes as a function

45

of the shear stress. The amount entrained into the flow depends only on the value of the eddy viscosity, i.e., the ability of the turbulence to entrain sediment. Equation 84 on the other hand implies that the entrainment itself is a function of the shear stress.

130. Matching the solution for the mean concentration implies that given enough time (approaching zero frequency) the quantity of sediment supplied by Equation 84 is the same as the quantity set by Equation 83. However, when considering periodic (non-zero frequency) components the flow will not have sufficient time to entrain as much sediment from the pick-up condition as from the reference concentration condition. Thus the periodic components will always be smaller when Equation 84 is used with the difference increasing with the frequency. Increased eddy viscosity and decreased fall velocity will also tend to increase this difference because these factors allow the flow to take up greater quantities of sediment through Equation 83 while Equation 84 limits the supply of sediment.

131. Thus the work of Soulsby (1991) shows that while the two formulations can be matched for the mean concentration, they will then give different results for the periodic components. Equation 83 has been selected as the bottom boundary condition for the model presented in this report. This selection is based on the conceptual bed load model of Madsen (1991) which indicates that the shear stress affects the sediment concentration in the bed load layer rather than the flux.

132. It is probable that this equation will show a lower reference concentration than actually exists during the interval where the shear stress decreases due to the effect of sediment settling from above. This error will definitely occur whenever the predicted reference concentration is zero. However this error will be balanced by the error involved in expressing the exact reference concentration as the sum of a few sinusoidal components. As an example, the approximation to the reference concentration in Figure 6 does not vanish while the exact value does.

133. The diffusion equation used to describe the suspended sediment profile is based on the assumption that grain-grain collisions are negligible. This is clearly not valid in the region very close to the bed where the concentration is high and the transport is due primarily to rolling and small jumps rather than to the suspended grains being carried

by the fluid. As a result the transport process has long been considered as taking place due to two mechanisms—bed load transport which takes place very near the bed and suspended sediment transport which takes place in the main body of the flow. The boundary condition for the diffusion equation is applied at the border between the two regions. Since the separation of the flow into these two regions is somewhat artificial this border is not well defined and therefore it must be specified and used consistently.

134. As the sediment that is brought into suspension is entrained from the bed load layer it is apparent that the reference concentration must depend on processes in this layer. Furthermore, while this report is concerned with the development of a model for the transport of susended sediment, it is desirable to have a means of estimating how much bed load transport may take place under the same conditions so that the relative contribution of each component to the total transport can be assessed. Therefore this section will begin with a discussion of a simple conceptual model of bed load transport put forward by Madsen (1991).

Conceptual model of bed load transport

135. Madsen (1991) considered the case of fully rough turbulent flow over a flat sand bed. By assuming that the logarithmic velocity profile was valid very close to the grains he related the fluid velocity seen by the stationary grains to the shear velocity based on the bottom shear stress. A simple force balance between the drag force on a sediment grain and the static friction of the sand bed showed that the initiation of motion was indicated by a constant value of the Shield's parameter, a result that is supported by experimental data.

136. Madsen (1991) then used the equation of motion for a sediment grain rolling on the bed to examine the response of such a grain to changes in the fluid motion. The analysis showed that the response time of grains with diameters in the range commonly found in coastal regions is on the order of 0.1 seconds. This time is much smaller than the wave period, which is the time scale for changes in the external flow under wave conditions. The above result means that the sediment grains can be assumed to react instantaneously to changes in the near bottom flow and that bed load formulations derived assuming steady external flow conditions can be

47

extended to wave dominated conditions by using the shear velocity based on the instantaneous shear stress.

137. A simple model of bed load transport by rolling and sliding grains was derived by balancing the excess bottom shear stress, i.e., the difference between the bottom shear stress and the shear stress required to initiate motion, with the flow resistance due to the moving grains. The resulting expression for the transport was found to be similar in form and magnitude to the empirical bedload transport formula of Meyer-Peter and Muller.

138. Since the idea of transport solely by rolling and sliding is realistic only for shear stresses that are slightly above the critical value for the initiation of motion, Madsen (1991) next considered the case of grain motion by saltation. By simplifying the equation of motion he was able to obtain solutions for quantities such as the jump length, the jump time, and the height of the jump. A balance of the momentum lost by the grains when they hit the bed with the excess shear stress resulted in a transport formula that was once again quite similar to the Meyer-Peter Muller formula.

139. The fact that very similar formulae for the bed load transport resulted from these two quite different conceptual models coupled with the demonstration that the bed load transport reacts very quickly to changes in the mean flow led Madsen (1991) to propose a generalized form of the Meyer-Peter and Muller formula for the calculation of the instantaneous bed load transport under wave-current conditions. This equation relates the non-dimensional bed load transport, $\vec{\Phi}_b$, to the skin friction shear stress by

$$\vec{\Phi}_b(t) = \begin{cases} \dfrac{8}{1\pm\dfrac{\tan\beta(t)}{\tan\phi_m}} \, (|\psi'(t)| - \psi_{cr})^{3/2}\dfrac{\vec{\tau}_b'(t)}{|\vec{\tau}_b'(t)|} & |\psi'(t)| > \psi_{cr} \\[20pt] 0 & |\psi'(t)| < \psi_{cr} \end{cases} \tag{85}$$

140. In this equation $\vec{\tau}_b'(t)$ is the instantaneous skin friction shear stress, $\psi'(t)$ is the Shields parameter based on the instantaneous skin friction shear stress given by

$$\psi'(t) = \frac{|\vec{\tau}_b'(t)|}{\rho(s-1)gd} \tag{86}$$

and ψ_{cr} is the critical Shields parameter for the initiation of motion. In Equation 86 ρ is the density of water, s the specific gravity of the sediment grains, g the acceleration due to gravity, and d the grain diameter.

141. The angle $\beta(t)$ in Equation 85 is the slope of the bed in the direction of $\vec{\tau}_b'(t)$, the positive sign is to be used when $\vec{\tau}_b'(t)$ is upslope and the negative sign when $\vec{\tau}_b'(t)$ is downslope. $\beta(t)$ can be calculated from the maximum bed slope angle β_0 and the angle between the direction of upward slope and the wave direction. ϕ_m is the friction angle of the sediment which for quartz sand is taken as 36° (Madsen, 1991).

142. The concept of skin friction, which will be discussed in a later section in this part, has been introduced here to account for the case of a rippled bed. The non-dimensional transport, $\vec{\Phi}_b$, is related to the dimensional value, $\vec{q}_b$, in units of volume per unit length per unit time, by

$$\vec{\Phi}_b = \frac{\vec{q}_b}{\sqrt{(s-1)gdd}} \tag{87}$$

143. In the calculation of the bed load, $\vec{\tau}'_b(t)$ is calculated from the wave and current skin friction shear stresses derived from the selected skin friction model. The directional instantaneous transport, $\vec{\Phi}_b(t)$, can be calculated from Equation 85. Integration of the components of $\vec{\Phi}_b(t)$ in the wave and wave-normal directions over a wave period will give the net transport in these directions.

144. It should be noted that the conceptual models discussed by Madsen (1991) assume fully rough turbulent flow over a plane bed with negligible intergranular forces. Therefore the predictions made using this equation for rippled beds and for high shear stresses, where grain-grain interactions could be significant, should be viewed with caution.

Reference concentration for steady flows

145. Most of the theoretical development and experimental verification for the reference concentration has been done for steady open channel flow. The most commonly used formulation for unsteady flows is simply an extension of a steady flow approach. Therefore the development of the reference concentration for steady flow will be discussed first.

146. As mentioned above, it is natural to expect the magnitude of the reference concentration, $\bar{c}_r$, for the suspended sediment to depend on the magnitude of the bed transport. Einstein (1950) suggested that $\bar{c}_r$ for steady channel flow be defined by the average concentration in the bed load layer, i.e., by

$$\bar{c}_r = \frac{q_B}{h_T u_B} \tag{88}$$

where q_B is the bed load transport, h_T the height of the bed load layer, and u_B the velocity of the grains in the bed layer. He used his own expressions for these quantities to derive a formulation for the reference concentration.

147. However Equation 88 can be used with any bed load transport formulation that calculates the three quantities on the right-hand side. For example the bed load load formulation of Yalin (1963) assumes that the concentration in the bed load layer is proportional to s' where s' is a measure of the excess bottom shear stress and is given by

$$s' = \frac{\psi'}{\psi_{cr}} - 1 \tag{89}$$

where as ψ' is the Shields parameter based on the skin friction shear stress and ψ_{cr} is the critical Shields parameter for the initiation of motion.

148. Smith (1977) used Yalin's bed load transport equation in Equation 88 to derive

$$\bar{c}_r = \frac{c_b \gamma_0 s'}{1 + \gamma_0 s'} \tag{90}$$

where c_b is the volume concentration of a loose sand bed and γ_0 is an undetermined constant that is known as the resuspension coefficient. The value of c_b is usually taken as 0.65. The term in the denominator was included in order to insure that $\bar{c}_r$ does not exceed c_b when S' becomes very large. However since γ_0 is found to $O(10^{-4}\text{—}10^{-3})$ and S' is $O(10)$ Equation 84 is effectively a linear relationship between S' and the reference concentration.

149. Smith and McLean (1977) used velocity and suspended sediment measurements from the Columbia River to derive a value of 2.4×10^{-3} for γ_0. They set the reference level for the application of Equation 84 to be equal to z_0 where $z_0 = k_n/30$ with k_n being the Nikuradse roughness of the sand grains. If Equation 90 is to be used with their value of γ_0 it is important that this same reference level be used.

150. This formulation of the reference concentration has been widely adopted and many researchers have attempted to verify Equation 90 using data from various types of flows. These comparisons have resulted in γ_0 values ranging from $O(10^{-5}\text{—}10^{-2})$. Several attempts to verify Equation 90 using steady flow data from the laboratory and the field were reviewed by Zettler (1991). He found that some of the analyses done had been inconsistent with the Smith and McLean method in that different reference levels had been used to determine γ_0 and in one case the total bottom shear stress was used instead of the skin friction shear stress.

151. A consistent analysis of some steady flow data was attempted by Zettler (1991). He found that the data did not support the simple relationship of Equation 84. He then conducted a regression analysis allowing the reference concentration to be a function of both the grain size and S'. The reference level was taken as $7d$ where d is the grain diameter. The results of the analysis were plotted as curves of reference concentration against S' for each grain size. It was found that for grain sizes less than about 0.1 mm the relationship between $\bar{c}_r$ and S' was approximately linear with a constant of proportionality that was 3×10^{-4}, 4×10^{-3}, and 2×10^{-2} for grain diameters of 0.04 mm, 0.07 mm, and 0.1 mm, respectively. For grains sizes greater than 0.1 mm the behavior is more complicated with $\bar{c}_r$ decreasing with S' for small values of S'. It

51

should be noted that for the larger grain sizes the experimental values of s' were not very large.

152. The expressions for the bed load transport and the height of the saltating layer derived in the saltation model of Madsen (1991) can be substituted in Equation 90 to derive a formula for the reference concentration. The relation obtained in this fashion shows that the reference concentration is proportional to s'. The constant of proportionality in this equation is weakly dependent on s' and for moderate to large values of the ratio ψ'/ψ_{cr} it is found to be in the range 0.6—1.0×10^{-2}. The height of the saltating layer for these conditions is estimated to be in the range 3—$10 \ d$.

153. In summary, it can be said that while the data do not validate the general applicability of Equation 90, both the data and the conceptual bed load model of Madsen (1991) support the idea of a linear relationship between the non-dimensional excess shear stress, s', and the reference concentration with a constant of proportionality that may depend on the grain diameter. Therefore, it is proposed to adopt a reference concentration equation of the form

$$\bar{c}_r = c_b \gamma_0 s' \tag{91}$$

for the model presented in this report. The value of the resuspension coefficient γ_0 must be determined using field measurements of suspended sediment. The reference level will be taken as $7 \ d$. This reference level is supported by the result for the height of the saltating layer in the bed load model and is also more realistic than the level z_0 used by Smith and Mclean (1977) because z_0 may be less than the grain diameter when the bed form height is small.

Mean reference concentration under waves

154. The discussion so far has considered only steady flows. Glenn and Grant (1987) suggested that the Smith and McLean equation could be used to calculate the mean reference concentration for wave and wave-current conditions. This was based on the demonstration by Grant and Madsen (1982) that sand grains rolling on the bottom, i.e., grains in the bed load layer, would respond to changes in the near-bottom velocity with a time scale that

52

was much smaller than the wave period. Therefore Glenn and Grant (1987) assumed that the instantaneous reference concentration, $c_r(t)$, was given by

$$c_r(t) = \begin{cases} \dfrac{c_b \gamma_0 s'(t)}{1 + \gamma_0 s'(t)} & s'(t) > 0 \\ 0 & s'(t) < 0 \end{cases} \qquad (92)$$

where $s'(t)$ was calculated from Equations 86 and 89 using the instantaneous skin friction shear stress. The mean concentration was obtained by averaging this value over a wave period. They set the reference level at z_0 and set γ_0 to be 0.002, a value that was based on experimental data.

155. There have been some attempts to verify this reference concentration using data from field experiments. Drake and Cacchione (1989) reported the results of a field experiment conducted in about 90 m depth on the California shelf. The mean sediment size ranged from 0.016 to 0.024 mm. Velocity was measured 20, 50, 70, and 100 cm above the bottom and suspended sediment concentrations were measured 190 cm above the bottom using optical methods, and the pressure was measured at a height of 200 cm. The wave-current model of Grant and Madsen (1979) and the suspended sediment model of Glenn and Grant (1987) were used to analyze the data and predict the reference concentrations and shear stresses.

156. The analysis resulted in γ_0 values ranging from 2×10^{-5} to 3×10^{-4}. The observed value of γ_0 was seen to decrease with increasing s' . Drake and Cacchione attributed this to armoring of the bed and to increasing substrate cohesiveness. This variation could equally well be explained by saying that $\bar{c}_r$ is proportional to $s'^{0.9}$ with a constant of about 1×10^{-4}. However the possible sources of error in these estimates, such as the effect of sediment sorting and flocculation and the fact that a single measured concentration is extrapolated to the near-bed level, make such speculation unwarranted.

157. Similar experiments are reported by Wiberg and Smith (1983) and Shi et al. (1985). Using the same models for the wave-current-sediment interaction results in estimates for γ_0 of 1×10^{-5} and $1.4-4.4\times10^{-4}$ from the

two studies. The field experiment reported by Vincent and Green (1990), which will be discussed in greater detail later, yielded estimates of 1— 1.7×10^{-4} for γ_0 but with the reference level set at 2 cm above the bed instead of at z_0 as recommended by Glenn and Grant (1987).

158. As far as the verification of the mean reference concentration recommended by Glenn and Grant (1987) is concerned the results of these field experiments are mixed. On the one hand the trend of decreasing γ_0 with s' observed by Drake and Cacchione is evidence that it is not perfect. However, when considering the widely varying conditions of measurement and the possible sources of error involved, it is encouraging that the estimates of γ_0 fall in the range 1×10^{-5}—4.5×10^{-4}.

159. A major weakness of the first three field experiments is that only a single measurement of the sediment concentration is made and that this is at an elevation above the bottom much larger than the wave boundary layer length scale. This results in the measured concentration being multiplied by a very large factor to obtain the near-bottom value, a procedure which would magnify errors in measurement. The experiment reported by Vincent and Green (1990) had concentration measurements every 1 cm above the bottom. In theory each of these measurements could be used to estimate a value of γ_0 . However the values reported by them are based only on the measured concentration at a height of 2 cm.

Time-varying reference concentration under waves

160. The discussion so far has considered only the reference value for the mean component of the concentration. In order to solve the equations formulated in this chapter a reference concentration is required for the periodic components as well. When specifying the reference value for these components the ratio of the time-varying component to the mean component is of interest in addition to the absolute value of the components because it is this ratio that will determine the significance of the time-varying concentration in the calculation of the mean sediment flux.

161. Madsen (1991) showed that the motion of the sediment grains very near the bottom could be assumed to react instantaneously to changes in the external flow. Therefore Equation 91, which was selected for the calculation of the reference concentration in steady flows, can be extended to the case of unsteady flow in the form

$$c_r(t) = \begin{cases} c_b \gamma_0 s'(t) & s' > 0 \\ 0 & s' < 0 \end{cases} \tag{93}$$

where $c_r(t)$ is the instantaneous reference concentration and $s'(t)$ is the instantaneous value of the non-dimensional excesss shear stress given by

$$s'(t) = \frac{|\psi'(t)| - \psi_{cr}}{\psi_{cr}} \tag{94}$$

In Equation 94 ψ_{cr} is the critical Shields parameter for the initiation of motion and $\psi'(t)$ is the Shields parameter based on the instantaneous skin friction shear stress, $\tau'(t)$, defined as

$$\psi'(t) = \frac{\tau'(t)}{\rho(s-1)gd} \tag{95}$$

Skin Friction Models

162. Most of the reference concentration models discussed in the previous section related the near bed reference concentration to the shear stress at the bed. For a flat bed the only scale for the bed roughness is the diameter of the sediment grains that make up the bed. In this case it is reasonable to expect that the total bottom shear stress, τ_b, will act to mobilize the grains and make them available for suspension.

163. The situation changes when bedforms are present. The bottom shear stress is now the sum of the two components—the form drag due to the ripple shape and the skin friction drag on the ripple surface. The roughness due to the form drag is scaled by the bedform height while the roughness due to the skin friction is scaled by the grain diameter. Since the bedform height is generally much greater than the grain size, the roughness seen by the flow at heights that are much greater than the bedform height will be scaled by the bedform height.

164. However, the entrainment of sediment occurs in a thin bed load layer of a thickness that is usually much less than the bedform height. Therefore it is apparent that the appropriate shear stress necessary to

55

describe this process should be the skin friction shear stress and not the bed shear stress which is dominated by the form drag. Thus the skin friction shear stress must be estimated before using an equation, such as Equation 93, to predict the reference concentration.

165. The values τ_{CW} , τ_W , and τ_C , which are combined wave and current, wave, and current shear stresses, respectively, are calculated using the wave-current model outlined in Part II, which uses the full bed roughness. The equivalent Nikuradse roughness for a movable bed under field conditions can be calculated using the empirical formulae given in Part II. The problem is to estimate the skin friction shear stresses τ_W' and τ_C' , due to the waves and the current respectively. These can then be used to calculate the instantaneous skin friction shear stress.

166. Glenn and Grant (1987) suggested that τ_W' and τ_C' could be estimated by running the wave-current model with the same wave and current specifications but with the roughness taken as the grain roughness. The current was specified for this model by a given value of the mean velocity at an elevation that was usually well above the wave boundary layer.

167. This specification implies that the current velocity calculated with the shear velocities u_{*c} and u_{*cw} , and using the full roughness, should match the specified value. If the same specification is used to calculate u_{*cw}' , and thence τ_C' , using the grain roughness, the value of τ_C' thus obtained would be dependent upon the level at which the current is specified. As this level is usually specified to be well above the wave boundary layer this method of calculating τ_C' is not consistent with the expectation that the skin friction shear stresses should only affect the flow within the boundary layer.

168. One way of removing this inconsistency is to require the matching of the current velocities to be done at the level δ defined in Equation 33. In other words the skin friction current shear stress τ_C' is estimated by running the wave-current model with the original wave specification, the roughness taken as the grain roughness and the current specified to be the value of the mean veloicty at the level $z = \delta$ calculated from the solution to the wave-current problem that used the full roughness.

Formulation of the Instantaneous Reference Concentration
and Calculation of the Suspended Sediment Fluxes

169. The skin friction shear stresses calculated using the procedure described in the preceding section can be used in Equation 88 to obtain the time-varying reference concentration. However, the solution to the governing equation derived in the first section of this part required the specification of the reference concentration as a reference value for each component of the concentration and not as an arbitrary function of time. The derivation of the reference values for each component will be done in this section. The situation considered here will be the case where wave asymmetry is simulated by two wave components in phase with each other, one having twice the frequency of the other. The computer program for this case is given in Appendix B.

170. Equations 93 and 94 can be combined to write the instantaneous reference concentration as

$$c_r(t) = \begin{cases} \dfrac{c_b \gamma_0 (|\psi'(t)| - \psi_{cr})}{\psi_{cr}} & |\psi'(t)| > \psi_{cr} \\ \\ 0 & |\psi'(t)| < \psi_{cr} \end{cases} \tag{96}$$

171. $\psi'(t)$ is the Shields parameter based on the instantaneous skin friction shear stress which can be written as

$$|\psi'(t)| = \frac{|\vec{\tau}'(t)|}{\rho(s-1)gd} \tag{97}$$

where $|\vec{\tau}'(t)|$ is the magnitude of the instantaneous skin friction shear stress vector and is given by

$$|\vec{\tau}'(t)| = [\tau_w'(t)^2 + 2\tau_w(t)\tau_c'\cos\phi_{cw} + \tau_c'^2]^{1/2} \tag{98}$$

with $\tau_w'(t)$ being the instantaneous wave skin friction shear stress, τ_c' the current skin friction shear stress, and ϕ_{cw} the angle between the waves and the current.

172. The hydrodynamic model was extended to include the case of many wave components in Part II. Once the parameters u_{*cw} and δ are defined it was shown that the individual shear stresses and phases could be obtained from Equation 34. As outlined in the previous section the skin friction shear stresses are obtained by using the grain diameter as the equivalent roughness with the current specified as the calculated mean velocity at the level $z = \delta$. For the case of two waves in phase with each other $\tau_w'(t)$ can be written as

$$\tau_w'(t) = \tau_{w1}' \cos(\omega t + \phi_{b1}) + \tau_{w2}' \cos(2\omega t + \phi_{b2}) \tag{99}$$

where τ_{w1}' and τ_{w2}' are the wave skin friction shear stresses for each component and ω is the frequency of the principal component.

173. Substituting from Equations 97, 98, and 99 into Equation 90, the instantaneous reference concentration, $c_r(t)$, can be written as

$$c_r(t) = \begin{cases} c_b \dfrac{\gamma_0 \psi_{w1}'}{\psi_{cr}} [([\cos\theta + r_\tau \cos(2\theta + \phi)]^2 \\ \qquad + 2\mu'^2 [\cos\theta + r_\tau \cos(2\theta + \phi)] \cos\phi_{cw} \\ \qquad + \mu'^4)^{1/2} - r_\varphi] & |\psi'(t)| > \psi_{cr} \\ 0 & |\psi'(t)| < \psi_{cr} \end{cases} \tag{100}$$

where ψ_{w1}' is the Shields parameter based on τ_{w1}', μ' is given by

$$\mu'^2 = \frac{\tau_c'}{\tau_{w1}'} \tag{101}$$

and r_τ, ϕ, and r_φ by

$$r_\tau = \frac{\tau_{w2}'}{\tau_{w1}'} \tag{102}$$

$$\phi = \phi_{b2} - \phi_{b1} \tag{103}$$

and

$$r_\varphi = \frac{\psi_{cr}}{\psi_{w1}'} \tag{104}$$

174. Equation 100 gives the time-variation of the reference concentration. In the formulation presented here we consider only two wave

components, with frequencies ω and 2ω . Therefore, the only components of the concentration that contribute to the time-averaged sediment flux will be those with the same frequencies. These components can be extracted by approximating the instantaneous reference concentration, $c_r(t)$, by

$$c_r(t) \approx \frac{c_b \gamma_0 \psi_{w1}'}{\psi_{cr}}(\bar{r} + r_1\cos(\theta+\phi_1) + r_2\cos(2\theta+\phi_2)) \qquad (105)$$

where θ is the phase of the shear stress τ_{w1}' and is given by

$$\theta = \omega t + \phi_{b1} \qquad (106)$$

175. The coefficients $\bar{r}$, r_1 , ϕ_1 , r_2 , ϕ_2 can be found by expanding Equation 100 as a Fourier series. In the case considered here ϕ in Equation 103 is very small so that τ_{w1}' and τ_{w2}' in Equation 99 are nearly in phase. The result is that ϕ_1 and ϕ_2 in Equation 105 are negligible, i.e., the coefficient of $\sin\theta$ and $\sin2\theta$ from the Fourier expansion are negligible. However, if a different formulation, for example one based on the measurements shown in Figure 1, is used where the peaks of $c_r(t)$ do not coincide with the peaks of τ_{w1}' , ϕ_1 , and ϕ_2 may be important. In this case r_1 and r_2 can be represented by complex numbers to include these phase differences.

176. The three term Fourier expansion of the instantaneous reference concentration of Equation 105 is compared to the exact value given by Equation 100 in Figure 6. The figure shows the reference concentration, normalised by the term $(c_b\gamma_0\psi_{w1}')/\psi_{cr}$, as a function of θ , the phase of τ_{w1}' . In this example μ_1' is 0.35 and the ratios r_φ and r_t are 0.27 and 0.25 respectively, while the coefficients $\bar{r}$, $r1$, and $r2$ are found to be 0.41, 0.17, and 0.36, respectively.

177. The figure shows that the three term approximation of Equation 105 is quite a good approximation of the exact form of Equation 100. The values of the Fourier coefficients show that the periodic components of the reference concentration are comparable to the mean component with the reference value for the secondary component found to be larger than that for the principal component. These differences are due to the assumed time variation of the reference concentration in Equation 100. Since the shear
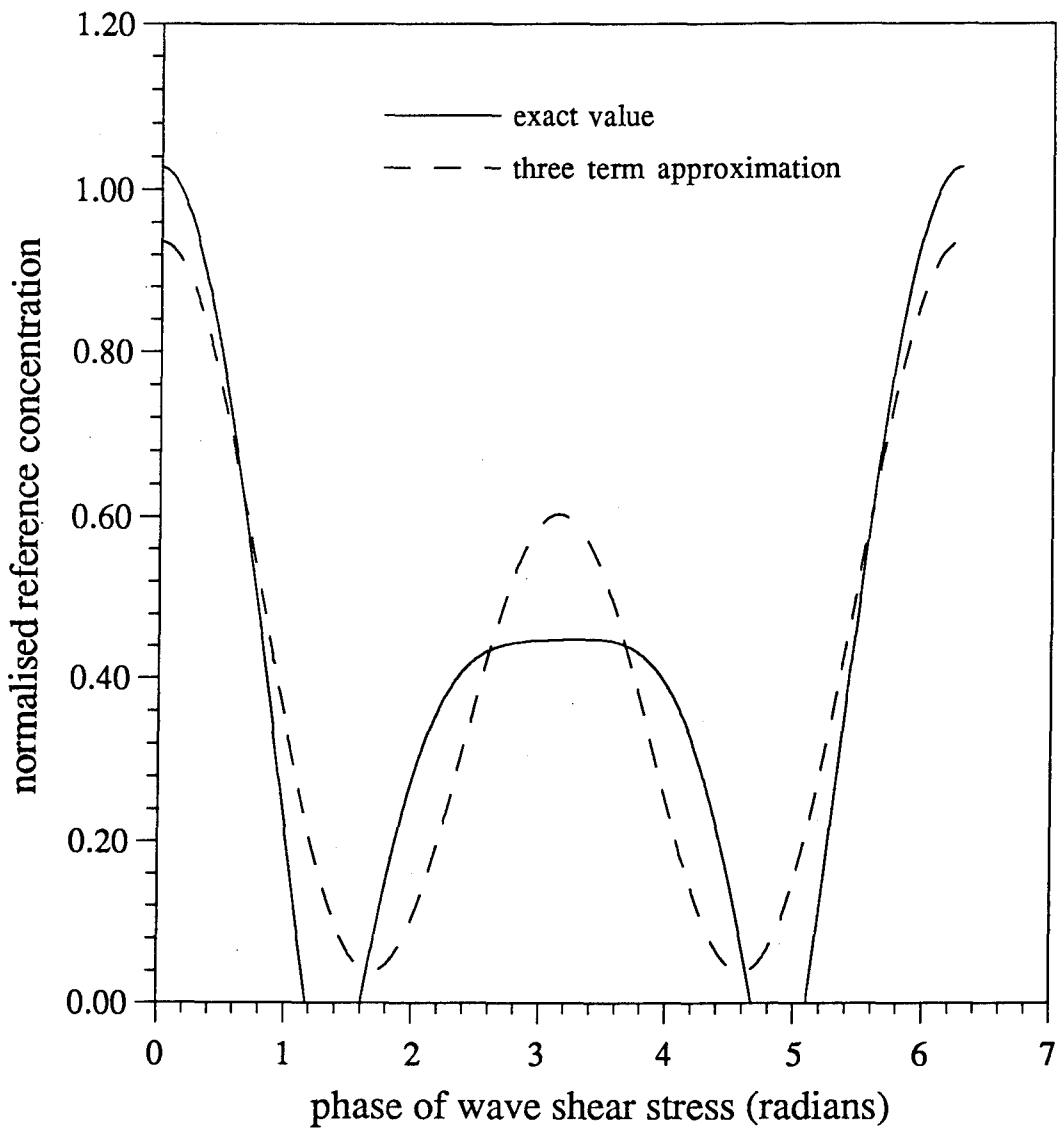
Figure 6. Comparison of the instantaneous reference concentration of
Equation 100 with its three-term approximation in Equation 105.

stress $\tau'(t)$ has two peaks for each wave cycle there will be a pronounced component of frequency 2ω. A component of frequency ω can exist only if there is some asymmetry in the shear stress. In this case, where the wave asymmetry is simulated by two waves, the component of frequency ω is caused both by the wave asymmetry and by the presence of a current.

178. The procedure outlined in this section forms the link between the hydrodynamic and sediment problems. The instantaneous bottom shear stress obtained from the hydrodynamic problem is converted into the instantaneous reference concentration using Equation 96. The reference concentration can then be approximated by the required number of sinusoidal components to obtain the reference value for each component. These values can then be used in the solution derived earlier in this chapter to obtain the concentration at any depth.

179. Once the concentration and velocity distribution are known the flux of sediment, $\vec{T}$, can be found as

$$\vec{T} = \vec{T}_W + \vec{T}_C \tag{107}$$

where $\vec{T}_W$ is the flux due to the time-varying components of velocity and concentration while $\vec{T}_C$ is the flux due to the mean components. $\vec{T}_W$ and $\vec{T}_C$ are denoted as vectors in Equation 107 because the transport caused by the wave and current motions will be in the directions of the wave and current velocity vectors, respectively.

180. $\vec{T}_W$ can be found from

$$\vec{T}_W = \overline{\vec{\tilde{u}}\tilde{c}} \tag{108}$$

where $\vec{\tilde{u}}$ is the wave velocity vector and the overbar denotes the average over the period, while $\vec{T}_C$ is given by

$$\vec{T}_C = \vec{\bar{u}}\bar{c} \tag{109}$$

where $\vec{\bar{u}}$ is the current velocity vector.

181. The calculation of $\vec{T}_w$ in Equation 108 requires the phase difference between the velocity and concentration component. This phase difference can be found because ϕ_1 and ϕ_2 in Equation 105 link the phase of the concentration component to the phase of T_{w1}' , which in turn is linked to the phase of the near-bottom wave velocity through ϕ_{b1} .

Summary of Model Development

182. The present report builds on the work of Madsen and Wikramanayake (1991) and Wikramanayake and Madsen (1990), which dealt with wave-current interaction and movable bed roughness, respectively, to develop a sediment transport model for wave-current flow. The hydrodynamic model, reviewed in Part II, calculates the velocities and relevant bed shear stresses using given wave, current, and sediment characteristics.

183. The sediment transport component of the model was developed in this part. The equations governing the mean and time-varying suspended sediment concentrations were solved. As the concentrations depend on the specific near-bottom reference value, the next step was to select a method that related the bottom shear stress to this reference value. After a review of proposed models the relatively simple model of Equation 93, which related the reference concentration to the excess skin friction shear stress, was selected. The level at which the boundary condition is to be applied was chosen as seven times the grain diameter. The procedure for the calculation of the skin friction shear stress in wave-current flows was also given, as was a simple formulation for the bed-load transport.

184. The sediment transport model thus developed is completely deterministic except for the value of the resuspension coefficient, γ_0, of Equation 93. Once this parameter is known it is possible to calculate the suspended sediment concentration and flux, given the wave, current, and sediment characteristics. Therefore the next part of the report will be the determination of an appropriate value for the resuspension coefficient. It must be remembered that the value of γ_0 that is derived in the next part is valid only for the reference concentration model selected in this report, i.e., Equation 93, with the reference level of 7d and the skin friction shear stress calculated as outlined above. The use of the model

for calculation of sediment transport will be fully detailed in Part V and Appendix B.

PART IV : DETERMINATION OF THE RESUSPENSION COEFFICIENT γ_0

185. The only undetermined parameter in the suspended sediment model developed in Part III is the resuspension coefficient, γ_0 . The conceptual model of bed load transport developed by Madsen (1991) indicates that γ_0 lies in the range $6-10 \times 10^{-3}$. However, the conceptual model was developed for the restricted conditions of relatively low shear stress, where intergranular collisions are negligible, acting on a flat bed. Since the sediment suspension model is to be used for both rippled beds and sheet flow, where grain-grain interactions are significant, a value of γ_0 that is correct for these conditions is required. Due to the complicated nature of fluid-sediment interactions, it is not possible to derive a theoretical expression for the reference concentration under these conditions. Therefore the only way to obtain a value for γ_0 is by comparing the model predictions to experimental measurements.

186. Experimental measurements of the suspended sediment concentration under wave and wave-current conditions have been made in the laboratory and the field. Laboratory measurements have the advantage over field measurements in that they are made under well-controlled hydrodynamic conditions. Furthermore the sediment size and grading can be controlled and the bedforms observed during the experiments.

187. However, the range of wave and current conditions that can be realized in the laboratory is limited by the size of the apparatus. Wikramanayake and Madsen (1990) compared the dimensions of sand ripples generated under laboratory and field conditions and showed that there were significant differences in the geometries. These differences appeared to be caused by the longer wave periods seen in the field. Most of the recent measurements of instantaneous suspended sediment concentration have been made in the field. Many of these experiments have used acoustic backscatter sensors, which can make non-intrusive measurements close to the bed. It will be shown later in this part that the errors involved in the determination of γ_0 increase as the height of the measurement increases. For these reasons, and bearing in mind that the ultimate applications of the model will be for field conditions, the determination of γ_0 in this part will be done using field data.

Description of the Data Sets

188. The data sets to be used are those of Vincent and Green (1990), Wright et al. (1991), Hanes (1991), Bedford et al. (1990), and Vincent.[1] The cooperation shown by Drs. C. Vincent, P. Osborne, L. D. Wright, K. D. Bedford, and D. Hanes in giving us access to these data is acknowledged with gratitude. Some general information about each field site and the instrumentation is given in Table 1. All measurements were made outside the surf zone above sandy beds.

189. The data sets will be referred to by the code letters given in the table. The code letters VG , CW , CC , DK , and MB refer to the data of Vincent and Green (1990), Vincent,[1] Hanes (1991), Wright et al. (1991), and Bedford et al. (1990), respectively.

190. **The horizontal velocity in the experiments was measured by an electromagnetic current meter (EMCM) that measured two components of the velocity that were at right angles to each other. Wright et al. (1991) used a series of optical backscatter sensors (OBS) placed at different heights above the bottom to measure the instantaneous suspended sediment concentration, while the other investigators used acoustic backscatter sensors (ABS) to measure the instantaneous concentration.**

191. **OBS devices use a light source together with a sensor that records the backscattered light to make a point measurement of the suspended sediment concentration. The calibration of such sensors is described by Kim (1990). The ABS instrument utilizes the sound scattered by the sediment in suspension. The sound emitter and the measuring transducer are usually placed about 60-100 cm above the bed. A very short pulse of high frequency (1-5 MHz) sound is emitted and the backscattered signal recorded. By recording the scattered sound at several discrete times it is possible to estimate the concentration at several distances (range bins) from the instrument with the same pulse. The results of several closely spaced (within a few microseconds) pulses is averaged to obtain an estimate of the instantaneous concentration at each range bin. The interpretation of these**

---

[1] Personal Communication, 1990, C. E. Vincent, Professor, University of East Anglia, U.K.

Table 1

Site Location and Instrumentation for the Field Data Sets

Investigator	Location of site	Code	Velocity measurement	Concentration measurement	Frequency of sampling (Hz)	Duration of burst (min)
Vincent and Green (1990)	Holkham, UK	VG	EMCM at 20 cm	ABS every 1 cm	1.72	12.4
Vincent and Osborne (1991)	Cornwall, UK	CW	EMCM at 10 cm	ABS every 0.5 cm	4.22	4.2
Hanes (1991)	Cape Canaveral, FL	CC	EMCM at 15 cm	ABS every 0.5 cm	4	8.5
Wright et al. (1990)	Duck, NC	DK	EMCM at 20 cm	OBS at 15,35,65,105 cm	1	17.1
Bedford et al. (1989)	Mobile, AL	MB	EMCM at 114 cm	ABS every 1.16 cm	1-concentration 2-velocity	10

measurements and the calibration of ABS instruments is discussed by Thorne et al. (1991).

192.   Both the OBS and ABS instruments have been estimated to have an error of 10% under ideal conditions though this error may be much larger under field conditions. The advantages of the ABS over the OBS are that it does not disturb the flow and that it can measure the concentration at several points simultaneously. For these reasons it is possible to make measurements much closer to the bed with an ABS than is possible with an OBS.

193.   Table 2 shows the mean depth and grain diameter for each data set along with a description of the data obtained for this study. The quantities u and v in Table 2 are the horizontal velocities measured by the two-axis EMCMs in the experiments. It was possible to obtain the full time series for velocity and concentration only for the data sets CW and DK . However the method used to determine the value of γ_0 in this part requires only the mean of the measured concentration, the mean velocity, and a representative wave velocity and period. Therefore all the data sets in Table 2 could be used to calculate γ_0 .

Procedure to determine γ_0

194.   The data sets described above are to be used to determine γ_0 which is the constant of proportionality in Equation 93. Averaging both sides of this equation over a time that is large compared to the wave period results in

$$\bar{c}_r = c_b \gamma_0 \overline{s'}$$ (110)

which relates the time-averaged concentration at the reference level of $z_r = 7d$ to the time-averaged value of s' . The time-averaged value of s' can be computed from the solution to the hydrodynamic problem that is outlined in Parts II and III. Therefore if the mean concentration at the reference level can be measured γ_0 can be determined very easily from Equation 110.

67

Table 2.

Description of Available Measurements from the Field Experiments

Data set code	Number of runs available	Data Available Concentration	Data Available Velocity	Bed Condition	Mean depth (m)	Mean Grain diameter (cm)
VG	2	c̄ every 1 cm	ū, v̄ at 20 cm significant wave velocities at 20 cm	rippled	1.8	0.023
CW	1	c(t) at 4.22 Hz every 0.5 cm	u(t), v(t) at 10 cm	rippled (geometry measured)	1.75	0.03
CC	6	times series of c(t) averaged between 0.5 and 4.5 cm	u(t), v(t) at 15 cm	flat bed	2.0	0.18
DK	11	c(t) at 15, 35, 60, and 105 cm	u(t), v(t) at 20 cm	not observed	8.1	0.01
MB	12	c̄ every 1.16 cm	ū, v̄ at 114 cm significant near bottom wave velocity	not observed	5.7	0.023

68

195. However measuring the concentration at the reference level selected in this model, which is very close to the bed, is extremely difficult. The only available alternative is to estimate the concentration at the reference level using the measured mean concentration at a higher level. This estimation is done using the solution for the mean concentration given by Equations 50, 52, and 54 . The parameters a , ϵ , and δ that appear in these equations can be calculated using the solution to the hydrodynamic model.

196. It should be noted here that Figure 3a shows that the mean concentration decreases quite rapidly with height above the bottom. The estimation of the concentration at the reference level from a measured mean value will therefore be a process of magnification. Any errors in the measured mean value will be magnified by a corresponding amount. Furthermore, small changes in the parameters a , ϵ , and δ could result in large changes in the estimated value. The potential for error is particularly large in the case of the parameter a , the ratio of the sediment fall velocity to the shear velocity defined in Equation 48, because it appears as an exponent in Equations 50, 52, and 54.

197. The functional form of these equations, and also the curve in Figure 3a, indicate that the possible error in the estimation of the concentration at the reference level increases with the height from which the estimation is made. Therefore it is desirable to use data sets where the concentration was measured as close to the bottom as possible. It was mentioned in Part II that a major drawback of many previous measurements used to determine γ_0 was the relatively large height--sometimes as much as 2 meters above the bottom--at which the concentration was measured.

198. Some researchers, for example Hill et al. (1988), have attempted to avoid the estimation of concentrations very close to the bed by defining the reference level to be the level of the lowest concentration measurements. However, definition of the reference level in this way is quite arbitrary and has no physical relation to the level dividing the bed load and suspended load regions, unlike the reference concentration model used in this report. Furthermore, as this definition is not related to the boundary layer length scale δ , which scales the variation of the concentration, the values of γ_0 derived in this manner will depend on the

hydrodynamic conditions of each particular data set and will not be generally applicable.

199. The estimation of the reference concentration requires that the hydrodynamic problem be solved first. The input values needed for the hydrodynamic model are the wave and current conditions and the sediment properties. In the data sets selected here, there is only one measurement of the velocity. Thus the current is simply specified by the measured mean velocity at the level of the current meter. All the researchers have reported the mean grain diameter. Vincent and Green (1990) measured the fall velocity of the bottom sediment. The fall velocity for the other data sets can be calculated from the empirical relation given by Madsen and Grant (1976).

200. The complete time series of the horizontal velocity in two directions at right angles to each other was obtained for the data sets CW , CC , and DK . The wave direction was defined as the direction in which the variance of the instantaneous velocity was the greatest. The angle between this direction and the direction of the mean velocity was taken as the angle between the wave and current directions, ϕ_{CW} . For the other data sets ϕ_{CW} was taken to be the given value.

201. The final requirement is to represent the irregular wave motion observed in the field by one or more periodic components. The simplest method is to use a single wave component, u_{br} , that is related to the power spectrum of the observed wave record, S_{ub} , by

$$u_{br} = \sqrt{2 \int S_{ub} d\omega}$$

(111)

202. Representing the wave motion by a single component neglects wave asymmetry, a feature that is present in velocity records obtained in shallow water. For example, consider the velocity record shown in Figure 2, which is a portion of the cross-shore velocity time series of data set CC1 . The record has a strong positive skewness with a coefficient of skewness of 0.52 . It is probable that the asymmetry of the wave motion would be important when considering the suspended sediment transport due to the periodic components. One way to represent the asymmetric wave motion is by considering two wave components, u_{b1} and

70

u_{b2} , that are in phase, with u_{b2} having twice the frequency of u_{b1} . The magnitudes of u_{b1} and u_{b2} can be obtained by analyzing the velocity record on a wave-by-wave basis as done by Vincent and Green (1990). The analysis results in a set of positive and negative peak velocities for each wave. The representative positive and negative wave velocities, u_{bp} and u_{bn} , are taken as the root-mean-square value of each set. The magnitudes of u_{b1} and u_{b2} are then found by

$$u_{b1} = \frac{u_{bp} + u_{bn}}{2} \tag{112}$$

and

$$u_{b2} = \frac{u_{bp} - u_{bn}}{2} \tag{113}$$

203. For the data sets for which the full velocity time series was available (CW , CC , and DK) it is found that u_{b1} obtained from Equation 112 was quite similar to u_{br} obtained from Equation 111. The total wave energy for the single wave and the two wave representations was also nearly the same. These results show that the representation of the wave motion by u_{b1} and u_{b2} calculated from Equations 112 and 113 preserves the observed wave energy while accounting for some of the observed wave asymmetry.

204. The most elementary method of selecting the period of the representative wave is to specify it as the peak period of the power spectrum of the velocity record. However, this method is not suitable when the spectrum is not narrow banded. Figure 7 shows the velocity spectrum for data set CC1 . The peak period of this spectrum is about 8 seconds (0.125 Hz). It may appear that the spectrum in Figure 7 shows a wave motion consisting of an 8-second principal wave and its higher harmonics. However, analysis of the velocity record for this data sets shows a zero down-crossing period of 3.5 seconds, a result that does not support this hypothesis. Therefore it can be concluded that the peak period is not a good representative value for the spectrum.

205. Madsen (1992) showed that the representative frequency, ω_r , for the interaction of a current with an irregular wave motion was given by
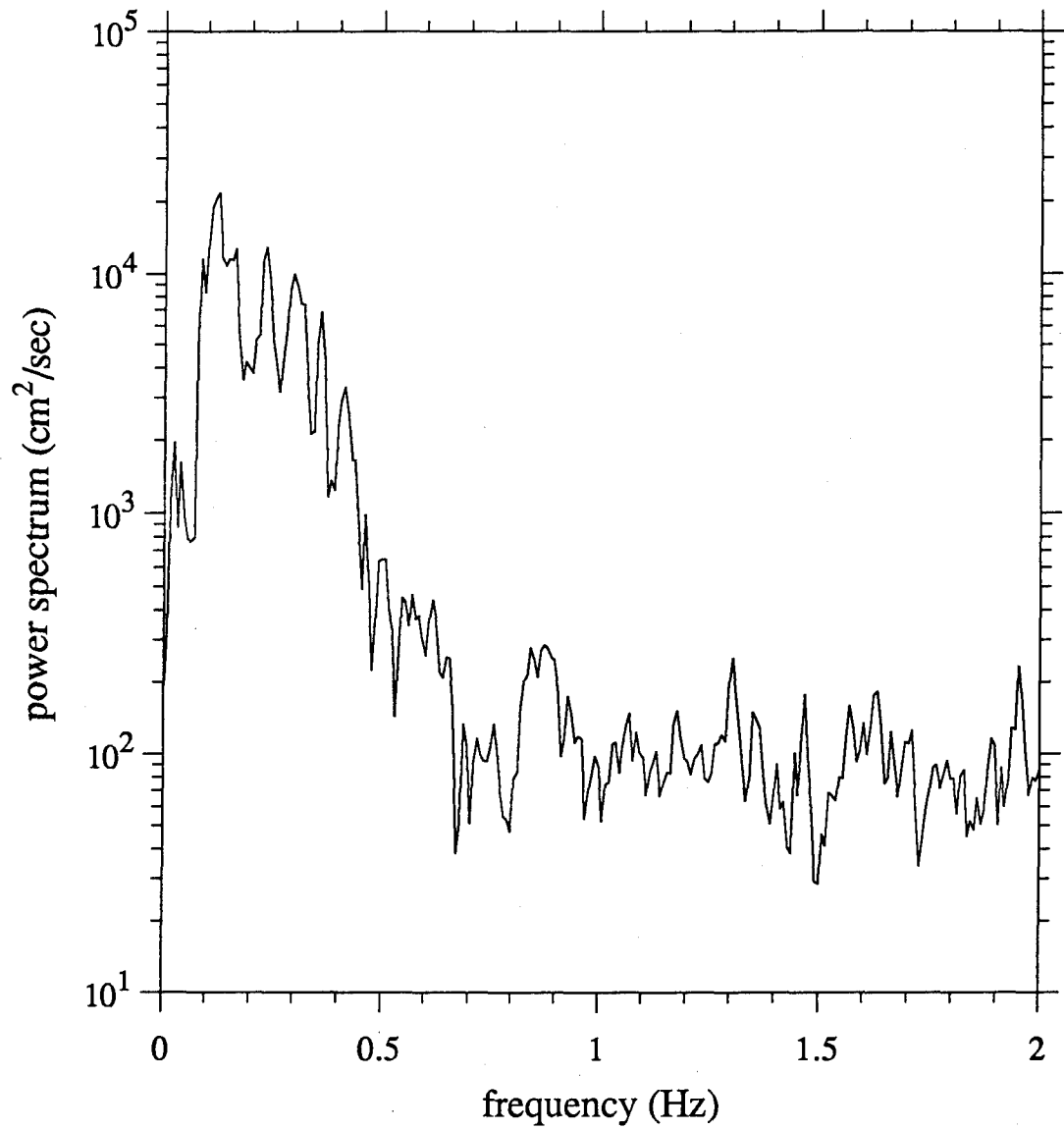
Figure 7. Power spectrum of wave velocity for data set CC2 .

$$\omega_r = \frac{\int S_{ub}\omega d\omega}{\int S_{ub}d\omega} \qquad (114)$$

where S_{ub} is the power spectrum of the wave velocity. Use of Equation 114 for the spectrum shown in Figure 7 results in a period of 3.8 seconds (0.26 Hz), which is obviously a much better representative value than the peak period.

206. Vincent and Green (1990) have given the wave period as the zero-downcrossing period from their wave-by-wave analysis of the velocity record. For the sets CC , CW , and DK it was found that Equation 114 gave nearly the same value for the wave period as the zero-downcrossing period. Therefore it seems reasonable to use the wave periods given by Vincent and Green (1990) when analyzing their data. The periods given by Bedford et al. (1990) for the MB data set was the peak period. In these sets however, inspection of the velocity spectra in Bedford et al. (1990) shows that the Equation 114, which gives the period of the centroid of the spectrum, would have given wave periods similar to the peak period.

207. The ranges of wave and current parameters for each data set to be used to solve the hydrodynamic model are given in Table 3. The table shows that the analysis of the velocity records for the data set DK resulted in very small values of u_{b2} . This result is expected as this data set was obtained in relatively deep water (8 m) where the effects of wave non-linearity--which is the cause of wave asymmetry--are negligible. The only wave information available for the MB data set was the significant wave velocities. The values in Table 1 were obtained by dividing the given velocities by a factor of $\sqrt{2}$ to obtain a representative velocity that corresponds to the definition of Equation 111.

208. The details of the calculations are described in Part V. In this part the main concern is to use the calculated shear velocities to extrapolate the measured mean concentrations down to the reference level so that γ_0 can be found from Equation 110. In the case of the CC data set, where available information is the average concentration between 0.5 cm and 4.5 cm, the calculated concentration is averaged between these two levels assuming $\gamma_0 = 1$ and the true value of γ_0 obtained by dividing the measured value of the average concentration by the calculated value using

73

Table 3.

Input Parameters for the Wave-Current-Sediment Model from the Data Sets used to Determine γ_0

Data Set	Uh1 (cm/s)	Uh2 (cm/s)	T (s)	Specified current velocity (cm/s)	Level of current specification (cm)	Mean grain diameter (cm)	Fall Velocity Measured (cm/s)	Calculated (cm/s)
VG	34.7-35.0	7.4-7.8	5.8-5.9	14.8-18.0	20	0.023	2.25	
CW	27.7	7.5	5.2	4.7	10	0.03	--	4.0
CC	47.4-62.9	7.7-15.0	3.5-5.4	19.8-37.0	15	0.018	--	1.95
DK	30.3-47.6	0.4-1.1	5.9-8.2	7.4-35	20	0.01	--	0.80
MB	19.7-31.0	--	5.6	15.8-23.9	114	0.023	--	2.78

74

$\gamma_0 = 1$. It should be noted here that even though the bottom ripple
geometry was measured for data set CW , it is not used in the initial model
calculations. This is because the model is developed as a fully predictive
model with the ripple geometry calculated as part of the solution of the
hydrodynamic problem.

Results of the Calculations

209. Some of the results of the hydrodynamic model for the various data
sets are given in Table 4. Ranges have been given for the sets that
included more than one run. The model predicted a rippled bed for the sets
VG , CW , MB , and one run of set CC while a flat bed was predicted for
the remaining five runs of CC and the set DK . However, Hanes (1991)
reported a flat bed for all the runs in the set CC . The value of the
parameter Z in Equation 36, which was used to calculate the ripple
height, was 0.17 . This value is very close to 0.18 which is the upper
limit for ripples observed in the field.

210. The calculated ripple height for the set CW was 1.6 cm while
Vincent and Osborne (personal communication) report a ripple height between
3 and 4 cm, i.e., the predicted ripple height is too low by a factor of
about 2. This error is comparable to the relative error of Equation 36,
which is 1.84. These differences between the observed and predicted
bedforms demonstrate the need for independent measurement of the bedforms
in field experiments.

211. As described earlier, each measurement of the mean concentration
can be used to obtain an estimate of γ_0 . The values of γ_0 obtained from
the two runs of the set VG , named VG2046 and VG2047 , respectively, are
plotted in Figure 8. The figure shows the values of γ_0 on the horizontal
axis while the vertical axis indicates the level of the measured mean
concentration from which the estimate was made. The estimates of γ_0
cluster around the value 1×10^{-3} in the region near the bottom and then
increase with increased elevation of the measuring point.

212. If all the estimated values of γ_0 had been the same it would
have meant that the predicted mean concentration profile has exactly the
same shape as the measured profile. The increase in γ_0 with height

75

Table 4

Some Important Output Parameters of the Hydrodynamic Model for the Data Sets Used to Determine γ_0

Data set	Current shear velocity u_{*c} (cm/s)	Combined shear velocity u_{*cw} (cm/s)	Boundary layer length scale δ (cm)	Shields parameter based on wave skin friction stress ψ'_w	Critical Shields parameter ψ_{cr}	Non-dimensional parameter for ripple geometry Z	Calculated ripple height η (cm)
VG	2.0-2.3	6.84-6.86	2.53-2.58	0.217	0.046	0.062	0.68-0.71
CW	1.1	6.0	2.0	0.123	0.040	0.023	1.62
CC	2.3-3.1	5.2-6.8	1.3-2.3	0.40-0.61	0.055	0.17-0.32	5 runs flat bed 1 run 0.25-cm ripples
DK	0.7-2.2	2.6-4.1	1.1-1.5	0.26-0.53	0.092	0.27-0.54	flat bed
MB	1.3-1.9	4.7-6.0	1.7-2.2	0.063-0.125	0.046	0.018-0.036	1.2-1.7
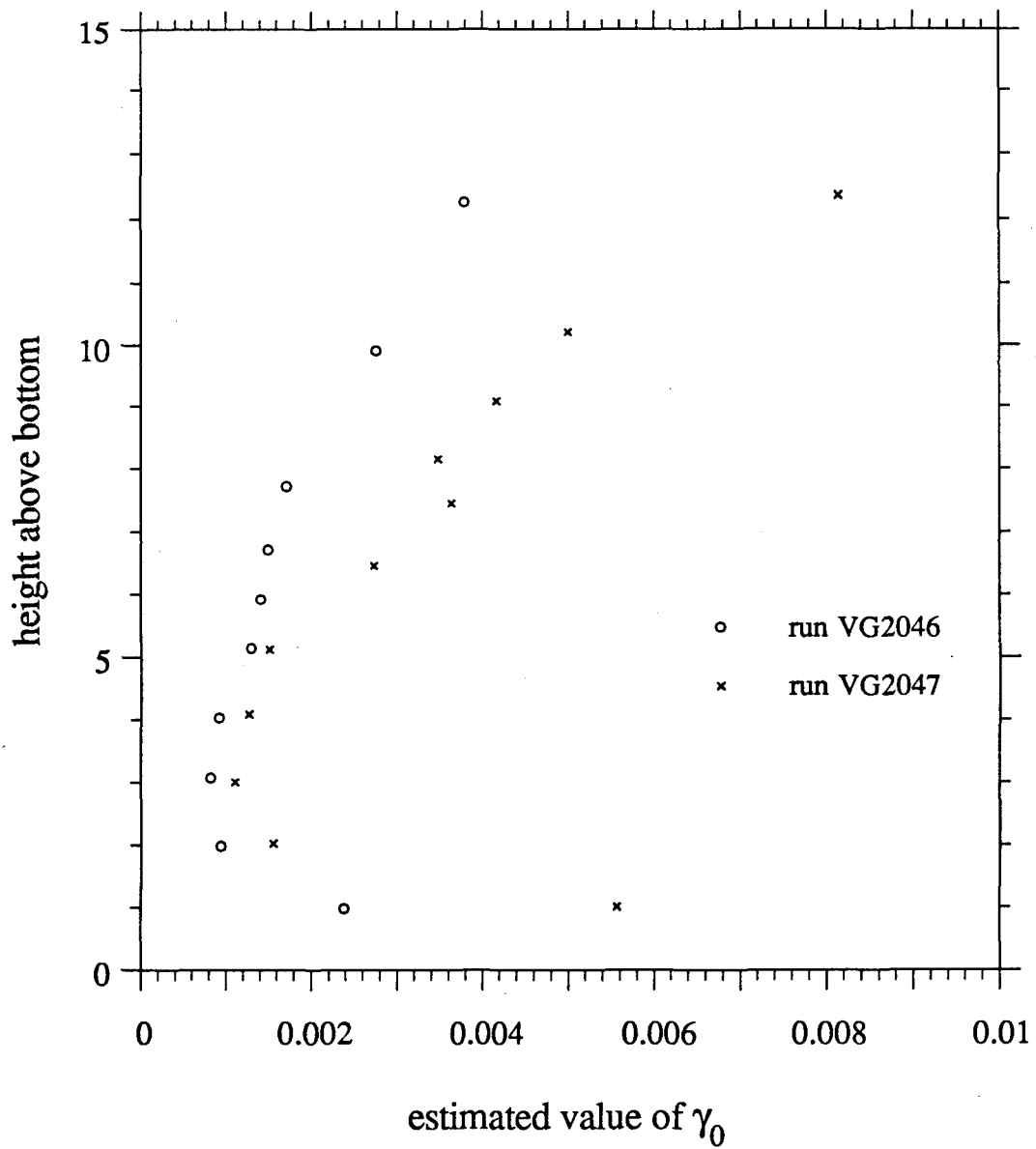
Figure 8. Variation of the estimated values of γ_0 with the height of the measurement for runs 2046 and 2047 of data set VG .

indicates that the predicted profile decreases with height more rapidly than the measurements. This difference in the profiles can be seen in Figures 15 and 16 of Part V where the profiles are discussed in detail. The most probable cause of this difference is the presence of many different grain sizes in the bed.

213. The reference concentration model of Equation 93 assumes that γ_0 is a constant and therefore it is necessary to select a single value of this parameter. As discussed earlier, the uncertainties in the estimates of γ_0 increase with the elevation of the measuring point. Thus it appears that γ_0 should be estimated from the lowest measuring points. However, Vincent and Green (1990) point out that due to the uncertainty in the bed level the real elevation of the measuring points is not precisely known. The effect of this uncertainty will be the greatest for the lowest points.

214. Therefore it is decided to select γ_0 by taking an average of the estimates from the lowest set of measurements. The upper limit of this set will be taken as twice the boundary layer length scale, δ. From the values in Table 4 it is seen that the upper limit is about 5.1 cm for the set VG , so that the lowest five points will be included for the two runs shown in Figure 8. This upper limit was chosen to include as many points as possible while excluding the region over which γ_0 shows a rapid increase with height. The boundary layer length scale is the appropriate choice because it is this length that controls the decrease of the predicted concentration. For the runs VG2046 and VG2047 the estimates of γ_0 in this subset are in the ranges 0.83-2.4×10^{-3} and 1.1-5.6×10^{-3}, respectively, with means of 1.3×10^{-3} and 2.2×10^{-3}.

215. Figure 9 shows the estimates of γ_0 for the single run of data set CW . As the predicted ripple height was too low by a factor of two, another calculation was done using a fixed bed roughness of 14 cm--a value that is based on the observed mean ripple height of 3.5 cm. Both sets of estimates increase with the height of the measurement and the estimates made using the predicted roughness (6.4 cm) increase more rapidly than those made using the observed roughness.

216. As in the case of the VG data set the increase in the γ_0 estimates with height is due to the predicted mean concentration profile decreasing more rapidly than the measured profile, as shown in Figure 17 of
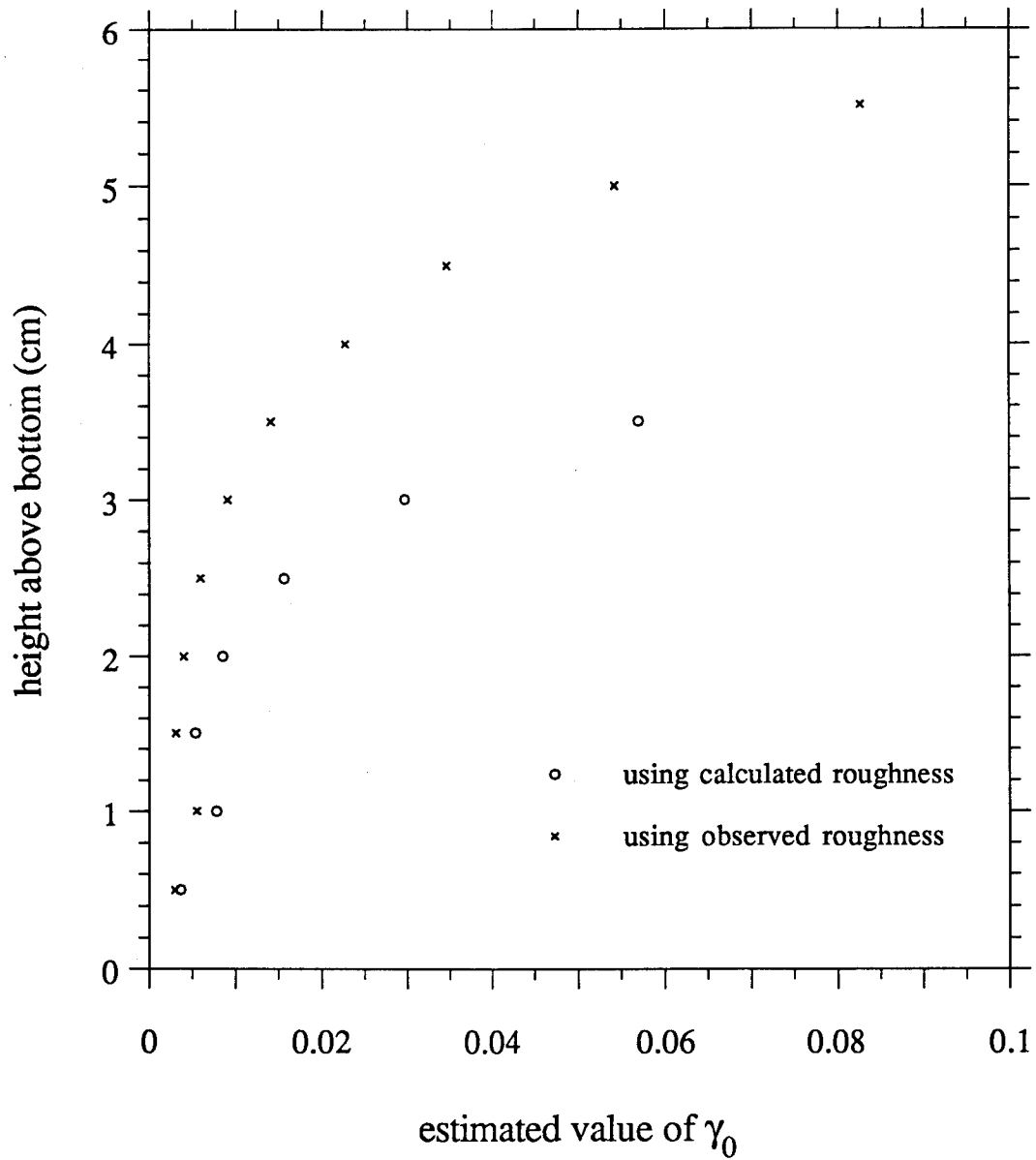
Figure 9. Variation of the estimated values of γ_0 with the height of the measurement for the data set CW using both the calculated and observed roughness

Part V. When the predicted roughness, which is too low, is used the shear velocity and therefore the eddy viscosity will be smaller than if the observed roughness is used. The lower eddy viscosity leads to a more rapid decrease of the mean concentration and a correspondingly more rapid increase in the predicted values of γ_0.

217. The boundary layer length scale, δ, for the CW set is 2.4 cm using the predicted roughness and 2.3 cm using the observed roughness. Using the same region, up to 2δ, as for the VG data set to obtain an average value of γ_0 results in mean values of 8.0×10^{-3} and 2.9×10^{-3}, from ranges of 2.6–22.5×10^{-3} and 1.5–5.8×10^{-3}, for the runs using the predicted and observed roughnesses, respectively. If only the values at heights less than δ are used the estimates of γ_0 reduce to 3.3×10^{-3} and 2.0×10^{-3} for the two roughnesses.

218. The sediment fall velocity for the VG data set was measured by Vincent and Green (1990) while that for the CW data set was obtained from the relationship between the grain diameter and the fall velocity. The fall velocity, through the parameter a defined in Equation 48, is one of the most important factors controlling the vertical variations of the concentration profile. Therefore the estimates of γ_0 from the VG set are probably more reliable, particularly when estimating γ_0 from the higher measurement points. For this reason the estimate of γ_0 for the CW set will be made from the points lower than δ and not 2δ as in the case of the VG set. As the measurements are made every 0.5 cm there will still be four points in this region while the points that show a rapid increase will be neglected. Furthermore, as the purpose of the calculations here is to derive as accurate a value of γ_0 as possible, the estimates obtained using the observed roughness will be used.

219. Thus the three estimates of γ_0 from the two runs of the set VG and the single run of set CW are 1.3×10^{-3}, 2.2×10^{-3}, and 2.0×10^{-3}, respectively. The mean of these three values is 1.8×10^{-3} which is proposed as a value of γ_0 that is appropriate for rippled beds. The other data set that was predicted to have a rippled bed, in addition to those considered here, was the MB data set. However, as discussed below, it was found that the calibration of the ABS instrument in this experiment was done in such a manner that the observed near bottom concentrations, which are critical in

determining γ_0 , may have been incorrect. Therefore the results from this data set were not used.

220. The estimated γ_0 values from the six runs of data set CC are plotted in Figure 10, with ψ_w' , the Shields parameter due to the wave skin friction shear stress, on the horizontal axis. It should be recalled here that only one estimate is possible for each run because only an average concentration between 0.5 cm and 4.5 cm was available. The single + symbol shows the value of γ_0 that would have been obtained from run CC4 if the ripple roughness predicted by Equation 36 had been used. However, as the bed had been observed by Hanes (1991) to be flat for all the runs, it will be the estimates shown by the O symbols, obtained using a flat bed roughness of $k_n = 10\ d$, that will be used in this study. It should be noted that Table 4 shows the range of δ in these runs to be 1.3 cm to 2.3 cm so that the estimates are made using measurements in the region below 2δ to 3.5δ . This region is similar to the region considered for the VG data set.

221. Figure 10 shows that the estimated γ_0 values decrease with increasing ψ_w' . Such a decrease in γ_0 was also observed by Drake and Cacchione (1989) from the results of their field experiment and attributed by them to bed armoring. However, bearing in mind the small number of runs considered here and the many uncertainties in these estimates, it seems reasonable to adopt the mean value as an estimate of γ_0 for flat bed conditions. Therefore it is proposed that 1.8×10^{-4} is an suitable value for flat bed conditions.

222. The 11 runs of data set DK yielded estimates for γ_0 in the range 1.8×10^{-2} to 4.2×10^2. However, it is seen from Tables 1 that the lowest measurement point for this set is 15 cm while Table 4 shows that boundary layer length scale, δ , ranges from 1.1 cm to 1.5 cm. In other words the estimates are made from at least 10δ for the lowest point and as much as 100δ for the highest measuring point at 105 cm. At these large heights it is very probable that the mean grain diameter of the bottom (given as 0.01 cm) is no longer representative of the sediment that is in suspension. Therefore estimates of γ_0 made using the given mean diameter are likely to be very unreliable.
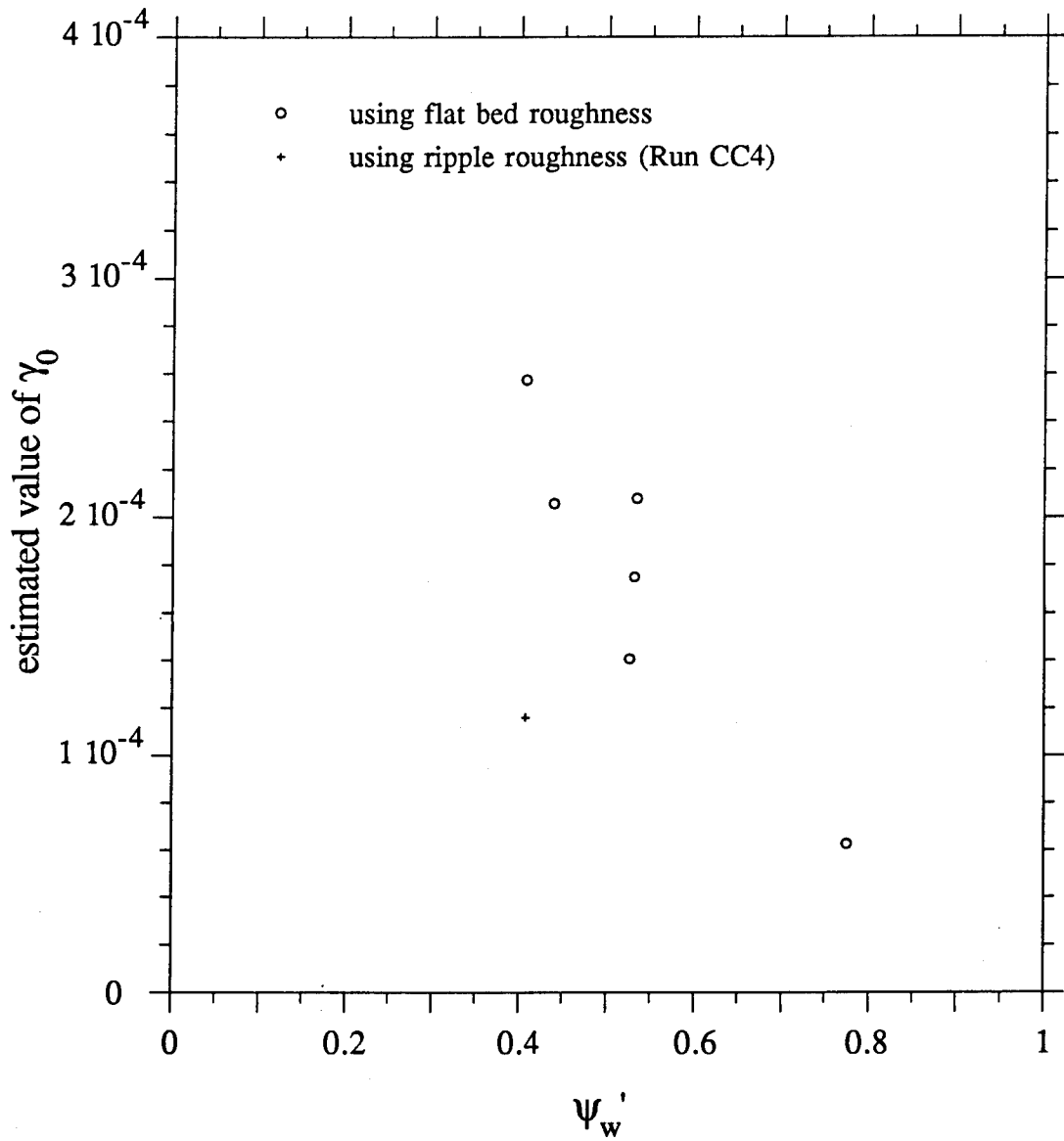
Figure 10. Variation of the estimated values of γ_0 with ψ_w' , the Shields parameter based on the wave skin friction shear stress, for the six runs of data set CC .

223. This point is illustrated by the comparison of the predicted and calculated mean concentration profile for run VG2046 given in Figure 15 of Part V. The figure shows that the predicted value at 15δ (which is about 37.5 cm for this run) is less than the measured value by more than an order of magnitude. Thus if the estimation of γ_0 had been done using the value measured at this height the estimated value would be greater than the value obtained from the near bottom points by the same amount. For this reason it appears that the DK data will not give estimates of γ_0 as reliable as the near bed measurements of the VG , CC , and CW sets, and the results will not be used in this part.

224. The data set MB had measurements of the mean concentration at every 1.16 cm over the first 101 cm above the bottom. Table 4 shows that the length scale δ ranged from 1.7 cm to 2.2 cm for the 12 runs in this set. Therefore the first three points would be inside the range 2δ above the bottom. The 36 γ_0 values obtained from these points range from 8×10^{-3} to 5.9. However, these values of γ_0 will not be considered in this study because of the methodology that appears to have been used by Bedford et al. (1990) to calibrate their ABS instrument.

225. The calibration of the instrument seems to have been done using the grain size distribution obtained from samples taken in the beam of the instrument at a height of 100 cm above the bottom. The dominant grain size in these samples was 0.004 cm to 0.006 cm. In contrast grab samples taken from the bottom near the measurement site indicate that the mean grain diameter of the bottom was 0.023 cm with only about 1-3% of the sediment being in the size classes sampled 100 cm above the bottom. Thus it seems likely that the concentration very near the bottom would be dominated by the larger grains. As the instrument was calibrated using the smaller grain size it is likely that the measurements made very near the bottom would be in error. Since it is these measurements that provide the most reliable estimates of γ_0 it was decided not to use this data set in the determination of γ_0 .

Discussion of the Results

226. The calculations performed in this part have led to the conclusion that the parameter γ_0 takes on a different value depending on whether the bed is rippled or flat. In the model development of Part II it is the parameter Z, defined in Equation 37, that determines the nature of the bed. Therefore, for the model presented in this report γ_0 can be defined as

$$\gamma_0 = \begin{cases} 1.8 \times 10^{-3} & z < 0.18 \\ 1.8 \times 10^{-4} & z \geq 0.18 \end{cases} \tag{115}$$

It should be remembered that γ_0 in Equation 115 is based on just nine runs from three different field experiments. Furthermore, the definition of the onset of the flat bed by $Z = 0.18$ is itself based on a limited number of field ripple geometry measurements. Nevertheless Equation 115 is the first step towards quantifying the reference concentration so that the suspended sediment model can be applied in the field. Comparison with more good quality data sets will serve to make the model applicable to a wider range of grain diameters, bed forms and wave and current conditions.

227. The existence of two different values of γ_0 for rippled and flat beds can be justified physically by considering the vortex shedding mechanism that was described in detail in Part II. The increased flow velocity over the ripple crest combined with the ejection of sediment into the flow during velocity reversal would mobilize more sediment than the action of the shear stress on a flat bed. It is likely that γ_0 decreases smoothly from the higher value to the lower value as the ripples respond to increasing flow intensity by growing smaller and finally vanishing. Data sets in the ripple disappearance region that include actual ripple measurements should help determine this variation of γ_0.

228. The apparent decrease of γ_0 with increasing flow intensity has been observed by Vincent et al. (1991). They considered a succession of mean concentration profiles, taken with an ABS instrument over a 0.015-cm sand bed, through the course of a mild storm event. The model of Glenn and Grant (1987), with ripple geometry predicted by the laboratory relations of

84

Grant and Madsen (1982), was used to estimate a value of γ_0 from the mean concentration measured 2 cm above the bottom.

229. The calculations showed that γ_0 was about 1×10^{-2} before the storm and then decreased to a value of about 2×10^{-4} over a period of nine hours. The value of γ_0 then increased and stabilized at a value of about 3×10^{-3} four hours later. The lowest value of γ_0 corresponded to the highest wave intensity. Whereas the ripple geometry relations used by Vincent et al. (1991) predicted the bed conditions to be rippled for the duration of the experiment, use of Equation 36 indicates that the bed would have been flat when the lowest values of γ_0 were obtained. The values of γ_0 calculated by Vincent et al. (1991) are not directly comparable to the values obtained in this part because of the different eddy viscosity model and reference level used. However, they do indicate that γ_0 could be expected to decrease smoothly between the two limits established in Equation 115. The values of Vincent et al. (1991) are also of the same order of magnitude as those derived here.

230. The parameter γ_0 is the only undetermined coefficient of the model. Therefore all the uncertainties present in the calculation will be reflected in a scatter of the resulting values of γ_0. These uncertainties include errors in measurement, in the calculations of the ripple geometry, the equivalent bottom roughness and the current and wave-current shear velocities, in the representation of the irregular wave motion by one or two components, and in the grain diameter and fall velocity. This fact should be kept in mind when considering the scatter of estimates of γ_0.

231. The model presented here calculates the equivalent bottom roughness, k_n, by first estimating the bed condition and the ripple height from Equation 36 and then calculating k_n from either Equation 35 or Equation 41, depending on whether the bed was rippled or flat. The estimation of ripple height using Equation 36 involves a considerable error. Therefore it is desirable to have independent estimates of the ripple geometry by making on site measurements during the experiments. This task is usually carried out by divers. However, measurements made by divers, particularly of the ripple height, are not very accurate. A more sophisticated method is to use a high resolution tracking sonar as described by Greenwood et al. (1990).

232. Once the ripple height is known the equivalent roughness can be calculated using Equation 35, which was obtained by Wikramanayake and Madsen (1990) after analysis of laboratory measurements of energy dissipation under waves. Equation 41 however, which is assumed to give the equivalent roughness for the case of sheet flow, has limited experimental backing. An alternative method of estimating the bottom roughness is by measuring the mean velocity at more than one point in the vertical.

233. If the measurement is done at two points, independent estimates of both the current shear velocity, u_{*c} , and the equivalent roughness, k_n , can be made once the wave conditions are known. Measuring the current at more than two points will increase the confidence in these estimates. While the roughnesses calculated in this way will be specific to the wave-current model used, the method has the advantage of avoiding the uncertainty in the prediction of the ripple geometry. If the ripple height and bed condition are observed independently this method will also serve to check the validity of Equations 35 and 41 for wave-current interaction in the field.

234. Another advantage in using several current meters at different elevations to measure the horizontal velocity is that checking the internal consistency between the readings at the different levels will indicate the "quality" of the data. For example, if the mean velocity is measured at four elevations, the values would be expected to show that the mean velocity is proportional to the logarithm of the height. However, the four two-axis current meters should also show that the direction of the mean velocity was the same at the four elevations. If the directions at the four elevations are very different it would be an indication of some problem with the instruments. This type of check is particularly important in the case of field experiments because the instruments are usually left on the bottom for long periods between calibrations and other adjustments.

235. Another contribution to the uncertainty in the estimates of γ_0 is the fact that sediment beds in the field consist of many different grain sizes. The distribution of grain sizes in suspension will vary with height above the bottom. This variation will affect the calibration of the concentration measuring device. Furthermore, as the model uses a single grain size, it can be expected that the predicted concentrations will

decrease with height faster than the observed concentration. This difference is caused by the finer grain sizes being suspended to greater heights than predicted by the model. Estimates of γ_0 made from heights where this difference is significant will result in values of γ_0 that are too large. As discussed above, this was the situation for the DK data set.

236. The effect of the non-uniform grain size distribution can be assessed by taking suction samples of the sediment laden water at several levels during the experiment. These samples would verify the calibration of the instruments and at the same time indicate whether the representation of the sediment by a single diameter was valid. Another method of obtaining the grain size distribution as a function of the height is to use an ABS instrument that operates at several frequencies as described by Hay (1992). In the absence of such measurements of the change in the size distribution with height it should be concluded that the reliability of the estimates of γ_0 decreases with the height of measurement.

237. The fall velocity of the sediment is another quantity that is often neglected in field measurements. If the sediment is specified solely by the grain diameter the fall velocity can be computed using the empirical relation given by Madsen and Grant (1976). However, this relation is based on a certain shape of grain and would also require an assumption regarding the specific density of the grains. The inaccuracy that may be caused by the use of this relation can be seen in the values for the fall velocity for the sets VG and MB in Table 3. Both sets have the same mean grain diameter. Vincent and Green (1990) measured the fall velocity of 100 grains and obtained a mean fall velocity of 2.25 cm/s. The empirical relation, used for data set MB , assuming s = 2.65 , resulted in a value of 2.78 cm/s. The two values differ by about 20% so that the corresponding values of the parameter a , defined by Equation 48, will also differ by 20%. This change in a could result in quite different estimates of γ_0 .

238. The critical Shields parameter for the initiation of motion, ψ_{cr} , is calculated in the model using the modified Shields curve proposed by Madsen and Grant (1976). This curve is based on experimental data that show considerable scatter. Uncertainty in psicr would result in uncertainty in the mean value of S' that appears on the right-hand side of

87

Equation 110 thus affecting the estimates of γ_0. Equation 93 shows that this uncertainty will decrease as the ratio of the wave skin friction shear stress, ψ_w', to ψ_{cr} increases. Therefore the reliability of the estimates of γ_0 increases as the excess skin friction shear stress increases. Based on this criterion the values in Table 4 show that the data sets CC and VG would be considered more reliable while some of the estimates of γ_0 from the sets DK and MB would be subject to large uncertainties because the excess skin friction shear stress is small.

239. Thus the reliability of the estimated values of γ_0 can be improved by using data from experiments that include the measurements discussed above. These are measurements of the ripple geometry, measuring the current at more than one point in the vertical, measuring the grain size distribution with height and direct measurement of the fall velocity. Though this list may seem difficult to fulfill there are some experimental programs, for example that outlined by Greenwood et al. (1990), that include all the features mentioned above. Data from these experiments would be ideal for testing the present wave-current-sediment model.

PART V : EXAMPLE CALCULATIONS AND COMPARISON WITH MEASURED CONCENTRATION AND FLUX PROFILES

240. The model results for two sets of wave, current, and sediment conditions are presented in this part. The objective of these calculations is to outline the procedure used by the model to calculate the suspended sediment concentrations, fluxes, and transports. Following the example calculations the model results for the data sets VG and CW, i.e., those of Vincent and Green (1990) and Vincent and Osborne (personal communication), will be compared to the measured values. The differences between the predicted and measured values will be discussed and the results of a simple formulation to account for non-uniformity in the grain size will be presented.

Example Calculations

241. Two sets of input parameters, corresponding to runs VG2046 and CC2, have been selected for the example calculations. These sets have been chosen to include both rippled and flat beds. The FORTRAN program that carries out all the calculations in this part is listed in Appendix B. The outline presented here will refer to sub-routines and variables of that program. All the program variables referred to here will be denoted by upper case characters to avoid any ambiguity. The correspondence between the variable name used in the program and the symbol used in this report for some important quantities is given in Table A1 of the appendix. The units of the input values should be in cm and cm/s for lengths and velocities, respectively, as the program uses these units consistently throughout. All angles should be input in units of degrees though the program uses radians in the calculations. The concentration will always be the volumetric concentration.

242. The basic organization of the main program is shown in the flow chart of Figure 11. The different sections of the main program will be described below. The program listing includes comments that identify these sections in order to make it easy to follow the explanation given below. The sub-routine WAVEC, which handles the wave-current solution, will be described after the main program while the other important sub-routines

Read input values from file WCSTRANS_IN

Set current specification according to FLAGC
Set FLAGKB . Calculate the variables DIAM, FALLV,
S and TEMP if they have been input as zero
Calculate SSTAR and PSICR
If FLAGKB = 0 calculate an initial estimate of the
roughness, KB, by calling WAVEC and FINDKB

SOLUTION

OF THE

WAVE -

CURRENT

AND SKIN

FRICTION

PROBLEMS

Call WAVEC to solve wave-current problem and obtain
USC, USW, USWC, DELTA, ZE0, SOLU1 AND SOLU2

Calculate UMD the mean velocity at the level DELTA

Call WAVEC with KB=DIAM, T1=UMD, T2=DELTA
and FLAGC=2 to solve the skin friction problem

Calculate ZW1 - a new value of the parameter Z

Calculate a new value
for the roughness KB

NO

Does the value of
Z converge?

YES

Is FLAGKB = 0 ?

YES

NO

Hydrodynamic problem solved

Figure 11. Flow chart for program WCSTRANS

REFERENCE
CONCENTRATION
SECTION

Calculate GAMMA0 from the final value of
Z. Calculate RTAU, RATPSI, MUP1 and DELPHI
Call COEFF to obtain the Fourier expansion
of the instantaneous reference concentration
Calculate the mean reference concentration
CSCALE and the ratios R1 and R2

CALCULATION OF THE
BED LOAD TRANSPORT

Call the sub-routine BEDLOAD

SOLUTION OF THE
CONCENTRATION PROBLEM

Calculate ZER and A
Call TCONCCOEFF to obtain the solution
for the periodic components of the concentration

CALCULATION OF THE
OF THE SUSPENDED
SEDIMENT TRANSPORTS

Set the upper and lower limits of integration
Call FLUXMEAN for the mean transport
Call FLUXWAVE for the transport due to
the periodic components

CALCULATION OF THE
VELOCITY, CONCENTRATION
AND TRANSPORT PROFILES

Set the evaluation levels in the vector Z
Calculate the mean and periodic velocity
components using VELMEAN and TCONC
Calculate the mean and periodic concentration
components using MCONC and TCONC
Calculate the mean and wave fluxes

OUTPUT OF THE RESULTS

Write the calculated velocity, concentration and
flux profiles to the files WCSTRANS_VELO,
WCSTRANS_CONC and WCSTRANS_FLUX
Write the calculated transport values and other
important parameters to the file WCSTRANS_RES

Figure 11 (cont.). Flow chart for program WCSTRANS

are described along with the section of the main program from which they are called.

Input Section

243. The program requires input values that describe the wave, current, sediment, and bed conditions. These values are read from a file named WCSTRANS_IN. The required format for the input file is given in Table 5. The program reads the input values in free format. Therefore the values in each row should be separated by spaces. Variables for which the default value is to be used should be given as zero. The input values for the two selected data sets are given in Table 6. As described in Part IV the wave conditions are specified by two waves, one with twice the frequency of the other. The required input values are the magnitudes of the velocities of the two components, UB1 and UB2 in the program, where UB1 is the principal component, and ω , the radian frequency of UB1 , which is denoted by the variable FRE in the program. A value of zero for UB2 would indicate a symmetric, periodic wave motion. If either UB1 or FRE is zero the program will terminate with an error message. The periodic velocity and concentration components with frequency ω (or FRE) will be referred to as the principal component while the components with frequency 2ω will be referred to as the secondary component.

244. The input values for the current are a flag FLAGC , two input parameters T1 and T2 , and the anticlockwise angle between the wave and current directions PHICWD . The method of specifying the current depends on the value of FLAGC . FLAGC = 1 would indicate that the current was specified by a given current shear velocity, i.e., the mean bottom shear stress is known. In this case the current shear velocity (variable USC) is read from T1 while T2 will be zero. A value of 2 indicates a specification by a given mean (current) velocity--variable UCR which is read from T1 --at a given elevation--variable ZCR which is read from T2 . If FLAGC = 3 the program will expect the current to be specified by a depth averaged velocity--variable UAVE which is read from T1 --and the flow depth--variable HEI which is read from T2 . Any other value of FLAGC will generate an error message.

245. The sediment is specified by the mean grain diameter, the fall velocity, and the specific density of the grains, represented by the

Table 5

Format of Input File WCSTRANS_IN for the program WCSTRANS

listed in Appendix B

Row number	Column number			
	1	2	3	4
1	UB1	UB2	FRE	
2	FLAGC	T1	T2	PHICWD
3	DIAM	FALLV	S	
4	KB			
5	SLOPED	PHISWD		
6	HEI			
7	TEMP			

Table 6

Input values for the program WCSTRANS for the example runs VG2046 and CC2

Input parameter	Unit	Symbol in report	Variable in program	Example run VG2046	Example run CC2
Principal wave velocity	cm/s	u_{b1}	UB1	34.7	62.9
Secondary wave velocity	cm/s	u_{b1}	UB2	7.8	15.4
Frequency of principal component	rad/s	ω	FRE	1.08	1.15
Current specification flag			FLAGC	2	2
Current specification values			T1	18.0	37.1
			T2	20.0	15.0
Angle between waves and current	deg		PHICWD	−70.6	96.1
Mean grain diameter	cm	d	DIAM	0.023	0.018
Sediment fall velocity	cm/s	w_f	FALLV	2.25	0
Sediment specific gravity		s	S	0	0
Equivalent bottom roughness	cm	k_n	KB	0	0
Bottom slope	deg		SLOPED	0	0
Angle between bottom slope direction and wave direction	deg		PHISWD	0	0
Flow depth	cm	h	HEI	180.0	200.0
Water temperature	°C		TEMP	0	0

variables DIAM , FALLV and S , respectively. If S is given as zero a value of 2.65 is assumed for the specific density. If either one of DIAM or FALLV is zero it is calculated using the empirical relation given by Madsen and Grant (1976) . If both values are zero the program terminates with an error.

246. The model outlined in Parts II and III used the empirical relationships of Equations 35 and 41 to calculate the equivalent roughness of the bottom. However, the program has been written to accomodate the need to use some other value for the roughness. This is done by including the roughness, variable KB , as an input parameter. If KB is given as zero the roughness is calculated using the iterative procedure described below while this procedure is not used if a non-zero value is given.

247. The bed is specified by the slope of the bed given as an angle made with the horizontal, variable SLOPED , and the anticlockwise angle between the wave direction and the direction of upward slope, variable PHISWD . The last two parameters required are the depth of the flow, variable HEI , and the water temperature in °C, variable TEMP . If TEMP is given as zero a value of 20°C is assumed.

248. The PARAMETER statement at the beginning of the listing of the main program sets the values of the Von Karman's constant, κ , to 0.4 , the model parameter α to 0.5 , the volume fraction of the grains in the bed, c_b , to 0.65 , the angle of repose of the sediment, ϕ_m , to 36° , and the acceleration due to gravity to 981 cm/s^2 . These quantities are represented by the variables KAP , ALPHA , CB , PHIFD , and GEE respectively.

Data Processing Section

249. This section processes the values read from the input file. The current specification is set according to the value of FLAGC . The temperature, the specific density of the grains, the grain diameter, and the fall velocity are calculated if they have not been given. The parameters S_* , ψ_{cr} , and ν , denoted by variables SSTAR , PSICR , and VIS are found. A variable FLAGKB is set to zero if the equivalent roughness KB is not given and set to 1 if it is. If the roughness is not given, as would be the case when the model is used in its fully predictive mode, it is necessary to have an initial estimate of the

95

roughness that can be used in the solution of the wave-current problem in the next section.

250. An initial estimate of the roughness requires an initial estimate of the the parameter Z , defined by Equation 37, which depends on the wave skin friction shear stress. The initial estimate of this shear stress is made by calling the sub-routine WAVEC in its pure wave mode with the bed roughness specified as the grain diameter. The sub-routine WAVEC will be described after the discussion of the main program. The value of Z , variable ZW , calculated in this way is used in the routine FINDKB which incorporates Equations 35, 36, and 41.

251. The parameters calculated in the data processing section are listed in Table 7 for the two data sets considered here. The program has used the default values for the sediment specific density and the water temperature for both runs and has calculated the fall velocity for run CC2 . A value of zero was input for all these values in Table 6. As the equivalent bottom roughness was not given (FLAGKB = 0) the program has made an initial estimate of the bed conditions and the roughness. The table shows that a rippled bed is predicted for set VG2046 while set CC2 leads to sheet flow conditions.

Solution of the Wave-Current and Skin Friction Problems

252. The next section of the program is the wave-current solution module. The solution is done by the sub-routine WAVEC which will be discussed later. This sub-routine takes the wave, current, and roughness specifications as an input value and calculates the corresponding current, wave, and wave-current shear velocities, u_{*c} , u_{*w} , and u_{*cw} , denoted by the variables USC , USW , and USWC respectively, where u_{*w} is the shear velocity based on wave-component-only shear stress. The sub-routine also calculates the boundary layer length scale δ , variable DELTA , friction factors for the two wave components and the phase difference between the wave velocities and the corresponding bottom shear stresses. Also output are the vectors SOLU1 and SOLU2 which contain the five complex coefficients A , B , C , D , and E that are part of the solution for the wave velocity in Equations 67, 69, and 72 of Part III. The vectors SOLU1 and SOLU2 correspond to the velocities u_{b1} and u_{b2} , respectively.

Table 7

Results of data processing section of program WCSTRANS

for the example runs VG2046 and CC2

Input parameter	Unit	Symbol in report	Variable in program	Example run VG2046	CC2
Current specification					
Reference current velocity	cm/s		UCR	18.0	37.1
Current reference level	cm		ZCR	20.0	15.0
Bottom roughness flag			FLAGKB	0	0
Water temperature	°C		TEMP	20.0	20.0
Sediment specific density		s	S	2.65	2.65
Kinematic viscosity	cm^2/s	ν	VIS	0.01	0.01
Mean grain diameter 0.018	cm	d	DIAM	0.023	
Non-dimensional grain diameter		S_*	SSTAR	3.51	2.43
Sediment fall velocity	cm/s	w_f	FALLV	2.25	1.95
Critical Shields parameter for the initiation of motion		ψ_{cr}	PSICR	0.046	0.055
Initial estimate of bottom roughness					
Ripple geometry parameter		z	ZW	0.041	0.205
Ripple height	cm	η	HA	1.11	flat
Equivalent bottom roughness	cm	k_n	KB	4.5	0.18

253. Once the wave-current solution is obtained the mean velocity at the level $z = \delta$, variable UMD , is calculated using the sub-routine VELMEAN which incorporates the solution for the mean velocity given by Equation 10. The next step is to calculate the skin friction shear stresses. As detailed in Part III, this is done by solving the wave current problem with the roughness taken to be the mean grain diameter and the current specified as the mean velocity at the level $z = \delta$. Therefore the sub-routine WAVEC is called again with the roughness given by DIAM and the current specified by UMD at the level DELTA .

254. The important results of this calculation are the current, wave, and wave-current skin friction shear stresses, u_{*c}' , u_{*w}' , and u_{*cw}' , denoted by the variables USCP , USWP , and USWCP , respectively, and the phase differences between the wave velocities and the wave skin friction shear stresses, denoted by variables PHIBP1 and PHIBP2 for the principal and secondary components, respectively. If the equivalent bottom roughness, k_n , had been specified in the input file the hydrodynamic problem would now be solved completely. However, when k_n is not specified the problem will not be solved until the calculated skin friction shear velocities result in the same value of the roughness that was assumed in order to obtain the shear velocities.

255. The calculated value of u_{*w}' is used to obtain a new value for the parameter Z , denoted by the variable ZW1 . The program then checks the difference between ZW1 and ZW --which was the estimate of Z made prior to the solution of the wave-current solution. If the fractional change in z is less than 0.001 the program will advance to the next section while if the difference is greater ZW is set equal to ZW1 , a new roughness is calculated using ZW1 , and the calculations of this section are repeated until the calculated value of ZW1 coincides with ZW . This loop in the program structure is shown in the flow chart in Figure 11.

256. The results of the hydrodynamic model for the two data sets are given in Table 8. The table shows the values obtained for the first iteration, i.e., using the roughness given in Table 7, as well as the final converged values. The solution for run VG2046 took three iterations to converge because the ripple height had to be predicted as part of the solution. The table shows that the value of Z obtained after the first

Table 8

Initial and Final Results from the Wave-Current Section of the Program

WCSTRANS for the Example Runs VG2046 and CC2

Parameter	Unit	Symbol in report	Variable in program	Example runs			
				VG2046		CC2	
				First iteration	Final value	First iteration	Final value
Current shear velocity	cm/s	u_{*c}	USC	2.47	2.26	3.12	3.12
Wave shear velocity	cm/s	u_{*w}	USW	7.51	6.70	6.59	6.59
Combined shear velocity	cm/s	u_{*cw}	USWC	7.66	6.84	6.75	6.75
Boundary layer length scale	cm	δ	DELTA	2.84	2.53	2.34	2.34
Non-dimensional value of $z_0 = k_n/30$		ζ_0	ZEO	0.053	0.036	0.0026	0.0026
Mean velocity at the level $z = \delta$	cm/s		UMD	6.45	6.76	22.6	22.6
Skin friction shear velocities							
Current	cm/s	u_{*c}'	USCP	0.84	0.88	2.21	2.21
Wave	cm/s	u_{*w}'	USWP	2.85	2.85	4.75	4.75
Phase of skin friction shear stress of principal wave	rad	ϕ_{bl}'	PHIBP1	0.27	0.26	0.24	0.24
New value of ripple parameter		z	ZW1	0.062	0.062	0.32	0.32
Ripple height	cm	η	HA	0.69	0.68	flat	flat
Bottom roughness	cm	k_n	KB	2.75	2.74	0.18	0.18

iteration is very close to the final converged value, with the additional iterations required to satisfy the convergence criteria. In contrast the solution for run CC2 converged on the first iteration because the roughness for a flat bed, which is obtained for these conditions, is not dependent on the skin friction shear stress.

Reference Concentration Section

257. The final converged value of Z can be used to determine γ_0 from Equation 115. The skin friction shear velocities calculated in the previous section can be used to calculate the quantities $\mu_1{}'$, r_φ , r_τ , and ϕ --denoted by variables MUP , RATPSI , RTAU , and DELPHI , respectively, in Equation 100. These values are used by sub-routine COEFF which calculates the coefficients of the Fourier expansion of Equation 100 given in Equation 105. This sub-routine uses the sub-routine CONTROL to obtain the values of $\bar{r}$, r_1 , and r_2 by numerical integration. The values returned by COEFF are VALM , which is equal to $\bar{r}$, and R1 and R2 which are equal to $r_1/\bar{r}$ and $r_2/\bar{r}$, respectively.

258. Therefore R1 and R2 are the ratios of the magnitudes of the reference values for the principal and secondary concentration components, c_{1r} and c_{2r} , to the magnitude of the mean reference concentration component $\bar{c_r}$. The quantity $\bar{c_r}$ is represented in the program by the variable CSCALE . It should be remembered that the solution for the periodic concentration profiles obtained in Part III was scaled by the magnitude of the reference value, which will be R1*CSCALE and R2*CSCALE for the principal and secondary components, respectively.

259. The results of the reference concentration section for the two example data sets is shown in Table 9. The table shows that the periodic components of the reference concentration are of the same order as the mean reference concentration. The table also shows that ϕ , which is the phase difference between the two wave skin friction shear stresses, is very small. This small difference verifies the assumption made in the development of the reference concentration model in Part III that these two skin friction shear stresses were in phase.

Calculation of the Bedload Transport

260. The skin friction shear velocities can also be used to calculate the bed-load transport from Equation 85 which relates the instantaneous

Table 9

Table 9

Results of Reference Concentration Section of Program WCSTRANS

for the Example Runs VG2046 and CC2

Parameter	Unit	Symbol in report	Variable in program	Example run VG2046	CC2
Resuspension coefficient		γ_0	GAMMA0	1.8×10^{-3}	1.8×10^{-4}
Ratio of current to principal wave skin friction shear stress		$\mu_1{}'$	MUP1	0.35	0.53
Ratio of critical to principal wave Shields parameter		r_φ	RATPSI	0.27	0.09
Ratio of principal to secondary wave skin friction shear stress		r_τ	RTAU	0.25	0.27
Phase difference between wave skin friction shear stresses	rad	ϕ	DELPHI	0.011	0.008
Mean reference concentration	vol/vol	$\overline{C_r}$	CSCALE	1.8×10^{-3}	8.3×10^{-4}
Ratio of principal to mean reference concentration		$r_1/\overline{r}$	R1	0.40	0.13
Ratio of secondary to mean reference concentration		$r_2/\overline{r}$	R2	0.88	0.51

bed-load transport to the instantaneous skin friction shear stress. The calculation is done by sub-routine BEDLOAD . This sub-routine calls sub-routine CONTROL to integrate the expression for the flux in the wave and wave-normal directions, given by sub-routines BLOADW and BLOADN , respectively, over a wave period to compute the transports in these directions.

261. The bed-load transports for the two example data sets are given in Table 10. The table shows that the bed-load transport normal to the waves is in the direction of the mean current as would be expected. The difference in sign is due to the difference in the angles between the wave and current directions for the two runs as given in Table 6. The transport in the wave direction is with the waves for both cases even though the mean current was against the waves in run CC2 . This reversal of the expected transport is because of the strong wave asymmetry seen in this data set.

Solution of the Concentration Problem

262. The reference level for this model has been selected to be 7d where d is the mean grain diameter. Since the boundary layer length scale δ and the combined shear velocity, u_{*cw} , have been calculated during the solution of the wave-current problem, the parameters ζ_r , ϵ , and a , represented by the variables ZER , EP , and A respectively, can be found. These values are used by sub-routine TCONCCOEFF to calculate the five complex coefficients of Equation 67, 69, and 72 that define the solution for the periodic components of the concentration. The values of ζ_r and a for the two examples are given in Table 10.

263. As discussed later on, the parameter δ is defined in sub-routine WAVEC using the frequency of the principal wave, ω , as the representative frequency. Therefore for the solution of the principal component of concentration the ratio σ , defined by Equation 62, will be 1.0 while $\sigma = 2.0$ should be used for the secondary component. The parameter σ is denoted by the variable EN in the sub-routine.

264. The sub-routine TCONCCOEFF determines the five complex coefficients of Equations 67, 69, and 72 by solving the five simultaneous equations given by Equations 74, 75, 76, 77, and 78 . The sub-routine COMSOLVE is called to solve this system of equations. The kelvin functions and their derivatives are evaluated by the set of sub-routines

102

Table 10

Results of the Suspended Sediment Concentration, Bed Load Transport, and Suspended Load Transport Sections of Program WCSTRANS for the Example Runs VG2046 and CC2

Parameter	Variable in report	Variable in program	Example run VG2046	CC2
Non-dimensional fall velocity	a	A	0.82	0.72
Non-dimensional reference level	ζ_r	ZER	0.064	0.054
Bed load transports (10^{-4}cm^3/cm/s)				
Wave direction			87	171
Wave-normal direction			-36	241
Suspended load transports (10^{-4}cm^3/cm/s)				
Mean transport in wave direction			23	-18
Mean transport in wave-normal direction			64	170
Wave transport due to principal components			32	11
Wave transport due to secondary components			12	8
Total wave transport (in wave direction)			44	19
Total suspended load transport in wave direction			67	1

KELVINP , BERBEI , ASKELVINP , AB , GAMMA , DKELVINP , DBERBEI , and

ASDKELVINP . These sub-routines are based on the power series expansions

given by Young and Kirk (1964). The variable RHS in sub-routine

TCONCCOEFF is the value that is put on the right-hand side of the first

equation. As discussed in Part III, RHS is set to 1.0 when the periodic

concentration is being solved (Equation 74) and set to -1.0 when the

velocity problem is being solved. Similarly, the variable ZER in the

sub-routine is set to ζ_r , denoted by ZER in the main program, for the

concentration problem and set to ζ_0 , denoted by ZEO in the main program,

for the velocity problem.

265. When ϵ is very small the matching level for Equations 77 and 78,

given by $(a\delta)/\epsilon$, will become large. As the concentration and the velocity

deficit, i.e., u_{d1} of Equation 27, become very small at a height that is

several times the boundary layer length scale δ , it is not necessary to

evaluate these quantities at such high levels. Therefore when $\epsilon < 0.02$,

i.e., the level a/ϵ is greater than 25δ , the problem corresponding to a

pure wave motion is solved. In this case the solution for the periodic

components is given by Equations 67 and 69 with the coefficient C in

Equation 69 set to zero. These equations involve only three complex

coefficients which are obtained by solving Equations 74, 75, and 76 with C

set to zero.

Calculation of the Suspended Sediment Transports

266. The transport due to the various velocity and concentration

components is calculated in this section. The mean transport is obtained

from sub-routine FLUXMEAN . This sub-routine uses the sub-routine

CONTROL to integrate the sub-routine FLUXM between two specified levels.

FLUXM calculates the mean flux as the product of the mean velocity and the

mean concentration. The lower level of integration is set to be the larger

of the parameters z_0 and z_r , which are the levels at which the bottom

boundary conditions for the velocity and the concentration, respectively,

are defined. The upper level of integration is taken to be the flow depth.

267. The transport due to each wave component is calculated by sub-

routine FLUXWAVE , which integrates the sub-routine FLUXW between two

given levels. For the wave transport the upper level is set to be 30δ

while the lower level is the same as for the mean transport. The

calculated suspended sediment transports for the two example runs are shown in Table 10. The table shows that the transports due to the periodic components is of the same magnitude as the transport due to the mean components. The mean transport in the wave direction for run CC2 is nearly equal in magnitude to the wave transport. As the current opposes the waves in this case the result is a near zero value for the suspended sediment transport in the wave direction.

Calculation of the Velocity, Concentration and Transport Profiles

268. The output of the program includes the profiles of the mean and periodic components of the velocity and the concentration and the profiles of the fluxes due to each component as well as the total flux profile. The profiles are calculated at 100 levels between the larger of z_0 and z_r and the level 50δ. The lower limit is the lowest level at which both the velocity and concentration solution are defined. The upper limit was selected as a cutoff because the concentration, and therefore the fluxes, are generally very small above this level.

269. The mean velocity is calculated using the sub-routine VELMEAN, which uses Equation 10. The mean concentration is calculated by sub-routine MCONC which uses Equations 50, 52, and 54. These equations were based on the eddy viscosity model of Equation 7 which showed a linear increase above the wave boundary layer. While this variation of the eddy viscosity is appropriate near the bottom it would overestimate the eddy viscosity in the upper regions of the flow. Thus the calculation of the mean velocity and concentration at these levels, which is done during the integration of the mean flux over the entire depth, could be in error.

270. Therefore the sub-routines are based on the assumption that the eddy viscosity remains constant after it reaches 1/6 of the total depth. At heights greater than this the mean velocity, u_c, is calculated from the equation

$$u_c = \frac{u_{*c}}{\kappa}\left[\frac{\zeta}{\beta} + \ln\frac{\beta\epsilon}{a} + \epsilon\left[\ln\frac{a}{\zeta_0} - 1\right]\right] \tag{116}$$

and the mean concentration from the equation

$$\bar{c} = \bar{c}_r \left[\frac{a}{\zeta_{re}} \right]^{-a} \left[\frac{\beta\epsilon}{a} \right]^{-a/\epsilon} e^{-a\zeta/\epsilon\beta} \qquad (117)$$

where the parameter β , represented by the variable BETA in the program, is defined by

$$\beta = \frac{h}{6\delta} \qquad (118)$$

with h being the flow depth.

271. The complex number representing the periodic components of the velocity and the concentration are calculated by the sub-routine TCONC . This sub-routine evaluates the solution for the periodic components using one of Equations 67, 69, and 72 depending on the input value of the non-dimensional height ζ (denoted by ZZ in the sub-routine). The input vector SOL contains the five complex constants in these equations.

272. The input variable ZR is given as ζ_r for the concentration problem and as ζ_0 for the velocity problem. The ratio of the frequency of the component to the representative frequency, σ of Equation 62, is input as the variable EN . As for the sub-routine TCONCCOEFF the problem is assumed to be a pure wave problem when $\epsilon < 0.02$. Under this assumption only the first three values of SOL are used and the output parameter CT is calculated using Equations 67 and 69 with the coefficient C set to zero.

273. The output of TCONC is a complex number CT . The magnitude and phase of this value can be found from Equation 27 in the case of a velocity component and Equation 57 for a concentration component. The mean flux is calculated as the product of the means while the flux due to the periodic components is taken as the time average of their products. The phase of the concentration components with respect to the near bottom velocity is found by adding the phase of the reference concentration, ϕ_{b1}' , denoted by variable PHIBP1 , to the phase of the component with respect to the reference value.

Output of the Results

274. The profiles of velocity, concentration, and flux are written to the files WCSTRANS_VELO, WCSTRANS_CONC, and WCSTRANS_FLUX respectively.

The contents of the columns of each file are given in Table 11. The height above the bottom, velocities, phases, and fluxes are output in units of cm, cm/s, radians, and $cm^3/cm^2/s$, respectively, while the concentration given is the volumetric concentration. The input parameters, the calculated transport values, and some of the important intermediate parameters are written to the file WCSTRANS_RES. The corresponding output files for the two example runs are given in Tables 12 and 13.

275. The magnitudes of the mean, principal, and secondary components of the concentration for run CC2 are plotted as a function of z , the height above the bottom, in Figure 12. The figure shows that the periodic components of concentration decrease much more rapidly than the mean component, with the principal and secondary components decreasing to 1% of the reference value within 4.6 cm and 3.6 cm, respectively.

276. The mean, wave, and total fluxes in the wave direction for run CC2 are plotted in Figure 13. The mean flux is against the wave direction because the current opposes the waves in this run. The total flux is in the wave direction in the lower 2 cm of the flow and in the opposite direction above that level. However, as shown in Table 10, the depth-integrated values of the mean and wave fluxes are very similar resulting in the net suspended sediment transport in the wave direction being nearly zero. The concentration and flux profiles will be shown in the next section where the calculated profiles are compared to the measured values.

Description of Sub-routine WAVEC

277. The sub-routine WAVEC solves the wave-current problem. The input values are the wave parameters UB1 , UB2 , and FRE , the current which is specified by FLAGC , T1 , T2 , and PHICW , and the bottom roughness KB . The flowchart for the sub-routine is given in Figure 14. As shown in the figure, two different algorithms are used depending on whether a pure wave problem, specified by T1 = 0 , or a wave-current problem, i.e., a non-zero value of T1 , must be solved. The solution for the wave-curent problem will be described here as it is the more complicated of the two.

278. The extension of the wave-current model to include many wave components was described in Part II. The wave shear velocity, u_{*w} , was to be calculated using a representative wave defined by Equations 31 and 32.

Table 11

Format of the Output Files for the Profiles of Velocity,

Concentration, and Flux from the Program WESTRANS

Column number	Name of output file		
	WCSTRANS_VELO	WCSTRANS_CONC	WCSTRANS_FLUX
1	height above bottom	height above bottom	height above bottom
2	mean velocity	mean concentration	flux due to mass
3	magnitude of principal wave velocity	magnitude of principal concentration	flux due to principal components
4	magnitude of secondary wave velocity	magnitude of secondary wave concentration	flux due to secondary components
5	phase of principal wave velocity	phase of principal concentration component	total flux due to periodic components
6	phase of secondary wave velocity	phase of secondary concentration component	total suspended sediment flux

Table 12

Output File WCSTRANS_RES for Example Run VG2046

INPUT VALUES

   <u>Wave Specification</u>

first harmonic wave velocity	= 34.7 cm/s
second harmonic wave velocity	= 7.8 cm/s
wave frequency	= 1.080 rad/s

   <u>Current Specification</u>
current specified by a given reference value

given current velocity	= 18.0 cm/s
at an elevation	= 20.0 cm
anticlockwise angle	
between wave and current	= -70.6 deg

   <u>Sediment Specification</u>

given mean grain diameter	= 0.02300 cm/s
given sediment fall velocity	= 2.250 cm/s
given sediment specific density	= 2.650 cm/s
non-dimensional grain size (SSTAR)	= 3.508
critical Shields parameter for	
initiation of motion	= 0.0465

   <u>Flow Specifications</u>

flow depth	= 180.0 cm
bottom slope	= 0. deg
anticlockwise angle between	
wave direction and bottom slope	= 0. deg
assumed water temperature	= 20.000 C

   <u>Bottom Roughness Not Given</u>

OUTPUT VALUES

   <u>Results of Wave-Current Model</u>

current shear velocity	= 2.26 cm/s
wave shear velocity	= 6.70 cm/s
combined shear velocity	= 6.84 cm/s
value of parameter EP (= USC/USWC)	= 0.3301
boundary layer length scale	= 2.53 cm
non-dimensional z0	= 0.03601
relative roughness for wave 1	= 11.74

   <u>Results of Skin Friction Model</u>

current skin friction shear vel	= 0.8852 cm/s
wave skin friction shear vel	= 2.8518 cm/s
phase lead of wave skin friction shear stress	
over the near bottom velocity	= 0.260
shields parameter based on	
wave skin friction shear stress	= 0.21846
value of non-dimensional	
ripple parameter Z	= 0.62267×10^{-1}

<u>Bottom Roughness Not Given</u>

<u>Bottom is Rippled</u>
ripple height   = 0.6840 cm
ripple steepness   = 0.06667
calculated bottom roughness   = 2.736 cm

<u>Results of Reference Concentration Model</u>
resuspension coefficient $= 0.180 \times 10^{-2}$
mean reference concentration $= 0.181 \times 10^{-2}$
ratio of reference concentration of
   principal component to mean   = 0.39645
ratio of reference concentration of
   secondary component to mean   = 0.87781

<u>Results of the Solution of Sediment Problem</u>
non-dimensional fall velocity   = 0.8225
non-dimensional reference level   = 0.06356

RESULTS OF TRANSPORT CALCULATIONS
  <u>Bedload Transports</u>
    in wave direction $= 0.8672 \times 10^{-2} cm^3/cm/s$
    in wave normal direction $= -0.3650 \times 10^{-2} cm^3/cm/s$

SUSPENDED LOAD TRANSPORTS
  <u>Transport Due to Mean Components</u>
    in wave direction $= 0.2258 \times 10^{-2}$
    in wave normal dir. $= -0.6412 \times 10^{-2}$

  <u>Transport Due to Periodic Components (in Wave Direction)</u>
    principal components $= 0.3175 \times 10^{-2}$
    secondary components $= 0.1197 \times 10^{-2}$
    total wave transport $= 0.4373 \times 10^{-2}$
    total suspended load transport
      in wave direction $= 0.6631 \times 10^{-2}$

Table 13

Output File WCSTRANS_RES for Example Run CC2

INPUT VALUES
    Wave Specification
        first harmonic wave velocity   = 62.9 cm/s
        second harmonic wave velocity   = 15.4 cm/s
        wave frequency   = 1.156 rad/s

    Current Specification
    current specified by a given reference value
        given current velocity   = 37.1 cm/s
        at an elevation   = 15.0 cm
        anticlockwise angle
            between wave and current   = 96.1 deg

    Sediment Specification
        given mean grain diameter   = 0.01800 cm/s
        calculated sediment fall velocity   = 1.954 cm/s
        given sediment specific density   = 2.650 cm/s
        non-dimensional grain size (SSTAR)   = 2.429
        critical Shields parameter for
            initiation of motion   = 0.0551

    Flow Specifications
        flow depth   = 200.0 cm
        bottom slope   = 0. deg
        anticlockwise angle between
            wave direction and bottom slope   = 0. deg
        assumed water temperature   = 20.000 C

    Bottom Roughness Not Given

OUTPUT VALUES
    Results of Wave-Current Model
        current shear velocity   = 3.12 cm/s
        wave shear velocity   = 6.59 cm/s
        combined shear velocity   = 6.75 cm/s
        value of parameter EP (= USC/USWC)   = 0.4623
        boundary layer length scale   = 2.34 cm
        non-dimensional z0   = 0.00257
        relative roughness for wave 1   = 302.29

    Results of Skin Friction Model
        current skin friction shear vel   = 2.2146 cm/s
        wave skin friction shear vel   = 4.7518 cm/s
        phase lead of wave skin friction shear stress
            over the near bottom velocity   = 0.237
        Shields parameter based on
            wave skin friction shear stress   = 0.77499
        value of non-dimensional
            ripple parameter Z   = 0.31906×10^{0}

Bottom Roughness Not Given

Bottom is Flat
   calculated bottom roughness   = 0.180 cm

Results of Reference Concentration Model
   resuspension coefficient   = 0.18010^{-3}
   mean reference concentration   = 0.83410^{-3}
   ratio of reference concentration of
     principal component to mean   = 0.13472
   ratio of reference concentration of
     secondary component to mean   = 0.50782

Results of the Soultion of Sediment Problem
   non-dimensional fall velocity   = 0.7238
   non-dimensional reference level   = 0.05395

RESULTS OF TRANSPORT CALCULATIONS
   Bedload Transports
     in wave direction   = $0.1710 \times 10^{-1} cm^3/cm/s$
     in wave normal direction   = $0.7414 \times 10^{-1} cm^3/cm/s$

SUSPENDED LOAD TRANSPORTS
   Transport Due to Mean Components
     in wave direction   = -0.1812×10^{-2}
     in wave normal dir.   = 0.1696×10^{-1}

Transport Due to Periodic Components (in Wave Direction)
   principal components   = 0.1146×10^{-2}
   secondary components   = 0.8008×10^{-3}
   total wave transport   = 0.1947×10^{-2}
   total suspended load transport
     in wave direction   = 0.1347×10^{-3}
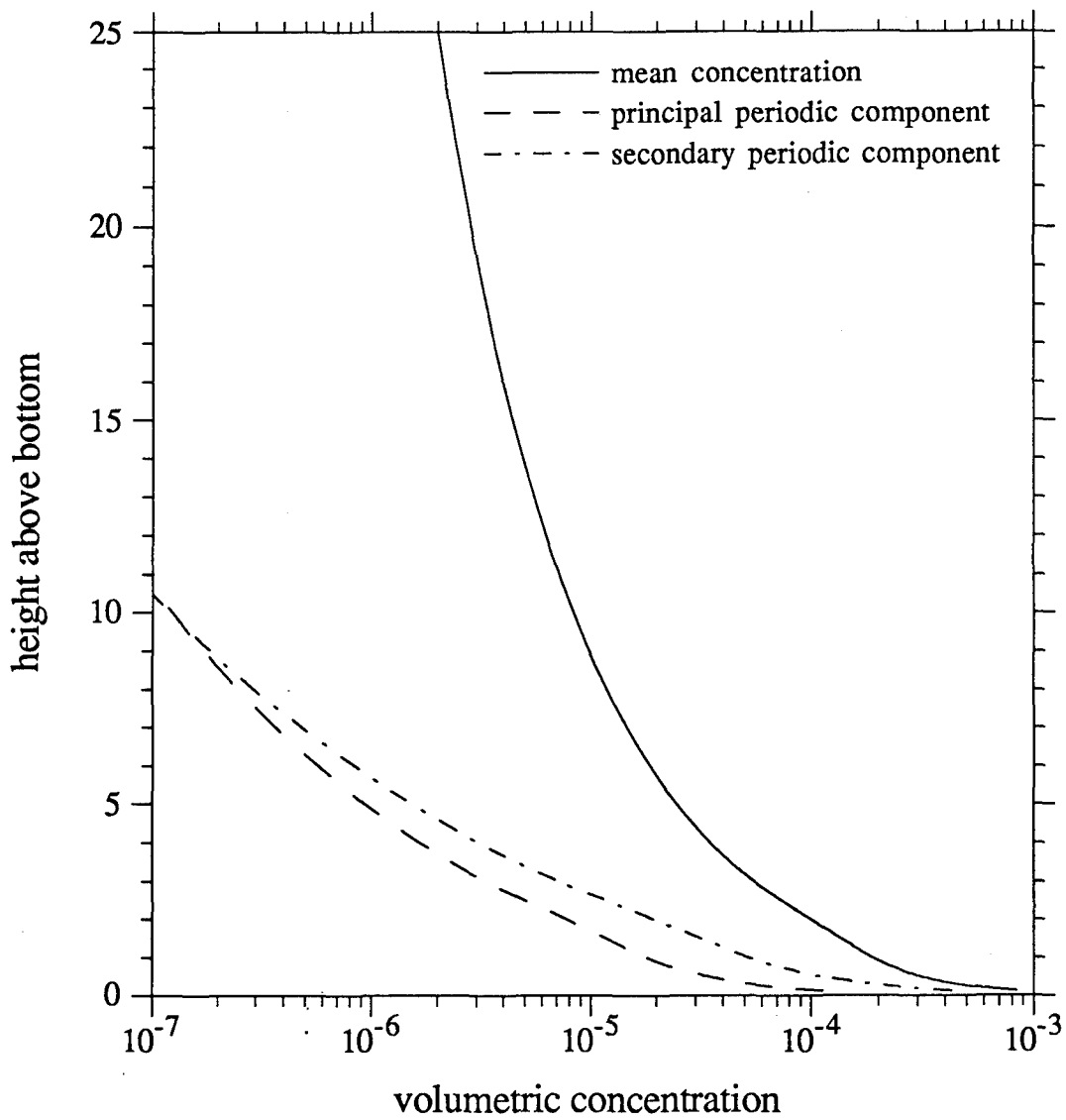
Figure 12. Profiles of the magnitudes of the mean, principal and secondary components of the concentration for example run CC2
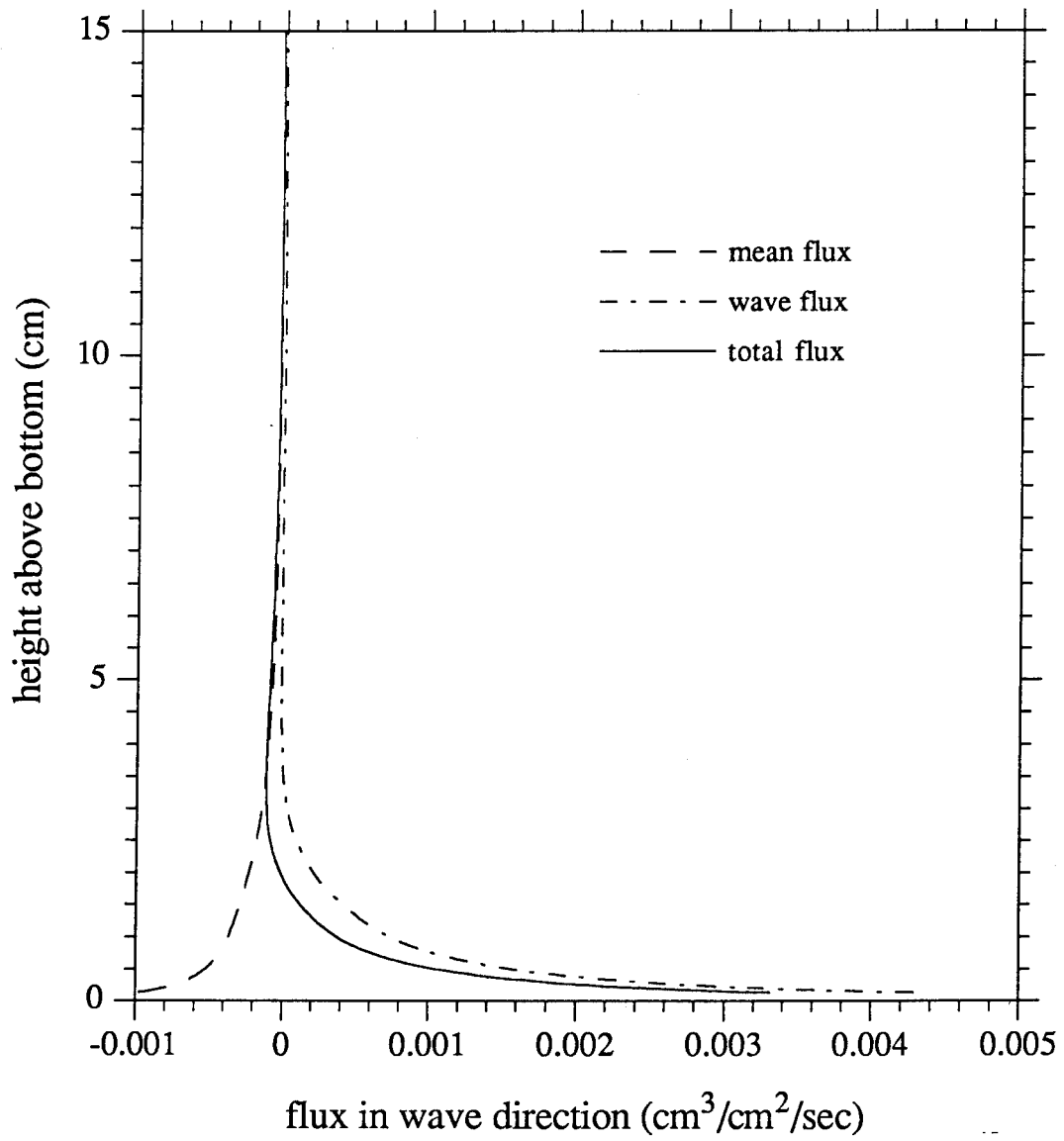
Figure 13. Profiles of the mean, wave and total suspended sediment fluxes for example run CC2

```
┌──────────────────┐      ┌─────────────┐      ┌──────────────────────┐
│ Pure wave problem │◄─────│ Is T1 = 0 ? │─────►│ Wave-current problem │
└──────────────────┘      └─────────────┘      └──────────────────────┘
         │                                                │
         ▼                                                ▼
┌──────────────────┐                      ┌──────────────────────────┐
│ Assume an initial │                     │ Assume initial values for │
│  value for the USW│                     │ USW and USC. Calculate    │
│                   │                     │ MU and EP                 │
└──────────────────┘                      └──────────────────────────┘
         │                                                │
         ▼                                                ▼
┌──────────────────────┐               ┌──────────────────────────┐
│ Calculate DELTA and  │◄──────        │ Calculate USWC, DELTA,    │
│ ZE0                  │       │        │ ZE0 and BETA              │
└──────────────────────┘       │        └──────────────────────────┘
         │                     │                          │
         ▼                     │                          ▼
┌────────────────────────────┐│       ┌──────────────────────────────┐
│ Call FINDUSWN for USWR1    ││       │ Call FINDUSWN for USWR1      │
│ the rough turbulent shear  ││       │ the rough turbulent shear    │
│ velocity for the principal ││       │ velocity for the principal   │
│ component. Calculate USWS1,││       │ component. Calculate USWS1,  │
│ the smooth turbulent shear ││       │ the smooth turbulent shear   │
│ velocity                   ││       │ velocity                     │
└────────────────────────────┘│       └──────────────────────────────┘
         │                     │                          │
         ▼                     │                          ▼
┌────────────────────────────┐│       ┌──────────────────────────────┐
│ Select USW1 as the larger  ││       │ Select USW1 as the larger of │
│ of USWR1 and USWS1. Find   ││       │ USWR1 and USWS1. Find the    │
│ the shear velocity of the  ││       │ shear velocity of the        │
│ secondary component, USW2  ││       │ secondary component, USW2    │
│ according to the regime of ││       │ according to the regime of   │
│ the principal component    ││       │ the principal component      │
└────────────────────────────┘│       └──────────────────────────────┘
         │                     │                          │
         ▼                     │                          ▼
┌────────────────────────────┐│       ┌──────────────────────────────┐
│ Calculate a new value for  ││       │ Calculate a new value for    │
│ USW, the wave shear        ││       │ USW, the wave shear velocity,│
│ velocity, using USW1 and   ││       │ using USW1 and USW2          │
│ USW2                       ││       └──────────────────────────────┘
└────────────────────────────┘│                          │
         │                     │                          ▼
         ▼                     │       ┌──────────────────────────────┐
┌──────────────┐  NO  ┌────────┴──┐    │ Update the current shear     │
│ Does USW     │─────►│ Update    │    │ velocity USC according to    │
│ converge?    │      │ USW       │    │ the current specification    │
└──────────────┘      └───────────┘    └──────────────────────────────┘
         │                                             │
        YES                                            ▼
         │                          ┌──────────────┐   ┌─────────────────┐
         │            ┌─────────────│ Update MU    │◄──│ Calculate new   │
         │            │             │ and EP       │NO │ values for MU   │
         │            │             └──────────────┘   │ and EP          │
         ▼            │                                 └─────────────────┘
┌────────────────────┐│                                 ┌─────────────────┐
│ Return to main     │◄──────────────────────────YES────│ Do MU and EP    │
│ program            │                                   │ converge?       │
└────────────────────┘                                   └─────────────────┘
```

Figure 14.   Flow chart for sub-routine WAVEC of the program WCSTRANS

However, this formulation was intended for a situation where an irregular wave motion was represented by several wave components of arbitrary frequency and phase. The wave motion considered in the model is one with just two components that are in phase, one at twice the frequency of the other. The combined velocity, obtained by summing the components, will be periodic with the period of the principal component. The peak wave shear stress will also be observed once in every cycle.

279. Therefore it is more appropriate to base the wave shear velocity in this case on the peak wave shear stress as is done for the case of a single wave component. The wave shear stress, τ_W , is given by

$$\tau_W = \rho u_{*w}^2 = \tau_{w1} + \tau_{w2} = \rho(u_{*w1}^2 + u_{*w2}^2) \tag{119}$$

with the individual wave shear stresses, τ_{w1} and τ_{w2} , being obtained using Equation 34. u_{*w1} and u_{*w2} are the shear velocities corresponding to τ_{w1} and τ_{w2} . The combined shear velocity, u_{*wc} , is defined by Equation 20 .

280. The parameter μ is defined as the ratio of the current shear velocity, u_{*c} , to the wave shear velocity, u_{*w} , i.e.,

$$\mu = \frac{u_{*c}}{u_{*w}} \tag{120}$$

and the combined shear velocity, u_{*wc} , is related to u_{*w} and μ by the equation

$$u_{*cw}^2 = u_{*w}^2(1 + 2\mu^2\cos\phi_{cw} + \mu^4)^{1/2} \tag{121}$$

The evaluation of the wave shear stresses by Equation 34 requires a knowledge of the shear velocities, u_{*c} , u_{*w} , and u_{*wc} , which are denoted by the variables USC , USW , and USWC respectively. However, all these values are also unknowns that are obtained as part of the solution. If the subroutine has been called for the first time (i.e., the value of USW passed from the main program is zero) the program begins by assuming values for these parameters. On subsequent calls the values of

USC and USW are taken as the values passed from the main program (i.e., the values calculated during the previous iteration). Using the previous values makes the solution for USC and USW converge faster. The parameters ζ_0 , δ , and ϵ , represented by the variables ZE0 , EP , and DELTA , can be calculated using these values and the given bottom roughness.

281. The solution of the wave velocity problem is done by the sub-routine FINDUSWN . This sub-routine uses the input values of ZETA0 , EP , KAP, ALPHA , USWC , and σ . The parameter σ , defined by Equation 62, is the ratio of the frequency of the wave component to the representative frequency. The representative frequency for the wave motion in this problem is taken as the frequency of the principal wave component. Therefore the parameter σ , represented by the variable EN in the subroutine, will take the values 1.0 and 2.0 for the solutions of the principal and secondary wave components, respectively. The first call of FINDUSWN is made to obtain the solution for the principal wave component.

282. Using these input values sub-routine FINDUSWN calls the sub-routine TCONCCOEFF to calculate the five complex coefficients, in vector SOLU , of Equations 67, 69, and 72 that give the solution for the periodic velocity component. The magnitude of the wave shear velocity, variable USW , and the phase of the wave shear stress, variable PHIB , for the given component are evaluated using Equation 34. The output of FINDUSWN is the values USW , PHIB , and SOLU .

283. The shear velocity returned by FINDUSWN is the value obtained by assuming fully rough turbulent flow. When the roughness is very small, as will be the case when the grain diameter is used as the roughness for the skin friction problem, the flow may be in the smooth turbulent regime. Therefore the shear velocity corresponding to smooth turbulent conditions is calculated using the sub-routine SMOOTHT which incorporates the smooth turbulent friction factor curve of Jonsson (1967). The actual shear velocity is chosen to be the larger of these two values. The next step is to calculate the shear velocity due to the secondary wave component. This value is taken from the smooth or rough turbulent regime depending on the result of the calculation for the principal component. The total wave shear velocity, USW , is found from Equation 119.

117

284. Once the wave shear velocity is found the assumed value of the current shear velocity, USC , can be improved by considering the values that specify the current motion. The method of specification is indicated by the value FLAGC . If FLAGC = 1 , USC is simply set to the given value of the current shear velocity. If FLAGC = 2 or FLAGC = 3 , the value of USC is updated based on the difference between the given and calculated reference velocity or depth-averaged velocity.

285. New values of the parameters μ and ϵ , denoted by MU1 and EP1 , can be calculated using the updated values of the shear velocities. If the differences between the new and old values are greater than a certain tolerance the solution of the wave problem is repeated using the updated values of the shear velocites until the values of MU and EP converge. This loop in the sub-routine is shown in Figure 14.

286. For the pure wave problem the parameters MU and EP will be zero. The eddy vicosity distribution will be bi-linear and based on the wave shear velocity USW . The sub-routine assumes an initial value for USW , solves the velocity problems for the two components using FINDUSWN , and computes a new value of USW . This procedure is repeated until the value of USW converges.

Comparison of Model Predictions with Measured Mean Concentration and Flux Profiles

287. The predictions of the mean concentration and flux profiles made by the model will be compared with the measured profiles from the data sets VG and CW . While measurements of the mean concentration were also available for the data sets DK and MB these data sets were not used as the analysis in Part IV showed that these data may not be reliable. Therefore only the runs VG2046 and VG2047 of set VG and the single run of set CW were used. The calculations were the same as those for run VG2046 described in detail earlier in this part. The calculations for the data set CW were also carried out using the observed ripple height to obtain the bed roughness.

Mean Concentration

288. The predicted and measured mean concentration profiles for runs VG2046 and VG2047 are plotted in Figures 15 and 16, respectively. The
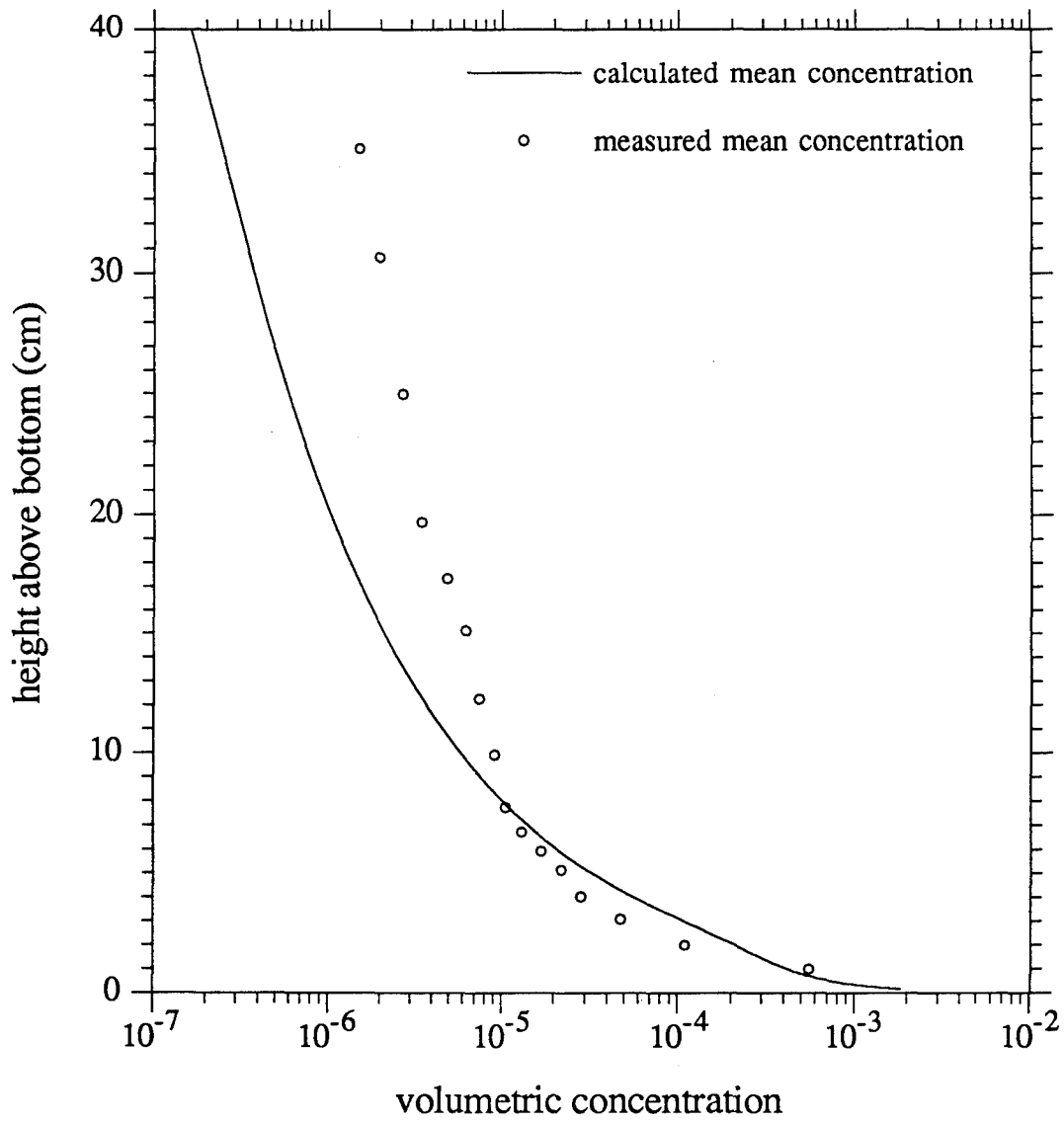
Figure 15. Comparison of predicted and measured mean concentration profiles for run VG2046 of data set VG
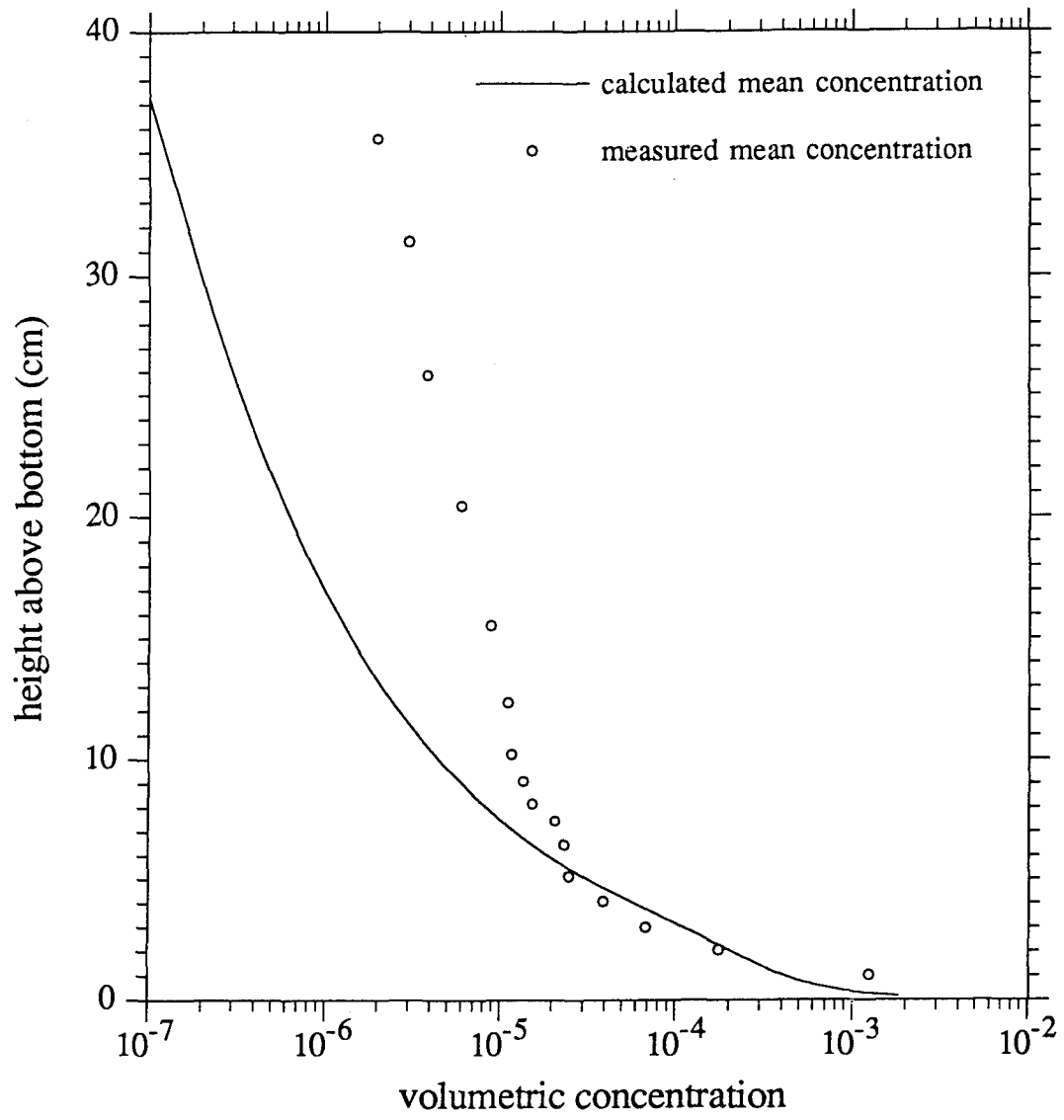
Figure 16. Comparison of predicted and measured mean concentration profiles for run VG2047 of data set VG

comparison for the set CW is shown in Figure 17 in which the predictions using both the observed and calculated bottom roughness are plotted. These figures show that the predicted values match the measured values near the bottom, with the predictions using the observed roughness showing better agreement for set CW than those made with the calculated roughness. This good agreement is hardly surprising in view of the fact that the value of γ_0 used for a rippled bed, which was the case for all three runs, was obtained using the same data sets.

289. Figures 15, 16, and 17 show that the predicted mean concentration drops off quicker than the observed values for all three sets, resulting in an increasingly large underprediction of the concentration as the height increases. It is this behaviour that causes the estimated value of γ_0 in Figures 8 and 9 to increase with increasing height. As pointed out in Part IV, the value of γ_0 that is predicted from the higher points would be much larger than those predicted from the lower points.

290. The differences at large elevations above the bed is probably due to a combination of the non-uniformity of the grain size and errors in the prediction of the shear velocities. Additional measurements that would reduce these uncertainities were discussed at the end of Part IV. The effect of considering a mixture of grain sizes will be considered in the next section.

291. Figure 17 shows that whereas using the observed roughness improves the agreement with the measurement for the set CW , the predictions are still much less than the measured value at heights greater than a few centimeters. The underprediction for this set is much larger than that for the comparisons with set VG in Figures 15 and 16. This difference may be due to the effects of non-uniform grain size being more important when the mean grain size is greater, as is the case for the CW data set.

292. Furthermore the fall velocity for the VG set was measured while it was estimated from the empirical relationship of Madsen and Grant (1976) for the CW data set. As shown in Part IV, this relationship was found to give a fall velocity of 2.8 cm/s for the VG set while the measured value was 2.25 cm/s. If the fall velocity for the CW data set is in reality less than the value predicted by the empirical relation the agreement

121
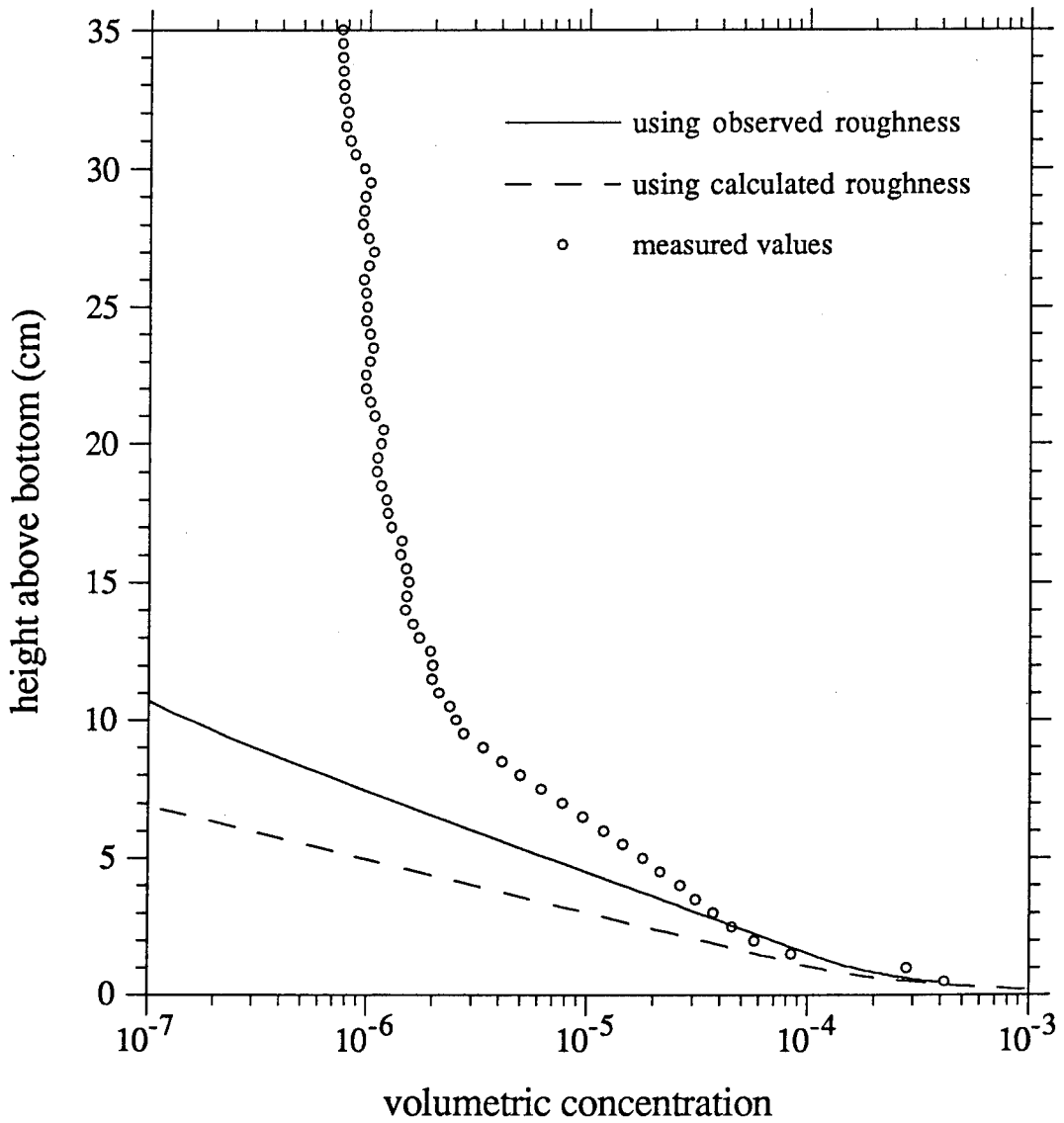
Figure 17. Comparison of the mean concentration profiles predicted using the observed and calculated roughness with the measured values for data set CW

between the predicted and measured concentrations in Figure 17 would improve.

293. An interesting feature of the observed mean concentration profiles is that they show different curvatures at different heights. This feature is particularly pronounced in the profile for the CW data set in Figure 17. The figure, which plots the logarithm of the concentration against the height, shows that the profile has a steeply decreasing bottom portion followed by a linear section of smaller slope that leads into another curved section that decreases more slowly with height. The observed profiles for runs VG2046 and VG2047 , in Figures 15 and 16, respectively, do not show such a well defined shape but a similar trend can be observed in Figure 16.

294. Comparing Figure 17 with Figure 3a shows that the observed mean concentration profile has a shape that agrees with the shape expected from the solution for the mean concentration given in Equations 50, 52 ond 54. However, while the shape of the observed profile is in agreement with the theory, the parameters a , δ , and ϵ that appear in Equations 50, 52, and 54 are different for the observed and predicted profiles. For example, the equations show that the levels at which the curvature changes are $z = a\delta$ and $z = a\delta/\epsilon$ for the lower and upper levels respectively. The slope of the linear section is given by a/δ .

295. These relations can be applied to the observed profile for the set CW to obtain approximate values of 4 cm , 0.22 , and 0.84 for the parameters δ , ϵ , and a , respectively. The model predicts values of 2.9 cm , 0.18 , and 1.13 for these parameters when the observed roughness is used. The boundary layer length scale, δ , which is defined by Equation 33, will increase with an increase in the combined shear velocity, u_{*cw} , and a decrease in the representative frequency, ω_r . The parameter a , defined in Equation 48, will decrease with a decrease in the fall velocity and an increase in u_{*cw} .

296. Therefore, if it is assumed that the eddy viscosity model of Equation 7 applies to the suspended sediment problem, the observed profile indicates some combination of a larger shear velocity, a smaller fall velocity, and a smaller representative frequency. For example, the shear velocity could be increased by using the significant wave velocity instead

of the root mean square value used to derive the values u_{b1} and u_{b2} in Equations 112 and 113. However, it is not possible to determine which of these parameters should be adjusted. If additional measurements, such as the fall velocity and the grain size distribution with height, had been made such an analysis may have resolved this issue.

Flux Profiles

297. The data sets VG and CW , described in Part IV, were obtained using an ABS instrument. This instrument measured the instantaneous suspended sediment concentration at several equally spaced points in the near bottom region. The instantaneous sediment flux is defined here as the product of the instantaneous concentration and velocity. However, the velocity in these experiments was measured at only a single point in the flow. Therefore, in order to obtain the flux profile, the velocity at each of the points at which the concentration was measured must be estimated.

298. Vincent and Green (1990) estimated the flux in several ways. The mean flux, i.e., due to the product of the mean velocity and concentration, was estimated using the predicted mean velocity from the wave-current model of Grant and Madsen (1979). The problem of estimating the instantaneous velocity over the whole depth was handled by Vincent and Green (1990) as follows. The measured velocity was split into a mean component and a wave-induced component. The wave-induced component above the wave boundary layer (as defined in the Grant and Madsen (1979) model) was assumed constant and equal to the measured irregular wave-induced velocity at 20 cm . The wave-induced component within the wave boundary layer was taken as the measured wave-induced value multiplied by an attenuation factor based on the solution for the wave velocity profile in the wave-current model. Finally, a temporal correction, based on the group speed of shallow water waves, was made to the velocity record to account for the fact that the EMCM and the ABS were 2 m apart.

299. Vincent and Green (1990) presented the mean and wave flux profiles estimated by this method. For the data set CW the time series of both velocity and concentration were available so that the fluxes could be estimated using the method described above with the mean velocity and attenuation factor based on the hydrodynamic solution of the present model.

The variation of the mean velocity and the attenuation factor with height is similar to the profiles shown in Figure 4.

300. The calculated and estimated flux profiles for runs VG2046 and VG2047 are shown in Figures 18 and 19. The figures are restricted to the first 10 cm above the bottom as the fluxes are quite small above this height. The wave flux was calculated as the sum of the fluxes due to the principal and secondary components. The figure shows that while the calculated flux profiles resemble the the estimated profiles in shape, the magnitude of the fluxes do not agree very well near the bed. The calculated mean and wave fluxes are the greatest at levels of 0.3 cm and 0.2 cm , respectively, while the lowest level of measurement is 1 cm .

301. As the height above the bed increases, both the estimated and calculated wave fluxes change sign and indicate a flux in the offshore direction, i.e., against the wave direction. However, the largest calculated values of the offshore wave fluxes are $2.6 \times 10^{-5} cm^3/cm^2/sec$ and $2.5 \times 10^{-5} cm^3/cm^2/sec$ for runs VG2046 and VG2047 , respectively, while the corresponding estimated values are $1.1 \times 10^{-4} cm^3/cm^2/sec$ and $1.4 \times 10^{-4} cm^3/cm^2/sec$, respectively. Figures 18 and 19 also show that the maximum offshore flux occurs at a slightly lower level for the estimated flux. The estimated offshore flux is sufficiently large to cause a net offshore flux between the levels $z = 3$ cm and $z = 8$ cm and the levels $z = 3$ cm and $z = 7$ cm for the runs VG2046 and VG2047 , while the calculated total flux is always onshore.

302. The calculated mean flux is greater than the estimated values in the region 2-7 cm above the bottom and less than the estimates above 7 cm . As the wave-current model used by Vincent and Green (1990) was quite similar to the model used here, and because the same current specification was used, these differences should be chiefly the result of under- or overprediction of the mean concentration. Inspection of the mean concentration profiles in Figures 15 and 16 shows that this explanation is correct.

303. The calculated and estimated flux profiles for the CW data set are shown in Figure 20. The calculated values were obtained using the observed bottom roughness. The mean fluxes are offshore because the observed mean velocity in the wave direction was offshore. The calculated
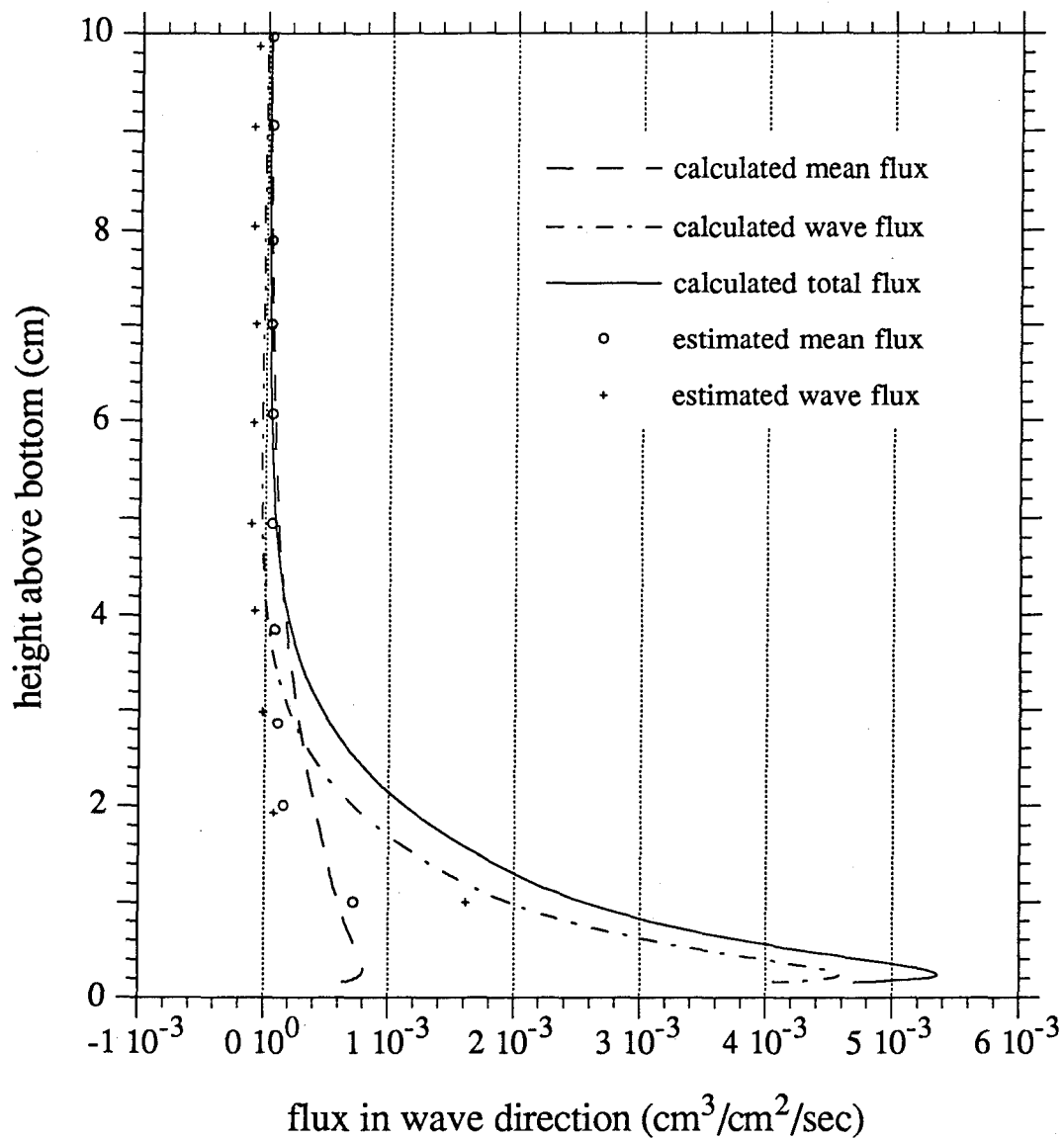
Figure 18. Predicted mean, wave and total flux profiles for run VG2046 of set VG compared to the estimated mean and wave flux profiles
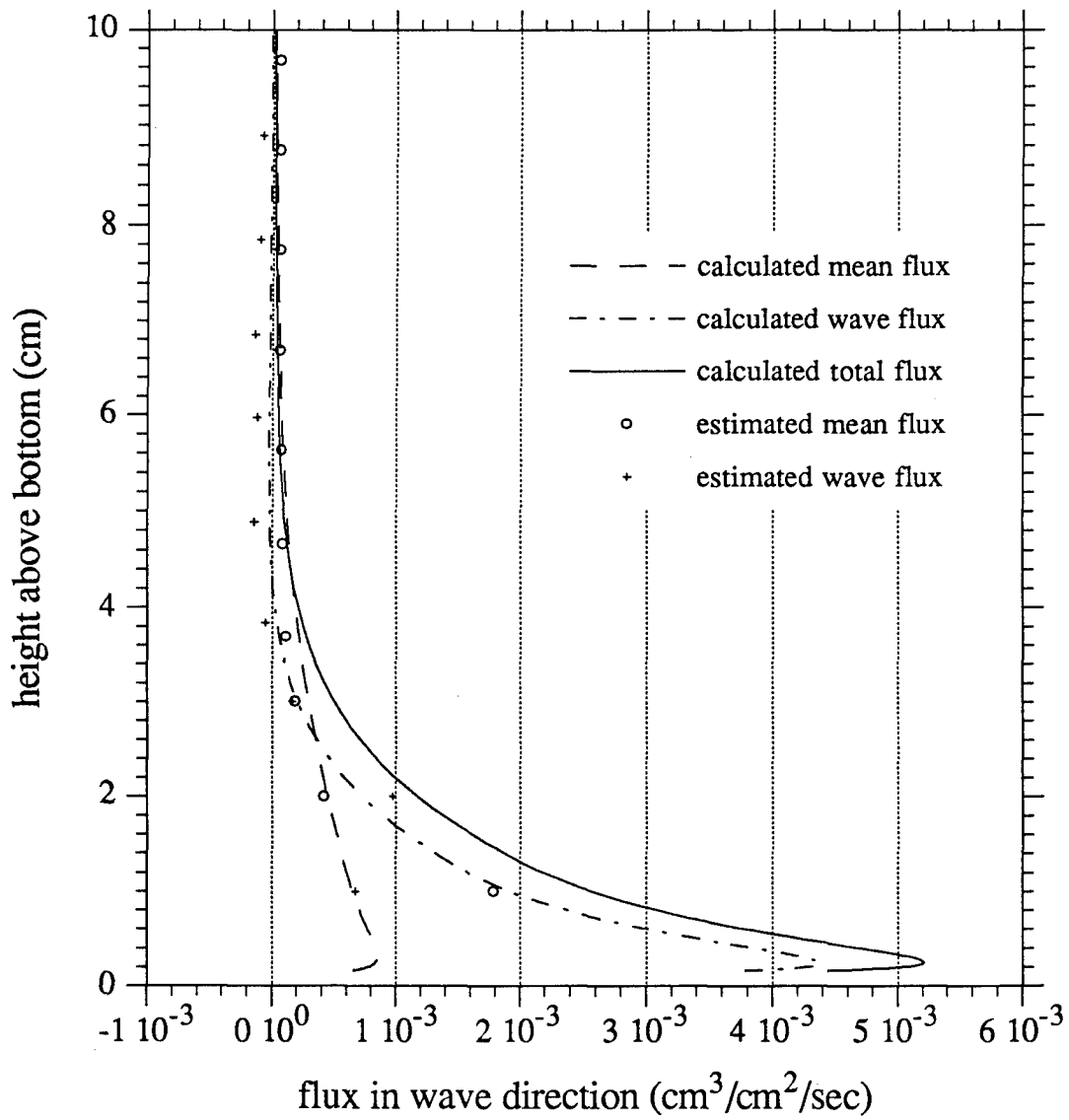
Figure 19. Predicted mean, wave and total flux profiles for run VG2047 of
set VG compared to the estimated mean and wave flux profiles
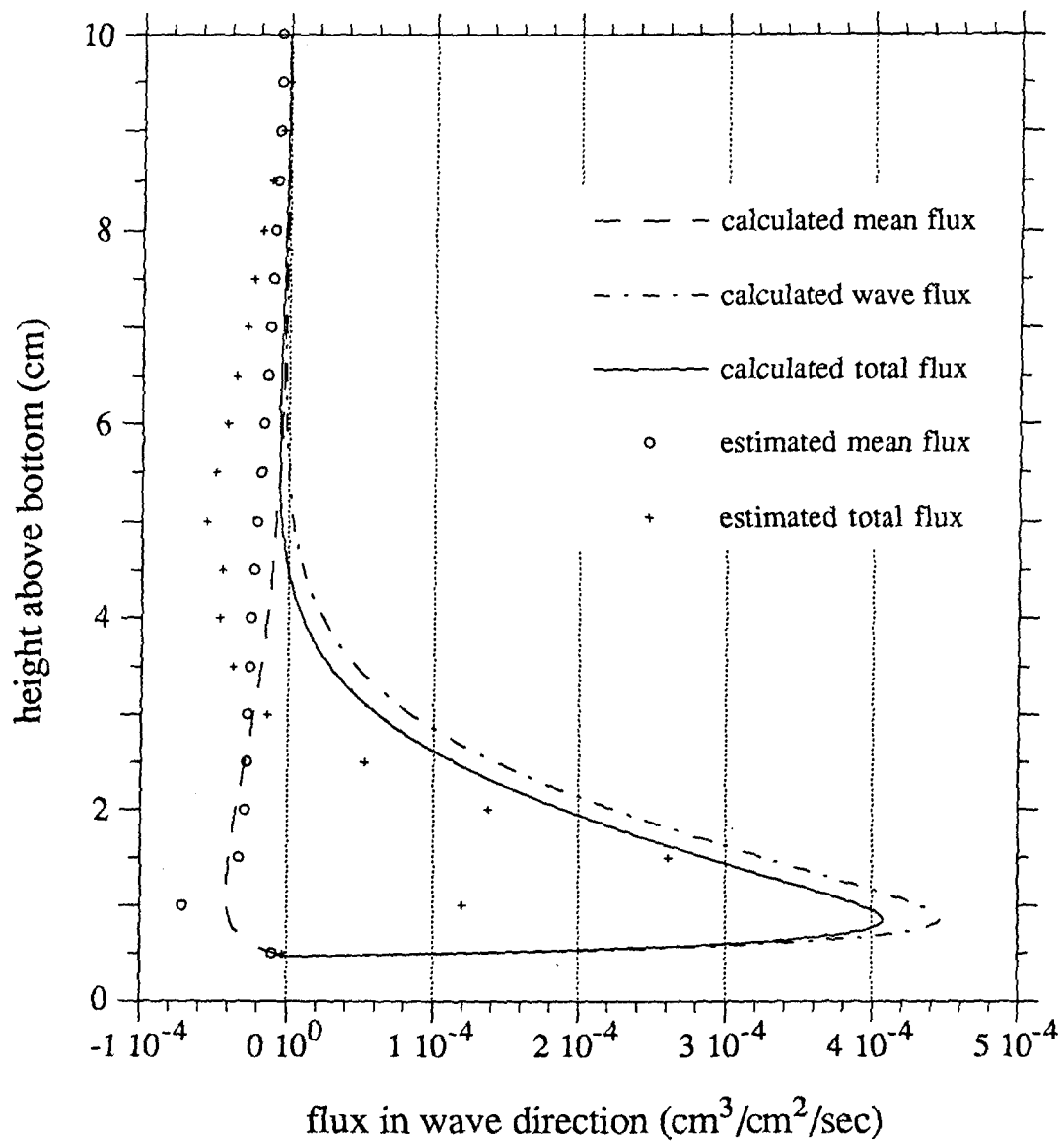
Figure 20. Mean, wave, and total flux profiles (predicted using the observed roughness) for set CW compared to the estimated mean and wave flux profiles

wave flux has a onshore maximum at about 0.8 cm and becomes offshore at about 5.4 cm . The estimated wave flux has a similar variation but the onshore peak is at about 1.5 cm and the flux becomes offshore at about 3 cm . The estimated values show quite a large offshore value of $6 \times 10^{-5} cm^3/cm^2/sec$ while the calculated offshore value is only about $2 \times 10^{-6} cm^3/cm^2/sec$.

304. Both the calculated mean and wave fluxes decrease with height more rapidly than the estimated values. This is because the predicted mean concentration, as shown in Figure 17, drops off much quicker than the observed values. The differences between the profiles in Figure 20 also show that the estimated profiles indicate a larger value of the boundary layer length scale, δ , than is calculated by the model.

305. The comparisons show that one of the most important differences between the calculated and estimated profiles is the relative magnitude of the mean and wave fluxes in the region $z = 3$ cm to $z = 8$ cm . The estimated wave flux in this region has a significant offshore value that is not shown in the calculated wave flux profile. A possible reason for this difference is that the calculated value of the periodic components decreases faster than the observed values. This decrease is probably important in the data set CW , where the predicted mean concentration also decreases faster than the observed value. However, another factor that enters the calculation of the wave flux is the phase difference between the velocity and the concentration components of the same frequency.

306. This phase difference is controlled by the type of boundary condition used for the periodic components. The calculations shown above were carried out using the boundary condition of Equation 93, which relates the reference concentration to the skin friction shear stress. This model was derived from models proposed for steady flow over flat beds. However, the beds over which the measurements for the data sets VG and CW were made were observed to be rippled. Vincent and Green (1990) present a short portion of the instantaneous concentration record obtained from the first 40 cm above the bed.

307. The record shows a pattern of suspension that is consistent with the entrainment from rippled beds by vortex shedding that was discussed in Part II. The reference concentration model of Equation 93 may not be the

appropriate model under these conditions. A model that does reflect the entrainment by vortex shedding would give different values for the ratios r1 and r2 of Equation 105 and lead to a difference in the relative magnitude of the mean and the wave fluxes.

Total Transport

308. The estimated flux profiles can be integrated over the depth to obtain estimates of the mean and wave suspended sediment transports. These values are presented in Table 14 along with the calculated bed-load and suspended load transports for runs VG2046 , VG2047 , and CW . The transport computations for the set CW were carried out using the observed roughness of 14.0 cm . The calculated values of the transports due to the principal and secondary components are calculated separately and then summed to obtain the wave transport.

309. Comparing the calculated and estimated transport rates for the data set VG shows that the mean transport rates for the run VG2046 are in good agreement while the agreement is not so good for run VG2047 . The reason for this difference is that the mean concentration prediction for VG2046 , shown in Figure 15, was greater than the observed value near the bottom and less at higher elevations. When the transport is computed these differences would tend to cancel each other out and result in a value close to the estimate. On the other hand, Figure 16 shows that the calculated concentration is almost always less than the observed value for run VG2047 resulting in the calculated mean transport also being less. Similarly, the calculated mean transport for the run CW was less than the estimated value because the calculated mean concentration decreased much more rapidly than the observed values.

310. The two runs VG2046 and VG2047 were taken within a period of 40 minutes and the hydrodynamic conditions are nearly identical. However, examination of the mean concentration profiles in Figures 15 and 16 and the transport estimates in Table 14 show that the mean concentration observed during run VG2047 is greater than that for run VG2047 by about a factor of 2 . The only possible explanation for this result within the framework of the present model is that the ripple height was significantly different for the two runs despite the wave and current motions being very similar. If this was not the case the observations indicate that mechanisms not

130

Table 14

Transport Calculations for Runs VG2046, VG2047, and CW

	Data Set		
	VG2046	VG2047	CW
	$10^{-4}\text{cm}^3/\text{cm/s}$	$10^{-4}\text{cm}^3/\text{cm/s}$	$10^{-4}\text{cm}^3/\text{cm/s}$
Calculated transports			
Suspended sediment transports			
Mean in wave direction	22.6	23.6	-1.3
Mean in wave-normal direction	-64.1	-43.9	-2.3
Principal wave	31.8	31.7	5.2
Secondary wave	12.0	11.5	2.0
Wave	43.8	43.2	7.2
Total	66.4	66.8	5.9
Bed load transport			
Wave direction	86.7	86.1	44.1
Wave-normal direction	-36.5	-25.3	-3.2
Estimated transport			
Mean in wave direction	19	40	-3.0
Wave	6	3	1.4
Total	25	43	1.6

Suspended sediment transports calculated using the lowest
measuring point as the lower level of integration

	VG2046	VG2047	CW
Mean in wave direction	16.6	17.2	-1.3
Principal wave	13.6	13.9	5.2
Secondary wave	2.9	2.8	2.0
Wave	16.5	16.7	7.2
Total	33.1	33.9	5.9

accounted for here play a significant role in the suspension process. An examination of the detailed velocity and concentration time series may shed some more light on this issue.

311. The calculations show that while the transport due to the secondary components are less than the transport due to the principal components they are still of the same order of magnitude. The calculated wave transport is significantly larger than the estimated values for all three runs. This difference is due to the larger negative values seen in the estimated wave fluxes of Figures 18, 19, and 20 which tend to cancel out the positive values near the bottom. Another possible reason is that the calculated transport is obtained by integrating the flux from the lower of the levels $z_0 = k_n/30$ and $z_r = 7d$, while the estimated values are integrated from the lowest measuring value.

312. Table 14 also includes calculations of fluxes where the lower limit was set to the level of the lowest measurement. The wave fluxes computed in this way for the runs VG2046 and VG2047 are reduced significantly, though they are still larger than the estimated values. The use of the lowest level, $z = 0.5$ cm , does not cause much change in the values for the set CW because the level z_0 is 0.47 cm , a value that is very close to the lowest measurement level.

313. The table also shows that the calculated bed-load transport is greater than the total suspended load transport for all three runs. This result is contrary to the results of Goud (1988) who used the model of Glenn and Grant (1987) and found that the bed-load transport was generally negligible. However, Goud (1988) carried out calculations for sand sizes ranging from 0.002 cm to 0.02 cm while the sand sizes for the data sets considered here were 0.023 cm and 0.03 cm . When the grain size decreases there will be much more sediment in suspension leading to an increase in the suspended sediment transport relative to the bed load transport. Another reason for the increased importance of the bed-load is that the model presented here includes the effect of wave asymmetry, a factor which will increase the net bed-load transport.

The Effect of Non-uniform Grain Size

314. The comparisons of the calculated and observed mean concentration profiles in the preceding section showed that while the values agreed quite

well in near bottom region, the predicted profiles decreased more rapidly than the observed values in the upper region of the flow. The most probable cause of this discrepancy is the existence of a mixture of grain sizes in the bed. The smaller grain sizes would be suspended to higher elevations and the result would be an increase in the computed concentration at these elevations compared to the value that would be obtained using the mean grain size as the representative diameter.

315. Vincent and Green (1990) measured the fall velocity of 100 grains from a bottom sample and found the fall velocity to be normally distributed with a mean of 2.25 cm/s and a standard deviation of 0.36 cm/s . These values indicate that the non-uniformity of the grain size may be a significant factor in the modeling of this experiment. Therefore the model of this report, which was based on a single grain size, will be extended in a relatively simple fashion to account for the effect of non-uniform grain size in this section.

316. The different grain sizes will be considered only for the calculation of the suspended sediment profiles. The model calculations up to this point, i.e., up to the calculation of the reference concentration, will be done using the mean grain diameter. The reference level will be taken as $7d_m$ where d_m is the mean diameter.

317. This method implies that if p_i is the volume fraction of the size class d_i in the bed, the mean reference concentration for that class, $\overline{c_{ri}}$, would be given by

$$\overline{c}_{ri} = p_i\overline{c}_r \tag{122}$$

where $\overline{c}_r$ is the mean reference concentration calculated using the mean grain diameter. Equation 122 shows that according to this formulation the proportion of the different size classes available for suspension at the reference level $7d_m$ is the same as the proportion of the size classes in the bed. Though this method of calculating the reference values may be oversimplified, the objective here is to investigate the effect of non-uniform grain size on the mean concentration profile while keeping the other factors the same.

318. As an example, the calculations will be carried out for run VG2046 of set VG . The grain size distribution will be represented by five size classes. The selected diameters and fall velocities for these classes are given in Table 15. These values have been selected so that the fall velocity is approximately normally distributed with the measured standard deviation.

319. The calculated mean reference concentration will be exactly the same as the value given in Table 9 for the example calculation. The reference concentration for each size class is found from Equation 122. The mean concentration profiles for each class are calculated using Equations 50, 52, and 54. The only parameter in this equation that has a different value for each size class is the non-dimensional fall velocity, a , defined by Equation 48. The values of a for each size class are given in Table 1. Once the mean concentration profiles for each class are calculated they can be summed to obtain the total concentration.

320. The calculated mean concentration profile is shown in Figure 21, along with the observed profile and the profile calculated using the mean grain size. The figure shows that the use of many grain size classes increases the concentration in the region more than 10 cm above the bottom. While the profile with many grain sizes is still not in full agreement with the observed profile, it accounts for about half the difference (in logarithmic terms) between the observed profile and the profile computed with a single grain size.

321. The concentrations of the different size classes at any level can be used to calculate a mean grain size for that level. The variation of the mean grain size with height above the bottom is shown in Figure 22. The figure shows that the mean grain size decreases linearly above the level $z = 7$ cm . This result agrees with the measurements of Hay (1992), who used a multi-frequency ABS instrument to obtain the variation of the grain size distribution with the height above the bottom. He found that the mean grain size decreased linearly above the wave boundary layer, with a change of about 25% over 50 cm .

322. The decrease in grain size with height will have an effect on the interpretation of the measured backscattered acoustic signal in terms of the concentration. Vincent and Green (1990) calibrated their ABS

Table 15

Parameters of the Different Grain Size Classes Used

to Simulate the Grain Size Distribution for Run VG2046

Size class i	Grain diameter d_i (cm)	Fall velocity wf_i (cm/s)	Proportion of bed p_i	Non-dimensional fall velocity a_i
1	0.0273	2.97	0.09	1.136
2	0.0252	2.61	0.24	0.998
3	0.023	2.25	0.34	0.860
4	0.0208	1.89	0.24	0.723
5	0.0185	1.53	0.09	0.585
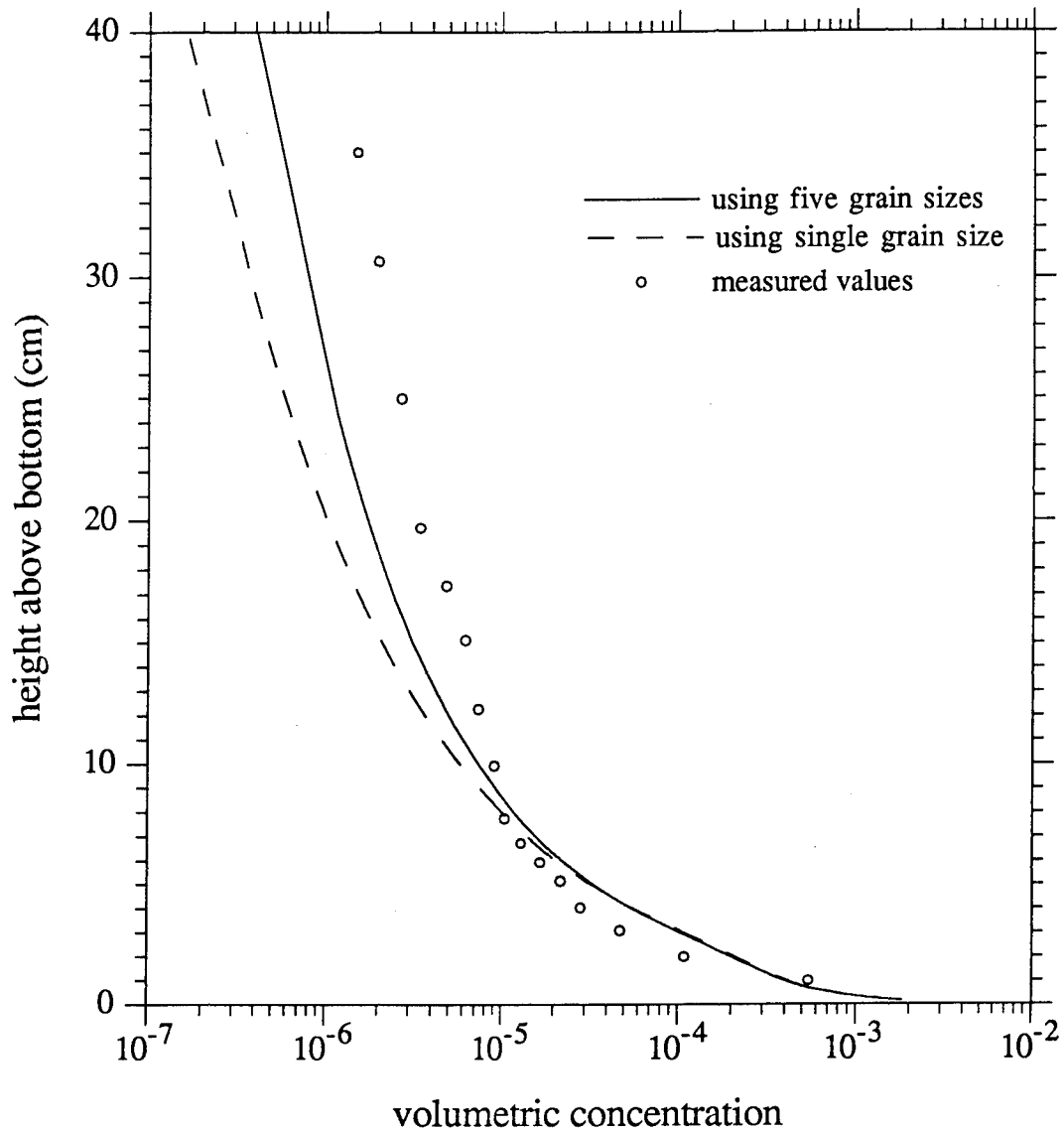
Figure 21. Mean concentration profile calculated using the grain size classes in Table 16 compared to the observed profile and the profile obtained with a single grain size, for run VG2046 of data set VG

136
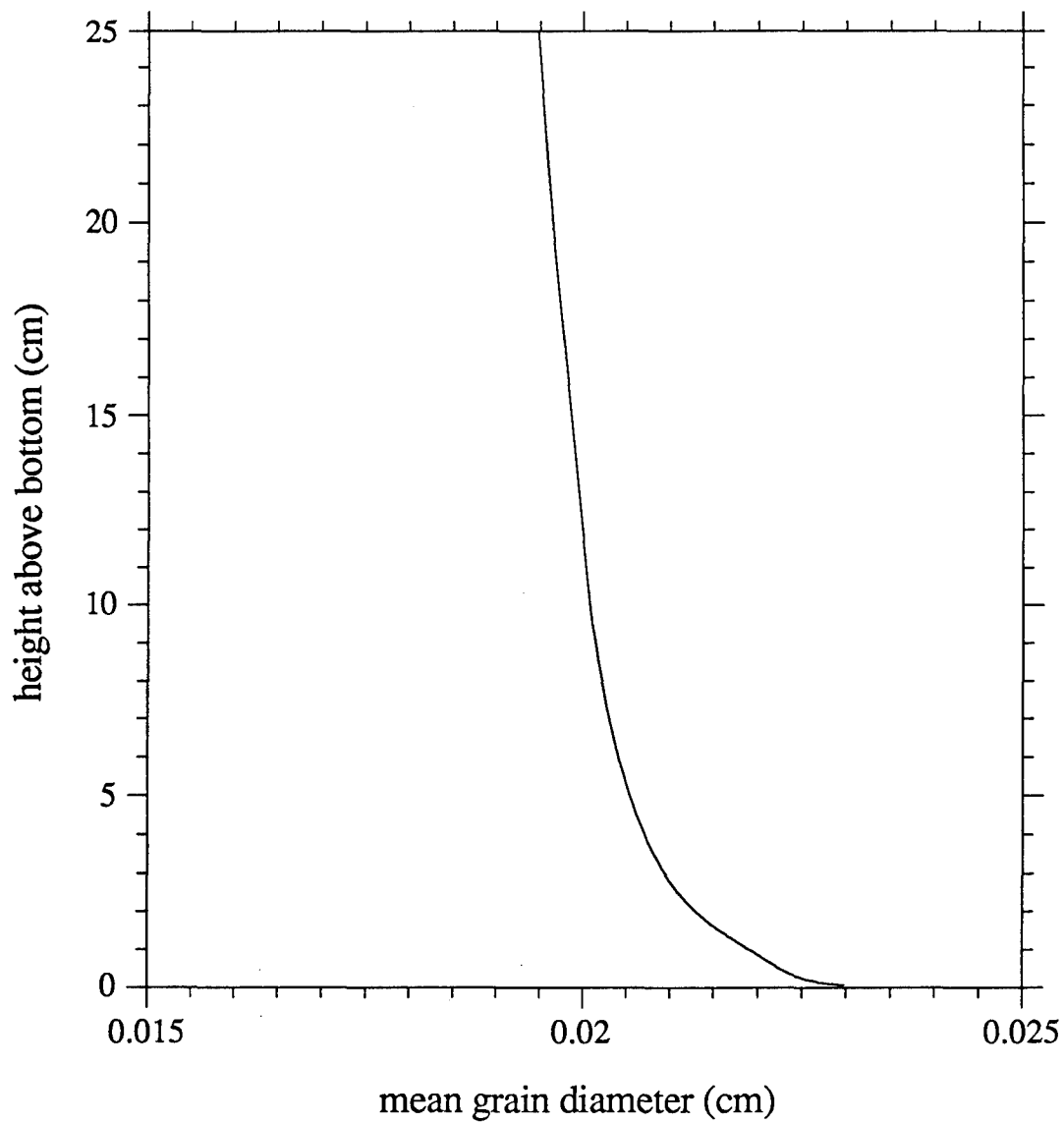
Figure 22. Variation of mean grain diameter with height for the calculation using the grain size classes of Table 16 for run VG2046 of data set VG

instrument using a sample of sand from the bottom. As the calibration is sensitive to the grain size distribution there is some uncertainity associated with the measurements at the higher levels because, as shown in Figure 22, the mean grain size at these elevations has decreased appreciably from the value at the bottom.

323.   The simple calculation presented in this section shows that non-uniformity of the bottom sediment could be the reason for the disparity observed between the computed and observed mean concentration profiles in the preceding section.   There are also other factors, such as an errors in the calculated current shear stress and uncertainity in the calibration, that are significant.   The relative effect of these factors can only be analyzed if the additional measurements discussed at the end of Part IV are available.

PART VI: SUMMARY AND CONCLUSIONS

324. The objective of this study was to investigate the application of simple eddy viscosity models, developed for wave-current interaction, to the problem of sediment suspension and transport. The motivation for this study was twofold. First, while the model of Glenn and Grant (1987) has been proposed and used widely for the calculation of suspended sediment in wave-current flows, the hydrodynamic aspect of this model was improved upon by the models of Madsen and Wikramanayake (1991).

325. Second, and more importantly, all proposed models calculate the suspended sediment transport by integrating the product of mean concentration and mean velocity. However, recent field experiments indicate that the flux due to the time-varying quantities is as important and sometimes dominates the flux due to the mean components. Therefore, the model developed in this report calculates the time-varying component of the concentration along with the mean.

326. After considering the ease of solution and the relatively small differences in the results compared to the uncertainties of the suspended sediment problem, the time-invariant eddy viscosity model of Madsen and Wikramanayake (1991) was chosen over the time-varying model of the same authors. The model was extended to include a wave motion specified by several periodic components. The solution for the various concentration components is derived in Part III. It was found that the solution for the periodic velocity components was a special case of the solution for the concentration components, thus allowing the solutions to be combined in the program. The magnitude of these components was found to be scaled by the reference concentration specified near the bottom. Second-order effects, such as those due to the vertical wave velocity, and the stratification induced by suspended sediment were ignored in the solution of the governing equation in Part III.

327. As most equations for the reference concentration were based on formulations of the bed load transport and also because it was desirable to calculate the bed load transport for comparison with the suspended load transport, the conceptual bed load model of Madsen (1991) was reviewed. Madsen (1991) showed that two different conceptual models, one for

139

transport by rolling and sliding and the other for transport by saltation, led to the conclusion that a generalized form of the Meyer-Peter Muller formula was suitable for the calculation of bed load transport in wave-current flows.

328. A review of the various formulations proposed for the mean reference concentration showed that while the most commonly used model was that of Smith (1977), comparison with field and experimental data cast doubts on its validity. However, the analysis of steady flow data by Zettler (1991) did suggest that the reference concentration was proportional to the non-dimensional excess shear stress, S' , for a particular grain size for fine-grained sands. As this conclusion was also supported by the saltation model of Madsen (1991), the simple relation of Equation 91 was selected for the mean reference concentration.

329. Considering the time-varying components of the reference concentration the review did not find any model that had been compared to experimental data. However, bearing in mind the demonstration by Madsen (1991) that the near-bed sediment grains can be assumed to respond instantaneously to changes in the external flow, it was decided to use Equation 93, which extended Equation 91 to relate the time-varying reference concentration to the instantaneous value of S' .

330. Two other parameters that must be specified as part of the reference concentration model are the reference level and the resuspension parameter γ_0 . Using the predictions for the height of the saltating layer of Madsen (1991) the reference level is selected as 7d , where d is the grain diameter. The value of γ_0 was chosen after comparison with field measurements in Part IV. The reference concentration model selected is a function of the skin friction shear stress, i.e., the shear stress exerted on the grains alone. A method of calculating this component that was more consistent with the wave-current model than the method proposed by Glenn and Grant (1987) was derived. An outline of the procedure used to derive the reference values of the mean, first and second harmonic components of the concentration from the variation of Equation 93 concluded the model development of Part III. This derivation was done for the case where an asymmetric wave motion is simulated by the two wave components that are in phase, with one having twice the frequency of the other.

140

331. The only undetermined parameter in the model was the resuspension coefficient, γ_0 , which is the constant of proportionality in Equation 93. The determination of γ_0 was presented in Part IV. It was decided to use concentration measurements from recent field experiments, some of which extended very near to the bed, for this purpose. After a thorough analysis it was concluded that the data sets VG , CW , and CC , obtained by Vincent and Green (1990), Vincent and Osborne (personal communication), and Hanes (1991), were the most reliable of the data sets considered.

332. The selected values of γ_0 are given in Equation 115. This equation indicates different values of γ_0 depending on whether the bed is rippled or flat. Some recent measurements by Vincent et al. (1991) indicate that there may be a smooth transition between the two values of Equation 115 as the ripples on the bed are washed away. The possible variation of γ_0 can be investigated by using data sets obtained from a wide range of wave, current, and sediment conditions.

333. The various uncertainties present in the calculation of γ_0 were discussed in detail in Part IV. The effect of all these uncertainties is reflected in the scatter of the estimates of γ_0 because it is the only free parameter in the model. The discussion of this aspect brought out some important measurements that can be made to minimize the uncertainty and provide checks of the internal consistency of field data. The measurements include

a) Measurement of the concentration as close to the bed as possible, preferably within a few multiples of the boundary layer length scale, δ , defined in Equation 11.

b) Measurement of the variation of the grain size distribution with height above the bottom. This can be done by actually collecting samples or by using a multi-frequency ABS instrument as done by Hay (1992).

c) Measurement of the mean velocity at more than one point in the vertical. Such measurements would provide a check on the current shear velocity, u_{*c}, and the bed roughness, k_n, which are calculated by the model.

d) Measurement of the bed forms during the experiment.

e) Measurement of the fall velocity.

334. The program WCSTRANS that carries out the model calculation was described in detail in Part V. This program calculates the velocity, concentration, and flux profiles and the bed load and suspended load transport. The wave motion can be prescribed either as a single wave component or as two components in phase, one with twice the frequency of the other, in order to simulate wave asymmetry. A listing of the program is given in Appendix B. The use of the program is outlined by two example calculations.

335. The calculated mean concentration and mean and wave flux profiles were compared to the observed values for the data sets VG and CW. The computed values were in good agreement with the measurements close to the bed. This agreement was to be expected because the selected value of γ_0 was chosen to fit these near-bed values. However, the predicted and observed mean concentration profiles diverged as the height increased. This divergence may have been due to non-uniformity of the grain size or the use of an incorrect value for the current shear velocity.

336. Observation of the shape of the observed mean concentration profiles showed that while their shape corresponded to the theoretical solution of Equation 10, these shapes indicated values of the parameters δ, ϵ, and a that were different from the calculated values. Again this difference could be caused by errors in the fall velocity or the shear velocity. However, it is not possible to distinguish among these possibilities because of the lack of additional measurements discussed earlier.

337. The calculated flux profiles were found to reproduce the shape of the estimated flux profiles quite well. However, the calculated wave flux did not show as large an offshore component as the estimated value. A possible reason for this difference is the use of Equation 93 for the reference concentration. The wave conditions and the observations of the suspended sediment concentration suggest a rippled bed for this experiment. The variation of the instantaneous concentration in Equation 93 was derived from the physical idea of entrainment from a thin bed load layer in a steady flow. While this idea may also apply in the case of a wave motion over a flat bed, i.e., condition of sheet flow, the situation is very different when ripples are present on the bed.

338. As described in Part II entrainment from a rippled bed has been observed to be caused by the periodic shedding of sand-filled vortices from the ripple crests. It is obvious that any reference concentration proposed to account for this process would vary strongly with time. Furthermore as the entrainment process is controlled by the reversal of the near-bottom flow and not by the bottom shear stress a form similar to Equation 93 may not be suitable.

339. It was noted that there has been no investigation of the time-variation of the reference concentration using experimental data. However, there are some experiments where the time variation of the concentration has been measured at various heights above the bottom. In the laboratory there have been the experiments of Horikawa, Watanabe, and Katori (1982) and Staub, Jonsson, and Svendsen (1984) over a flat bed, and those of Homma, Horikawa, and Kajima (1965), Nakato et al. (1977), Sleath (1982), and Hayakawa, Tsujimoto, and Hashimoto (1983) over a rippled bed.

340. These measurements could be used to develop a time-varying reference concentration over a rippled and a flat bed. An example of the laboratory measurements are the concentration records of Nakato et al. (1977) shown in Figure 1, which were made very close to a rippled bed under a pure wave motion. In the development of the governing equation for suspended sediment it was mentioned that the concentration was defined as the average value over a ripple length when ripples were present. Therefore in this case a possible method of developing a reference concentration from the data would involve averaging the records over a crest and a trough and using the result to develop a time-varying reference concentration.

341. The reference concentration model thus developed could be tested against detailed field data such as the measurements of Hanes (1991) shown in Figure 2. The comparison would be made either with a portion of the record, such as that shown in Figure 2, or with the spectrum of the concentration that is derived from the entire record. These are some possible methods of extending and developing the reference concentration model to account for a rippled bed.

342. The bed load transport calculation showed that the bed load transport was larger than the suspended load transport, though the two

values are of the same order of magnitude. This result is contrary to some previous calculations, which, however, were carried out for finer sediments than those observed in these experiments. A final decision on the relative importance of the bed load transport must be deferred until calculations are made for a wide range of wave, current, and sediment conditions. The bed load transport equation, Equation 85, has had only limited experimental verification under wave-current conditions. Such verification could be carried out using the recent experimental measurements made by Ribbenick and Al-Salem (1992) in a large wave tunnel.

343. The effect of a mixture of grain sizes was investigated by using a simple formulation of the reference concentration. A calculation was made using a grain size distribution selected to match the values observed by Vincent and Green (1990). The calculation of the mean concentration showed better agreement with their measurements than the calculation made using a simple grain diameter. The variation of the mean grain diameter with height above the bottom was found to agree with recent field measurements.

344. In summary it can be said that the model developed in this report is in fairly good agreement with available data. It is encouraging that the model was able to reproduce the shape of the wave flux profiles estimated from the field data despite the use of a boundary condition that was not derived for the case of a rippled bed. Some areas that require further investigation are the variation of γ_0 with different hydrodynamic conditions and grain diameters and the appropriate reference concentration for rippled beds. Further refinement of the model would require comparison with more detailed and comprehensive measurements than the sets used here.

REFERENCES

Abramowitz, M., I. A. Stegun (eds.). 1971. Handbook of Mathematical Functions, Dover Press, New York, New York.

Bakker, W. T. 1974. "Sand Concentration in an Oscillatory Flow," Coastal Engineering, Proceedings of the 14th International Conference, pp 1129-1148.

Bedford, K. W., O. Wai, R. Van Evra, P. Velissariou, J. Lee, C. Libicki. 1990. "The local near-bottom response of a dredged material placement site to wind and tide effects," Report prepared for the U.S. Army Corps of Engineers, Waterways Experiment Station, Coastal Engineering Research Center.

Davies, A. G., Soulsby, R. L., King, H. L. 1988. "A Numerical Model of the Combined Wave and Current Bottom Boundary Layer," Journal of Geophysical Research, Vol. 93, No. C1, pp 491-508.

Doering, J. C., Bowen, A. J. 1988. "Wave-Induced Flow and Nearshore Suspended Sediment," Coastal Engineering, Proceedings of the 21st International Conference, pp 1452-1463.

Drake, D. E., Cacchione, D. A. 1989. "Estimates of the Suspended Sediment Reference Concentration and the Resuspension Coefficient from Near-Bottom Observations on the California Shelf," Continental Shelf Research, Vol. 9, pp 51-64.

Einstein, H. A. 1950. "The bedload function for sediment transportation in open channels," Tech. Rep. 1026, U.S. Dept. of Agriculture, Soil Conservation Service.

Engelund, F., Fredsoe, J. A. 1976. "Sediment Transport Model for Straight Alluvial Channels," Nordic Hydrology, Vol. 7, pp 293-306.

Fredsoe, J., Anderson, O. H., Silberg, S. 1985. "Distribution of Suspended Sediment in Large Waves," Journal of Waterway, Port, Coastal and Ocean Engineering (ASCE), Vol. 111, No. 6, pp 1041-1059.

Glenn, S. M., Grant, W. D. 1987. "A Suspended Sediment Correction for Combined Wave and Current Flows," Journal of Geophysical Research, Vol. 92, No. C8, pp 8244-8264.

Goud, M. R. 1987. Prediction of Continental Shelf Sediment Transport using a Theoretical Model of the Wave-Current Boundary Layer, Ph.D. Thesis, Woods Hole Oceanographic Institution/Massachusetts Institute of Technology, Cambridge, Massachusetts.

Grant, W. D., Madsen, O. S. 1979. "Combined Wave and Current Interaction with a Rough Bottom," Journal of Geophysical Research, Vol. 84, No. C4, pp 1797-1808.

Grant, W. D., Madsen, O. S. 1982. "Movable Bed Roughness in Unsteady Oscillatory Flow," Journal of Geophysical Research, Vol. 87, No. C1, pp 469-481.

Greenwood, B., P. D. Osborne, A. J. Bowen, D. G. Hazen, A. E. Hay. 1990. "Nearshore sediment flux and bottom boundary dynamics: The Canadian coastal sediment transport programme (C-COAST)," Proc. 22nd Coastal Engineering Conference (ASCE) pp 2227-2240.

Greenwood, B., Osborne, P. D., Bowen, A. J. 1991. "Measurements of Suspended Sediment Transport: Prototype Shorefaces," Coastal Sediments '91, Proceedings of the ASCE Specialty Conference, pp 284-299.

Hagatun, K., Eidsvik, K. J. 1986. "Oscillating Turbulent Boundary Layer with Suspended Sediments," Journal of Geophysical Research, Vol. 91, No. C11, pp 13045-13055.

Hanes, D. M. 1991. "Suspension of Sand Due to Wave Groups," Journal of Geophysical Research, Vol. 96, No. C5, pp 8911-8915.

Hanes, D. M., Huntley, D. A. 1986. "Continuous Measurements of Suspended Sand Concentration in a Wave Dominated Nearshore Environment," Continental Shelf Research, Vol. 6, No. 4, pp 585-596.

Hay, A. E. 1992. "Vertical profiles of suspended sand concentration and size from multifrequency acoustic measurements," J. of Geophys. Res. (Oceans), in press.

Hayakawa, N., Tsujimoto, G., Hashimoto, H. 1983. "Velocity Distribution and Suspended Sediment Concentration Over Large Scale Ripples," Coastal Engineering in Japan, Vol. 26, pp 91-100.

Hildebrand, F. B. 1976. Advanced Calculus for Applications, Prentice-Hall, Englewood Cliffs, New Jersey, 2nd Ed.

Hill, P. S., A. R. M. Nowell, P. A. Jumars. 1988. "Flume evaluation of the relationship between suspended sediment concentration and excess boundary shear stress," J. Geophys. Res., Vol. 93, pp. 12,499-12,509.

Hom-ma, M., Horikawa, K., Kajima, R. A. 1965. "Study on Suspended Sediment Due to Wave Action," Coastal Engineering in Japan, Vol. 8, pp 85-103.

Horikawa, K., Watanabe, A., Katori, S. 1982. "Sediment Transport Under Sheet Flow Conditions," Coastal Engineering, Proceedings of the 18th International Conference, pp 1335-1352.

Huntley, D. A., Hanes, D. M. 1987. "Direct Measurement of Suspended Sediment Transport," Coastal Sediments '87, Proceedings of the ASCE Specialty Conference, pp 723-737.

Inman, D. L., A. J. Bowen. 1963. "Flume experiments on sand transport by waves and currents," Coastal Engineering Proc. of the 8th Int. Conf., pp. 137-150.

Jonsson, I. G. 1967. "Wave boundary layers and friction factors," Proc. 10th Conf. Coastal Engineering, Tokyo 1966, Vol. 1, pp 127-148.

Kennedy, J. F., Locher, F. A. 1972. "Sediment Suspension by Water Waves," Waves on Beaches, R. E. Meyer (ed.), Academic Press, pp 249-295.

Kim, S. C. 1990. "Inner Continental Shelf Benthic Boundary Layer Dynamics and Suspended Sediment Transport," Ph.D. Thesis, School of Marine Science, College of William and Mary in Virginia.

Madsen, O. S. 1991. "Mechanics of Cohesionless Sediment Transport in Coastal Waters," Coastal Sediments '91, Proceedings of the ASCE Specialty Conference, pp 15-27.

Madsen, O. S. 1992. "Spectral wave-current bottom boundary layer flows," to be presented at the 23rd Int. Conf. on Coastal Engineering, Venice, Italy.

Madsen, O. S., W. Grant. 1976. "Sediment Transport in the Coastal Environment," Report No. 209, Ralph M. Parsons Laboratory, Dept. of Civil Engineering, MIT, Cambridge, Mass.

Madsen, O. S., Wikramanayake, P. N. 1991. "Simple Models for Turbulent Wave-current Bottom Boundary Layer Flow," Final Report, submitted to the U.S. Army Corps of Engineers, Coastal Engineering Research Center.

Madsen, O. S., L. D. Wright, J. D. Boon, T. A. Chisholm. Wind Stress, Bottom Roughness and Sediment Suspension on the Inner Shelf during an Extreme Storm Event," submitted to Continental Shelf Research.

Nakato, T., Locher, F. A., Glover, J. R., Kennedy, J. F. 1977. "Wave Entrainment of Sediment from Rippled Beds," Journal of Waterway, Port, Coastal and Ocean Engineering (ASCE), Vol. 103, No. WW1, pp 83-99.

Nielsen, P. 1979. "Some Basic Concepts of Wave Sediment Transport: Lyngby, Denmark," Series Paper No. 20, Institute of Hydrodynamics and Hydraulic Engineering, Technical University of Denmark.

Nielsen, P. 1983. "Analytical Determination of Nearshore Wave Height Variation Due to Refraction, Shoaling and Friction," Coastal Engineering, Vol. 7, pp 233-251.

Nielsen, P. 1986. "Suspended Sediment Concentrations Under Waves," Coastal Engineering, Vol. 10, pp 23-31.

Nielsen, P. 1988. "Three Simple Models of Wave Sediment Transport," Coastal Engineering, Vol. 12, pp 43-62.

Osborne, P. D., B. Greenwood. 1992. "Frequency Dependent Cross-Shore Suspended Transport: 1, A Non-Barred Shoreface," Marine Geology, Vol. 106, pp 1-24.

Ribberink, J. S., A. Al-Salem. 1992. "Sediment Transport, Sediment Concentrations and Bedforms in Simulated Asymmetric Wave Conditions," Report H 840 Part V, Delft Hydraulics, Delft, The Netherlands.

Sato, S. 1992. "Sand Transport under Wave Groups," to be presented at the 23rd Int. Conf. on Coastal Engineering, Venice, Italy.

Shi, N. C., Larsen, L. H., Downing, J. P. 1985. "Predicting Suspended Sediment Concentration on Continental Shelves," Marine Geology, Vol. 62, pp 255-275.

Skafel, M. G., Krishnappan, B. G. 1984. "Suspended Sediment Distribution in Wave Field," Journal of Waterway, Port, Coastal and Ocean Engineering (ASCE), Vol. 110, No. 2.

Sleath, J. F. A. 1982. "The Suspension of Sand by Waves," Journal of Hydraulic Research, Vol. 20, No. 5, pp 439-452.

Smith, J. D. 1977. "Modeling of Sediment Transport on Continental Shelves," The Sea, Vol. 6., Goldberg, E. D., ed., Wiley Interscience: John Wiley and Sons, New York, pp 539-577.

Smith, J. D., Mclean, S. R. 1977. "Spatially Averaged Flow Over a Wavy Surface," _Journal of Geophysical Research_, Vol. 82, No. 12, pp 1735-1745.

Soulsby, R. L. 1991. "Aspects of Sediment Transport by Combined Waves and Currents," in Proc. IAHR International Symposium on the Transport of Suspended Sediments and its Mathematical Modelling, Florence, Italy.

Staub, C., Jonsson, I. G., Svendsen, I. A. 1984. "Variation of Suspended Sediment in Oscillatory Flow," _Coastal Engineering, Proceedings of the 19th International Conference_, pp 2310-2321.

Thorne, P. D., C. E.Vincent, P. J.Hardcastle, S. Rehman, N. Pearson. 1991. "Measuring Suspended Sediment Concentrations Using Acoustic Backscatter Devices," _Marine Geology_, Vol. 98, pp 7-16.

Vincent, C. E., Green, M. O. 1990. "Field Measurements of the Suspended Sand Concentration Profiles and Fluxes and of the Resuspension Coefficient Over a Rippled Bed," _Journal of Geophysical Research_, Vol. 95, No. C7, pp 11591-11601.

Vincent, C. E., D. M. Hanes, A. J. Bowen. 1991. "Acoustic Measurements of Suspended Sand on the Shoreface and the Control of Concentration by Bed Roughness," _Marine Geology_, Vol. 96, pp 1-18.

Vongvissesomjai, S. 1986. "Profile of Suspended Sediment Due to Wave Action," _Journal of Waterway, Port, Coastal and Ocean Engineering (ASCE)_, Vol. 112, No. 1, pp 35-53.

Wiberg, P., Smith, J. D. A. 1983. "Comparison of Field Data and Theoretical Models for Wave-Current Interactions at the Bed on the Continental Shelf," _Continental Shelf Research_, Vol. 2, pp 147-162.

Wikramanayake, P. N., Madsen, O. S. 1990. "Calculation of Movable Bed Friction Factors," Technical Progress Report, submitted to the U.S. Army Corps of Engineers, Coastal Engineering Research Center.

Wilson, K. C. 1989. "Friction of Wave Induced Sheet Flow," _Coastal Engineering_, Vol. 12, pp 371-379.

Wright, L. D., J. D. Boon, S. C. Kim, J. H. List. 1991. "Modes of Cross-Shore Sediment Transport on the Shoreface of the Middle Atlantic Bight," _Marine Geology_, Vol. 96, pp 19-51.

Yalin, M. S. 1963. "An Expression for Bed-Load Transportation," _J. of the Hydraulics Div. ASCE_, Vol. 89 No. HY3.

Young, A., A. Kirk. 1964. "Bessel Functions Part IV: Kelvin Functions" Royal Society Mathematical Tables Vol. 10, Cambridge University Press.

Zettler, D. T. 1991. "The Estimation of a Near-Bed Reference Concentration for Use in Suspended Load Computations," M.S. Thesis, Massachusetts Institute of Technology, Cambridge, Massachusetts.

APPENDIX A: NOTATION

a	non-dimensional fall velocity defined by Equation 48
A	complex constant
$A1$	real constant
$A2$	real constant
A_{br}	near-bottom excursion amplitude based on equivalent wave
B	complex constant
c	suspended sediment concentration
c'	turbulent fluctuation of the suspended sediment concentration
$\bar{c}$	mean suspended sediment concentration
c_1	normalized periodic component of concentration with frequency ω_1
$\tilde{c}_1$	periodic suspended sediment concentration with frequency ω_1
c_{1r}	magnitude of reference concentration for component with frequency ω_1
$\tilde{c}_{1r}$	reference concentration of component with frequency ω_1
$\tilde{c}_2$	periodic suspended sediment concentration component with frequency ω_2
c_b	concentration of the sediment bed
$\bar{c}_r$	mean reference concentration
$\overline{c_{ri}}$	mean reference concentration for ith grain size class
$c_r(t)$	instantaneous reference concentration
C	complex constant
d	grain diameter
d_i	grain diameter for the ith grain size class
d_m	mean grain diameter
D	complex constant
E	complex constant
F	complex constant
F_d	diffusive sediment flux
g	acceleration due to gravity
h	flow depth
h_T	height of bed load layer
i	$\sqrt{-1}$
k_n	equivalent Nikuradse roughness

p_i	fraction of bottom sediment in the ith grain size class
p_w	periodic pressure
p_{w1}	periodic pressure with frequency ω_1
$\vec{q}_b$	bed load flux
q_B	magnitude of bed load flux
$\bar{r}$	mean fourier coefficient of Equation 105
r_+	complex constant
r_-	complex constant
r_1	first harmonic fourier coefficient of Equation 105
r_2	second harmonic fourier coefficient of Equation 105
s	specific gravity of the sediment grains
s'	non-dimensional excess shear stress defined by Equation 89
$s'(t)$	instantaneous value of s'
S_{ub}	power spectrum of near-bottom velocity
t	time
T	wave period
$\vec{T}$	total suspended sediment transport
$\vec{T}_c$	suspended sediment transport due to mean components
$\vec{T}_w$	suspended sediment transport due to periodic components
u	horizontal velocity in wave direction
$\bar{u}$	current (mean) velocity
$\tilde{u}$	periodic velocity
u_1	periodic velocity component with frequency ω_1
u_b	magnitude of near-bottom wave velocity
$u_b(t)$	instantaneous near-bottom wave velocity
u_{b1}	near-bottom wave velocity with frequency ω_1
u_{b2}	near-bottom wave velocity with frequency ω_2
u_{bi}	near-bottom wave velocity of the ith wave component
u_{bn}	root-mean-square value of the offshore wave velocity obtained by a wave-by-wave analysis
u_{bp}	root-mean-square value of the onshore wave velocity obtained by a wave-by-wave analysis
u_{br}	representative near-bottom wave velocity
u_B	velocity of sediment in bed load layer
u_d	deficit wave velocity defined by Equation 27

u_∞ magnitude of near-bottom wave velocity

$u_{\infty 1}$ magnitude of near-bottom wave velocity with frequency ω_1

w_f sediment fall velocity

u_{d1} deficit wave velocity of component with frequency ω_1

u_w wave velocity

u_{w1} periodic velocity component with frequency ω_1

u_{w2} periodic velocity component with frequency ω_2

u_{*c} current shear velocity

u_{*c}' shear velocity based on current skin friction shear stress

u_{*cw} combined wave-current shear velocity

u_{*cw}' combined wave-current shear velocity based on the skin friction shear stress

u_{*w} wave shear velocity

u_{*w}' shear velocity based on wave skin friction shear stress

w' turbulent fluctuation in vertical velocity

x horizontal coordinate in wave direction

z vertical coordinate, height above bottom

z_r reference level at which concentration is specified

z_0 bottom roughness parameter $z_0 = k_n/30$

z_{oc} effective roughness due to wave-current interaction

z_a generalized Bessel function of order a

α free parameter in eddy viscosity model $\alpha = 0.5$

β parameter defined by Equation 118

$\beta(t)$ angle of bed slope in the direction of the instantaneous skin friction shear stress

β_0 angle of bed slope

γ_0 resuspension coefficient

δ boundary layer length scale defined by Equations 8 and 33

ϵ ratio of current shear velocity to combined shear velocity

ζ nondimensional vertical coordinate $\zeta = z/\delta$

ζ_r non-dimensional reference level

η ripple height

θ phase of bottom shear stress

κ Van Karman's constant $\kappa = 0.4$

μ'	ratio of current shear velocity to wave shear velocity based on skin friction values
ν	kinematic viscosity
ν_t	turbulent eddy viscosity
ρ	density
σ	relative frequency of periodic component defined by Equation 62
τ	bottom shear stress
$\tau'(t)$	- instantaneous skin friction shear stress
τ_b	magnitude of bottom shear stress
$\vec{\tau}_b'(t)$	instantaneous bottom skin friction shear stress
τ_c	bottom shear stress due to current
τ_{cw}	combined wave-current shear stress
τ_c'	current skin friction shear stress
τ_w	bottom shear stress due to waves
τ_w'	wave skin friction shear stress
τ_{w1}	bottom shear stress due to wave velocity with frequency ω_1
τ_{w2}	bottom shear stress due to wave velocity with frequency ω_2
τ_{wi}	bottom shear stress due to the ith wave velocity component
ϕ_1	phase near-bottom wave velocity component with frequency ω_1
ϕ_2	phase near-bottom wave velocity component with frequency ω_2
ϕ_{cw}	angle between waves and the current
$\vec{\phi}_b$	non-dimensional bed load flux
ψ'	Shields parameter based on skin friction shear stress
$\psi'(t)$	Shields parameter based on the instantaneous skin friction shear stress
ψ_{cr}	critical Shields parameter for the initiation of motion
ϕ_m	angle of repose of bottom sediment
$\vec{\phi}_b(t)$	instantaneous bed load transport
ψ_w'	Shields parameter based on the wave skin friction shear stress
ω	angular frequency
ω_1	frequency of wave component
ω_2	frequency of wave component
ω_i	frequency of ith wave component
ω_r	representative wave frequency

Re   real part of a complex number

| | modulus of a number

Diacritics

−   mean value of a quantity

→   vector quantity

Table B1. Correspondence between Variables in the Program
and the Symbols in this Report

A	a	nondimensional fall velocity (Equation 48)
ALPHA	a	model parameter
BETA	β	(Equation 118)
CB	c_b	volume fraction of sediment in bed
CSCALE	$\bar{c}_r$	mean reference concentration
DELPHI	ϕ	(Equation 103)
DELTA	δ	boundary layer length scale (Equation 9)
DIAM	d	mean grain diameter
EP	ϵ	(Equation 9)
FALLV	w_f	fall velocity of the sediment
FRE	ω	frequency of the principal component
GAMMA0	γ_0	resuspension coefficient
GEE	g	acceleration due to gravity
HA	η	ripple height
HEI	h	flow depth
KAP	κ	Von Karman's constant
KB	k_n	equivalent roughness of the bed
MU	μ	(Equation 120)
MUP1	μ_1'	(Equation 101)
PHICW	ϕ_{cw}	angle between waves and current (in radians)
PHICWD	ϕ_{cw}	angle between waves and current (in degrees)
PHIFD	ϕ_f	angle of repose of sediment
PSICR	ψ_{cr}	critical Shields parameter for the initiation of motion
PSIWP	ψ_w'	Shields parameter based on wave skin friction shear stress
R1	$r_1/\bar{r}$	ratio of reference concentration of principal component to mean reference concentration
R2	$r_2/\bar{r}$	ratio of reference concentration of secondary component to mean reference concentration
RATPSI	r_φ	(Equation 104)
RTAU	r_τ	(Equation 102)

S	s	specific density of sediment
SLOPED	β_0	bed slope (in degrees)
SSTAR	S_*	non-dimensional grain size
UB1	u_{b1}	magnitude of principal near bottom velocity
UB2	u_{b2}	magnitude of secondary near bottom velocity
USC	u_{*c}	current shear velocity
USCP	u_{*c}'	skin friction current shear velocity
USW	u_{*w}	wave shear velocity
USWP	u_{*w}'	skin friction wave shear velocity
USWC	u_{*wc}	combined shear velocity
VALM	$\bar{r}$	(Equation 105)
VIS	v	kinematic viscosity
ZE0	ζ_0	non-dimensional velocity reference level
ZER	ζ_r	non-dimensional current reference level
Z0	z_0	velocity reference level
ZR	z_r	current reference level
ZW	z	ripple geometry parameter

PROGRAM WCSTRANS

```
c    program to find velocity, concentration and flux profiles and bedload
c    and suspended load transports for combined waves and currents over a
c    sand bed uses a tri-linear time-invariant eddy viscosity model
c
c    All references are to the report "Calculation of Suspended Sediment
c    Transport by Combined Wave-Current Flows" (1992) by Wikramanayake,
c    P.N. and Madsen, O.S.
c
c    All program variables are capitalised when referred to in the comment
c    lines. The fully capitalised comment lines separate the main program
c    into the sections described in Part V and the flow chart of Figure 11.
c
c    The program reads the input data from the free format file
c    WCSTRANS_IN (i.e. numbers on each row must be separated by spaces)
c
c    The calculated profiles of velocity, concentration and flux are output
c    to the files WCSTRANS_VELO, WCSTRANS_CONC and WCSTRANS_FLUX
c    respectively. The format of these files are given in Table 11 and
c    also in the section of the code that deals with the output.
c
c    The calculated bedload and suspended load transports, shear velocities,
c    and some other important parameters are written to the file
c    WCSTRANS_RES
c
c    The correspondence between some of the variables in the program and
c    the symbols used in the report is given in Table B1 of the report


     character*44 spec

     complex*16 solu1(5),solu2(5),solc1(5),solc2(5),sold1(5),sold2(5)
     complex*16 uw1,uw2,ct1,ct2

     integer*2 i,j
     real*4 alpha,kap,ep,mup1,kb,pi,cb,gee,phifd
     real*4 ub1,ub2,fre,phicw,phicwd
     real*4 usc,usw,uswc,ucr,zcr,uave,hei,flagc,t1,t2
     real*4 diam,fallv,s,sloped,phiswd,temp,vis
     real*4 flagkb,flagt,flags,flagd,flagfv,flagz
     real*4 sstar,psicr,diamp,sstarp,fallvp,diamp1,wstar,wstarp
     real*4 dum1,dum2,dum3,dum4,dum5,dum6,dum7,dum8
     real*4 zw,zw1,ze0,zer,ab1,abkb,ha,st,zr,a
     real*4 fwc1,fwc2,delta,phib1,phib2,beta
     real*4 umd,uscp,uswp,uswcp,psiwp
     real*4 fwcp1,fwcp2,ze0p,deltap,phibp1,phibp2
     real*4 tauwp1,tauwp2,psiwp1,ratpsi,rtau,delphi,r1,r2,valm,uswp1
     real*4 zet,zeb,qw,qn,fm,gamma0,cscale
     real*4 fluxmw,fluxmn,fluxw1,fluxw2,fluxw,fluxws
     real*4 rat,fact,phic1,phic2,phiu1,phiu2,v,cm
     real*4 z(100),datau(100,6),datac(100,6),datat(100,6)
```

```
C       INITIALIZE PARAMETERS

        parameter(kap=0.4,alpha=0.5,cb=0.65,phifd=36.0,gee=981.0)
        pi=4.0*atan(1.0)

C       INPUT SECTION

c       read input data from file WCSTRANS_IN

        open(unit=2,file='wcstrans_in',status='old')

        read(2,*)ub1,ub2,fre
        read(2,*)flagc,t1,t2,phicwd
        read(2,*)diam,fallv,s
        read(2,*)kb
        read(2,*)sloped,phiswd
        read(2,*)hei
        read(2,*)temp

        close(unit=2)

C       DATA PROCESSING SECTION

        phicw=phicwd*(pi/180.0)
        ab1=ub1/fre

c       set current specification parameters according to FLAGC

        if (flagc.eq.1.0) then
           spec(1:44)='current specified by given shear velocity    '
           usc=t1
        else if (flagc.eq.2.0) then
           spec(1:44)='current specified by a given reference value '
           ucr=t1
           zcr=t2
        else if (flagc.eq.3.0) then
           spec(1:44)='current by depth averaged velocity and depth '
           uave=t1
           hei=t2
        else
           print *,' error in input - flagc is not 1, 2 or 3'
           go to 2000
        end if

c       set value of FLAGKB according to input value of KB

        if (kb.eq.0.0) then
           flagkb=0.0
        else
           flagkb=1.0
        end if
```

```
c      use default temperature if TEMP was input as zero and calculate VIS

       if (temp.eq.0.0) then
          flagt=0.0
          temp=20.0
       else
          flagt=1.0
       end if

       call viscosity(temp,vis)

c      use default specific density if S was input as zero

       if (s.eq.0.0) then
          flags=0.0
          s=2.65
       else
          flags=1.0
       end if

c      calculate grain diameter or fall velocity if DIAM or FALLV were given
c      as zero. program will terminate if both are zero. the values are
c      calculated using the empirical relationship of Madsen and Grant (1976)
c      that is contained in sub-routine FALLVEL

       if (diam.eq.0.0.and.fallv.eq.0.0) then
          print *,'error in input - both diam and fallv are zero'
          go to 2000
       end if

       if (diam.eq.0.0) then
          flagd=0.0
          diamp=0.01
   10     sstarp=(diamp/(4.0*vis))*sqrt((s-1.0)*diamp*gee)
          call fallvel(sstarp,wstarp)
          fallvp=wstarp*sqrt((s-1.0)*gee*diamp)
          if (abs((fallvp-fallv)/fallv).le.1.0e-3) go to 20
          diamp1=diamp*(1.0+0.1*((fallv-fallvp)/fallv))
          diamp=max(diamp1,diamp/2.0)
          go to 10
   20     diam=diamp
       else
          flagd=1.0
       end if

c      calculate non-dimensional grain size SSTAR (Equation 40) and critical
c      Shields parameter for the initiation of motion PSICR

       sstar=(diam/(4.0*vis))*sqrt((s-1.0)*diam*gee)
       call shields(sstar,psicr)
```

```
          if (fallv.eq.0.0) then
              flagfv=0.0
              call fallvel(sstar,wstar)
              fallv=wstar*sqrt((s-1.0)*gee*diam)
          else
              flagfv=1.0
          endif

c       if the equivalent roughness was not given (FLAGKB = 0) estimate the
c       roughness using the waves alone.

          if (flagkb.eq.0.0) then

c       call WAVEC with KB = DIAM and T1 = 0 (pure wave case)
              uswp=0.0
              call wavec(kap,alpha,ub1,ub2,diam,fre,phicw,2.0,0.0,0.0,hei,
     &vis,dum1,uswp,dum2,dum3,dum4,dum5,dum6,dum7,dum8,sold1,sold2)

c       calculate Z from Equations 37 and 39 (as ZW) using the wave skin
c       friction shear stress USWP and obtain the equivalent roughness by
c       calling FINDKB

              zw=(uswp**2.0)/(sstar*(s-1.0)*gee*diam)
              call findkb(zw,ab1,diam,kb,flagz,ha,st)

          end if

C       SOLUTION OF THE WAVE-CURRENT AND SKIN FRICTION PROBLEMS

          usw=0.0
          uswp=0.0


   30     continue

c       call wavec to solve the wave-current problem to obtain the shear
c       velocities USC, USW and USWC, the boundary layer length scale DELTA,
c       and the complex vectors SOLU1 and SOLU2 which contain the five complex
c       coefficients in Equations 67, 69 and 72 for the principal and secondary
c       velocity components respectively.

          call wavec(kap,alpha,ub1,ub2,kb,fre,phicw,flagc,t1,t2,hei,vis,
     &usc,usw,uswc,fwc1,fwc2,ze0,delta,phib1,phib2,solu1,solu2)

c       calculate the parameters BETA (Equation 118), EP (Equation 9) and the
c       relative roughness ABKB

          beta=hei/(6.0*delta)
          ep=usc/uswc
          abkb=ab1/kb

c       calculate the mean velocity at z = delta (UMD)

          call velmean(usc,alpha,ep,kap,beta,1.0,ze0,umd)
```

```fortran
c       calculate the skin friction shear stresses by calling WAVEC with the
c       roughness given by KB = DIAM , and the current by T1 = UMD , T2 = DELTA
c       and FLAGC = 2

        call wavec(kap,alpha,ub1,ub2,diam,fre,phicw,2.0,umd,delta,hei,
       &vis,uscp,uswp,uswcp,fwcp1,fwcp2,ze0p,deltap,phibp1,phibp2,sold1,
       &sold2)


c       calculate the Shields parameters based on the wave (Equation 39) and
c       combined skin friction shear stresses and an updated value of Z (ZW1)
c       from Equation 37

        psiwp=(uswp**2.0)/((s-1.0)*diam*gee)
        zw1=psiwp/sstar

c       if FLAGKB = 0 check for convergence of Z by checking the difference
c       between ZW and ZW1

        if (flagkb.eq.0.0) then

            if (abs((zw1-zw)/zw).lt.1.0e-3) go to 40

c       if the value of Z has not converged set ZW = ZW1 , calculate a new
c       value for the equivalent roughness, KB by calling FINDKB, and  go to
c       statement 30 to repeat the wave-current and skin friction solutions

            zw=zw1
            call findkb(zw,ab1,diam,kb,flagz,ha,st)

            go to 30

        end if

  40    continue
        zw=zw1


C       REFERENCE CONCENTRATION SECTION

c       calculate GAMMA0 from the final converged value of Z (ZW) using
c       Equation 115

        if (zw.le.0.18) then
           gamma0=1.8e-03
        else
           gamma0=1.8e-04
        end if
```

```
c       calculate the parameters RATPSI , MUP1 , RTAU  and  DELPHI (Equations
c       104, 101, 102 and 103) for Equation 100

        tauwp1=0.5*fwcp1*(ub1**2.0)
        uswp1=sqrt(tauwp1)
        mup1=uscp/sqrt(tauwp1)
        psiwp1=tauwp1/((s-1.0)*gee*diam)
        ratpsi=psicr/psiwp1

        if (ub2.eq.0.0) then
           rtau=0.0
           delphi=0.0
        else
           tauwp2=0.5*fwcp2*(ub2**2.0)
           delphi=phibp2-phibp1
           rtau=tauwp2/tauwp1
        end if

c       call COEFF to obtain the expansion of Equation 100 in terms of the
c       mean, principal and secondary concentration components given in
c       Equation 105

        call coeff(mup1,phicw,ratpsi,rtau,delphi,valm,r1,r2)

c       calculate the mean reference concentration CSCALE

        cscale=(gamma0*cb*valm)/(ratpsi)

C       CALCULATION OF THE BED LOAD TRANSPORT

c       the sub-routine BEDLOAD averages Equation 85 over the period of the
c       principal wave to obtain the bed load transports in the wave and
c       wave-normal directions (variables QW and QN)

        call bedload(mup1,uswp1,rtau,delphi,phicwd,phiswd,sloped,diam,s,
     &psicr,phifd,qw,qn)


C       SOLUTION OF THE CONCENTRATION PROBLEM

c       set the reference level ZR to seven times the grain diameter

        zr=7.0*diam

c       calculate the non-dimensional reference level ZER , and fall velocity A

        zer=zr/delta
        a=fallv/(kap*uswc)
```

```
c       calculate the solution for the principal component of the concentration
c       by calling TCONCCOEFF with input values EN = 1 and RHS = 1. SOLC1 is
c       a vector containing the five complex coefficients of Equations 67, 69
c       and 72.

        call tconccoeff(zer,a,alpha,ep,solc1,1.0,1.0)

c       call TCONCCOEFF with EN = 2 and RHS = 1 to obtain the solution for the
c       secondary component of concentration. SOLC2 contains the five complex
c       coefficients of Equations 67, 69 and 72 for this component

        call tconccoeff(zer,a,alpha,ep,solc2,1.0,2.0)

C       CALCULATION OF THE SUSPENDED SEDIMENT TRANSPORTS

c       set the upper and lower levels for the integration of the mean flux
c       and call FLUXMEAN to calculate the mean transport FM (FM is scaled by
c       CSCALE)

        zet=hei/delta
        zeb=amax1(zer,ze0)

           if (t1.eq.0.0) then
             fm=0.0
           else
             call fluxmean(alpha,kap,ep,ze0,zer,a,usc,zet,zeb,delta,
     &       beta,fm)
           end if

c       calculate the real mean transports in the wave and wave-normal
c       directions (FLUXMW and FLUXMN)

           fluxmw=fm*cos(phicw)*cscale
           fluxmn=fm*sin(phicw)*cscale

c       call FLUXWAVE to calculate the transport due to the principal
c       components

           call fluxwave(alpha,ep,ze0,zer,a,30.0,zeb,delta,
     &     r1,ub1,phibp1,1.0,solu1,solc1,fluxw1)

c       call FLUXWAVE to calculate the transport due to the secondary
c        components

           if (ub2.eq.0.0) then
              fluxw2=0.0
           else
              call fluxwave(alpha,ep,ze0,zer,a,30.0,zeb,delta,
     &        r2,ub2,phibp1,2.0,solu2,solc2,fluxw2)
           end if
```

```fortran
c       multiply by CSCALE to obtain the real wave transports

        fluxw1=fluxw1*cscale
        fluxw2=fluxw2*cscale

        fluxw=fluxw1+fluxw2
        fluxws=fluxw+fluxmw

C       CALCULATION OF THE VELOCITY, CONCENTRATION AND TRANSPORT PROFILES

c       set levels for profile calculation between the lower of ZER and ZE0
c       and the level 10 (in terms of the non-dimensional height defined by
c       Equation 11)

          rat=10.0/amax1(zer,ze0)
          fact=rat**(1.0/95)
          z(1)=amax1(zer,ze0)

          do 50 i=1,95
          z(i+1)=z(i)*fact
   50     continue


          z(97)=1.1*z(96)
          z(98)=1.5*z(96)
          z(99)=2.0*z(96)
          z(100)=5.0*z(96)

c       calculate velocity, concentration and transport profiles
c       note that the subroutines VELMEAN, MCONC and TCONC are all based on
c       the non-dimensional height defined by Equation 11
c       the matrices DATAU, DATAC and DATAT are filled with the profiles of
c       velocity, concentration and flux, respectively.

          do 60 i=1,100

c       set the first column to the dimensional height (in cm)

          datau(i,1)=delta*z(i)
          datac(i,1)=delta*z(i)
          datat(i,1)=delta*z(i)

c       call MCONC for the mean concentration

          call mconc(zer,a,alpha,ep,beta,z(i),cm)

c       call TCONC with EN = 1 for the complex magnitude of the principal
c       component of the concentration (CT1)

          call tconc(zer,a,alpha,ep,solc1,z(i),ct1,1.0)
```

```
c       call TCONC with EN = 2 for the complex magnitude of the secondary
c       component of the concentration (CT2)

        call tconc(zer,a,alpha,ep,solc2,z(i),ct2,2.0)

c       calculate the phases of the two periodic components of concentration
c       with respect to the reference value (Equation 57)

        if(ct1.eq.(0.0,0.0)) then
        phic1=0.0
        else
        phic1=atan2(dimag(ct1),dreal(ct1))
        end if

        if(ct2.eq.(0.0,0.0)) then
        phic2=0.0
        else
        phic2=atan2(dimag(ct2),dreal(ct2))
        end if

c       fill the columns of DATAC with the real value of the concentrations
c       (after multiplying by CSCALE) and the phases

        datac(i,2)=cscale*cm
        datac(i,3)=cscale*abs(r1*ct1)
        datac(i,4)=cscale*abs(r2*ct2)
        datac(i,5)=phic1
        datac(i,6)=phic2

c       call VELMEAN (which incorporates Equation 10) for the mean velocity

        call velmean(usc,alpha,ep,kap,beta,z(i),ze0,v)

c       call TCONC with EN = 1 for the complex magnitude of the principal
c       deficit velocity UW1 (ud1 of Equation 27)

        call tconc(ze0,0.0,alpha,ep,solu1,z(i),uw1,1.0)

c       call TCONC with EN = 2 for the complex magnitude of the principal
c       deficit velocity UW2 (ud1 of Equation 27)

        call tconc(ze0,0.0,alpha,ep,solu2,z(i),uw2,2.0)

c       calculate the phases of the periodic velocity components from Equation
c       27

        phiu1=atan2(dimag(uw1),(1.0+dreal(uw1)))
        phiu2=atan2(dimag(uw2),(1.0+dreal(uw2)))

        datau(i,2)=v
```

```fortran
c       calculate the magnitudes of the periodic velocity components from
c       Equation 27 and fill the columns of the matrix DATAU

        datau(i,3)=ub1*sqrt((1.0+dreal(uw1))**2.0+
     &  dimag(uw1)**2.0)

        datau(i,4)=ub2*sqrt((1.0+dreal(uw2))**2.0+
     &  dimag(uw2)**2.0)

        datau(i,5)=phiu1
        datau(i,6)=phiu2
        datau(i,7)=datau(i,2)*cos(phicw)

c       calculate the fluxes due to the mean and periodic components and fill
c       the matrix DATAT

        datat(i,2)=cos(phicw)*datau(i,2)*datac(i,2)
        datat(i,3)=0.5*datau(i,3)*datac(i,3)*cos(phibp1+phic1-phiu1)
        datat(i,4)=0.5*datau(i,4)*datac(i,4)*cos(phibp1+phic2-phiu2)
        datat(i,5)=datat(i,3)+datat(i,4)
        datat(i,6)=datat(i,2)+datat(i,3)+datat(i,4)

   60   continue

C    OUTPUT OF THE RESULTS

c       the velocity, concentration and flux profiles are written to the
c       files WCSTRANS_VELO, WCSTRANS_CONC and WCSTRANS_FLUX, respectively
c
c       the six columns of WCSTRANS_VELO are the height above the bottom
c       (in cm), mean velocity (in cm/sec), principal wave velocity
c       (in cm/sec), secondary wave velocity (in cm/sec), phase of the
c       principal wave velocity with respect to the near bottom velocity
c       (in radians) and phase of the secondary wave velocity (in radians)
c
c       the six columns of WCSTRANS_CONC are the height above the bottom
c       (in cm), mean concentration (volumetric), magnitude of the principal
c       concentration component (volumetric), magnitude of the secondary
c       concentration component (volumetric), phase of the principal
c       concentration component with respect to the reference concentration
c       (radians) and  phase of the secondary concentration component (radians)
c
c       the six columns of WCSTRANS_FLUX are the height above the bottom
c       (in cm), the flux due to the mean components in the wave direction
c       (in cm^3/cm^2/sec), the flux due to the principal components
c       (in cm^3/cm^2/sec), the flux due to the secondary components
c       (in cm^3/cm^2/sec), the total flux due to the periodic components
c       (in cm^3/cm^2/sec), and the total suspended sediment flux in the wave
c       direction

        open(unit=2,file='wcstrans_velo',status='unknown')

        write(2,70)((datau(i,j),j=1,6),i=1,100)
   70   format(6e13.5)
```

```fortran
      close(unit=2)

      open(unit=2,file='wcstrans_conc',status='unknown')

      write(2,70)((datac(i,j),j=1,6),i=1,100)

      close(unit=2)

      open(unit=2,file='wcstrans_flux',status='unknown')

      write(2,70)((datat(i,j),j=1,6),i=1,100)

      close(unit=2)


      open(unit=3,file='wcstrans_res',status='unknown')

      write(3,80)ub1,ub2,fre
80    format('        RESULTS OF PROGRAM WCSTRANS '//
     &' INPUT VALUES'//
     &'    WAVE SPECIFICATION'//
     &'        first harmonic wave velocity        = ',f6.1,' cm/s'/
     &'        second harmonic wave velocity       = ',f6.1,' cm/s'/
     &'        wave frequency                      = ',f6.3,' rad/s'//)

      write(3,90)
90    format('    CURRENT SPECIFICATION'/)

      write(3,100)spec
100   format(5x,a44/)

      if (flagc.eq.1.0) then

         write(3,110)usc
110      format(
     &'        given current shear velocity        = ',f6.1,' cm/s'/)

      else if (flagc.eq.2.0) then

         write(3,120)ucr,zcr
120      format(
     &'        given current velocity              = ',f6.1,' cm/s'/
     &'        at an elevation                     = ',f6.1,' cm'/)

      else

         write(3,130)uave,hei
130      format(
     &'        given depth average current velocity = ',f6.1,' cm/s'/
     &'        flow depth                          = ',f6.1,' cm'/)

      end if
```

```
      write(3,140)phicwd
140   format(
     &'       anticlockwise angle '/
     &'       between wave and current          = ',f6.1,' deg.'//)

      write(3,150)
150   format('    SEDIMENT SPECIFICATION'/)

      if (flagd.eq.1.0) then
       write(3,160)diam
160    format(
     &'       given mean grain diameter         = ',f8.5,' cm/s'/)
      else
       write(3,170)diam
170    format(
     &'       calculated mean grain diameter    = ',f8.5,' cm/s'/)
      end if

      if (flagfv.eq.1.0) then
       write(3,180)fallv
180    format(
     &'       given sediment fall velocity      = ',f6.3,' cm/s'/)
      else
       write(3,190)fallv
190    format(
     &'       calculated sediment fall velocity = ',f6.3,' cm/s'/)
      end if

      if (flags.eq.1.0) then
       write(3,200)s
200    format(
     &'       given sediment specific density   = ',f6.3,' cm/s'/)
      else
       write(3,210)s
210    format(
     &'       assumed sediment specific density = ',f6.3,' cm/s'/)
      end if

      write(3,220)sstar,psicr
220   format(
     &'       non-dimensional grain size (SSTAR)  = ',f6.3/
     &'       critical Shields parameter for'/
     &'       initiation of motion                = ',f7.4//)

      write(3,230)hei,sloped,phiswd
230   format('    FLOW SPECIFICATIONS'//
     &'       flow depth                        = ',f6.1,' cm'/
     &'       bottom slope                      = ',f6.3,' deg'/
     &'       anticlockwise angle between '/
     &'       wave direction and bottom slope   = ',f6.1,' deg')
```

```
      if (flagt.eq.1.0) then
       write(3,240)temp
240    format(
    &'        given water temperature         = ',f6.3,' C'//)
      else
       write(3,250)temp
250    format(
    &'        assumed water temperature       = ',f6.3,' C'//)
      end if


      if (flagkb.eq.1.0) then

       write(3,260)kb
260    format('   BOTTOM ROUGHNESS SPECIFIED'/
    &'        given bottom roughness          = ',f6.3,' cm'////)

      else

       write(3,270)
270    format('   BOTTOM ROUGHNESS NOT GIVEN'////)


      end if

      write(3,280)usc,usw,uswc,ep,delta,ze0,abkb
280   format(' OUTPUT VALUES'//
    &'     RESULTS OF WAVE-CURRENT MODEL'/
    &'        current shear velocity          = ',f6.2,' cm/s'/
    &'        wave shear velocity             = ',f6.2,' cm/s'/
    &'        combined shear velocity         = ',f6.2,' cm/s'/
    &'        value of parameter EP (= USC/USWC) = ',f6.4/
    &'        boundary layer length scale     = ',f6.2,' cm'/
    &'        non-dimensional z0              = ',f7.5,/
    &'        relative roughness for wave 1   = ',f7.2//)

      write(3,290)uscp,uswp,phibpl,psiwp,zw
290   format('     RESULTS OF SKIN FRICTION MODEL'/
    &'        current skin friction shear vel = ',f6.4,' cm/s'/
    &'        wave skin friction shear vel    = ',f6.4,' cm/s'/
    &'        phase lead of wave skin friction shear stress'/
    &'        over the near bottom velocity   = ',f7.3/
    &'        shields parameter based on '/
    &'        wave skin friction shear stress = ',f8.5/
    &'        value of non-dimensional '/
    &'        ripple parameter Z              = ',e13.5//)

      write(3,300)
300   format('     BOTTOM ROUGHNESS'/)

      if (flagkb.eq.0.0) then

        write(3,310)
310     format('     BOTTOM ROUGHNESS NOT GIVEN'/)
```

```
           if (flagz.eq.-1.0) then

               write(3,320)ha,st,kb
320            format('    NOTE : BOTTOM IS TREATED AS RIPPLED. HOWEVER'/
     &'     THE PARAMETER Z IS LESS THAN 0.0016 WHICH IS THE LOWER '/
     &'     LIMIT FOR RIPPLES OBSERVED IN THE FIELD'/
     &'        ripple height                  = ',f7.4,' cm'/
     &'        ripple steepness               = ',f7.5/
     &'        calculated bottom roughness    = ',f6.3,' cm'//)

           else if (flagz.eq.0.0) then

               write(3,330)ha,st,kb
330            format('    BOTTOM IS RIPPLED'/
     &'        ripple height                  = ',f7.4,' cm'/
     &'        ripple steepness               = ',f7.5/
     &'        calculated bottom roughness    = ',f6.3,' cm'//)

           else

               write(3,340)kb
340            format('    BOTTOM IS FLAT'/
     &'        calculated bottom roughness    = ',f6.3,' cm'//)

           end if

       else

           write(3,350)kb
350        format(
     &'        given bottom roughness         = ',f6.3,' cm'//)

       end if

       write(3,360)gamma0,cscale,r1,r2
360    format('    RESULTS OF REFERENCE CONCENTRATION MODEL'/
     &'        resuspension coefficient          = ',e10.3/
     &'        mean reference concentration      = ',e10.3/
     &'        ratio of reference concentration of'/
     &'        principal component to mean       = ',f7.5/
     &'        ratio of reference concentration of'/
     &'        secondary component to mean       = ',f7.5//)

       write(3,370)a,zer
370    format('    RESULTS OF THE SOLUTION OF SEDIMENT PROBLEM'/
     &'        non-dimensional fall velocity     = ',f7.4/
     &'        non-dimensional reference level   = ',f7.5//)
```

```
      write(3,380)qw,qn,fluxmw,fluxmn,fluxw1,fluxw2,fluxw,fluxws
380   format('     RESULTS OF TRANSPORT CALCULATIONS'//
     &'     BEDLOAD TRANSPORTS'/
     &'       in wave direction                = ',e12.4,
     &' cm^3/cm/s'/
     &'       in wave normal direction         = ',e12.4,
     &' cm^3/cm/s'//
     &'     SUSPENDED LOAD TRANSPORTS'//
     &'       TRANSPORT DUE TO MEAN COMPONENTS'/
     &'        in wave direction               = ',e12.4/
     &'        in wave normal dir.             = ',e12.4//
     &'       TRANSPORT DUE TO PERIODIC COMPONENTS (IN WAVE DIRECTION)'/
     &'        principal components            = ',e12.4/
     &'        secondary components            = ',e12.4//
     &'        total wave transport            = ',e12.4//
     &'       total suspended load transport'/
     &'        in wave direction               = ',e12.4/)

      close(unit=3)

      go to 3000

2000  print *,'program terminated with error'

3000  stop
      end
```

```
C     SUB-ROUTINES WAVEC AND FINDUSWN THAT SOLVE THE WAVE-CURRENT PROBLEM

      subroutine wavec(kap,alpha,ub1,ub2,kb,fre,phicw,flagc,t1,t2,hei,
     &vis,usc,usw,uswc,fwc1,fwc2,ze0,delta,phib1,phib2,solu1,solu2)

c     solves the wave-current problem given the wave, current and roughness
c     conditions. if t1=0 (i.e. no current) the pure wave problem is solved

      complex*16 solu1(5),solu2(5)

      real*4 ub1,ub2,kb,fre,phicw,kap,alpha,flagc,t1,t2,flags
      real*4 usc,usw,uswc,uswa,ze0,z0,ucr,zcr,uave,hei,delta,ucr1
      real*4 fac,mu,ep,mu1,ep1,phib1,phib2,usc1

      nc=0
```

```
c       calculate Z0 from the given roughness KB

        z0=kb/30.0

        if (t1.eq.0.0) then

         ep=0.0

c        pure wave case
c        if USW = 0 assume initial value for USW

         if (usw.eq.0.0) usw=ub1*sqrt(0.01/2.0)

c        begin iteration for USW
c        set USWC = USW (as there is no current)

   5     uswc=usw

c        calculate DELTA and ZE0 (Equations 11 and 12)

         delta=(kap*uswc)/fre
         ze0=z0/delta

c        call subroutine FINDUSWN to calculate the wave shear velocities
c        for the principal wave component (for rough turbulent flow)

         call finduswn(ze0,kap,alpha,ep,1.0,uswc,ub1,uswr1,phib1,
      &  solu1)

         fwcr1=2.0*((uswr1/ub1)**2.0)

c        limit FWRC1 (the rough turbulent friction factor to) 0.24

         if(fwcr1.gt.0.24) then
          uswr1=0.346*ub1
         end if

c        calculate the smooth turbulent friction factor FWS1 and select the
c        larger value to calculate USW1 (the shear velocity based on the
c        principal shear stress. FLAGS is set to 1 or 0 for smooth or rough
c        turbulent regimes, respectively

         re1=(ub1**2.0)/(fre*vis)
         call smootht(re1,fws1)
         usws1=sqrt(fws1/2.0)*ub1
         usw1=max(uswr1,usws1)

         if(usws1.gt.uswr1) then
            flags=1.0
         else
            flags=0.0
         end if
         fwc1=2.0*((usw1/ub1)**2.0)
```

```fortran
c       calculate the shear velocity for the secondary wave component
c       if FLAGS = 0 the rough turbulent value is used while if FLAGS = 0
c       the smooth turbulent value is used

        if (ub2.eq.0.0) then

          usw2=0.0
          fwc2=0.0

        else

          if (flags.eq.0.0) then

            call finduswn(ze0,kap,alpha,ep,2.0,uswc,ub2,uswr2,phib2,
     &        solu2)

            fwc2=2.0*((usw2/ub2)**2.0)

          else

            re2=(ub2**2.0)/(2.0*fre*vis)
            call smootht(re2,fwc2)
            usw2=sqrt(fwc2/2.0)*ub2

          end if

        end if

c       calculate the total wave shear velocity (i.e. a new value of USW)
c       as USWA from Equation 119

.       uswa=sqrt(usw1**2.0+usw2**2.0)

c         check for convergence of USW by calculating the fractional difference
c         between USW and USWA

        nc=nc+1
        if (nc.gt.200) pause '200 iterations done for usw'

c       if USW is converged go to the end of the sub-routine. If USW is not
c       converged repeat the calculation by returning to statement number 5

          if (abs((uswa-usw)/usw).le.1.0e-03) go to 20
          usw=uswa
          go to 5

        else
```

```
c      wave-current problem. set the current specification according to FLAGC

       if (flagc.eq.1.0) then
         usc=t1
       else if (flagc.eq.2.0) then
         ucr=t1
         zcr=t2
       else if (flagc.eq.3.0) then
         uave=t1
         hei=t2
       else
         pause 'flagc is not 1, 2 or 3'
       end if

c      assume initial values for USW and USC if they are zero

       if (usw.eq.0.0) then
         fwc1=0.01
         usw=ub1*sqrt(fwc1/2.0)
         if (flagc.ne.1.0) usc=0.1*usw
       end if

       mu=usc/usw
       ep=findep(mu,phicw)

c      begin iteration for USW and USC
c      calculate USWC, DELTA, ZE0 and BETA (Equations 9, 8, 12 and 118)

  10   uswc=usc/ep
       delta=(kap*uswc)/fre
       ze0=z0/delta
       beta=hei/(6.0*delta)

c      call subroutine FINDUSWN to calculate the wave shear velocities
c      for the principal wave component (for rough turbulent flow)

       call finduswn(ze0,kap,alpha,ep,1.0,uswc,ub1,uswr1,phib1,
     & solu1)

       fwcr1=2.0*((uswr1/ub1)**2.0)

c      limit FWRC1 (the rough turbulent friction factor to) 0.24

       if(fwcr1.gt.0.24) then
        uswr1=0.346*ub1
       end if
```

```fortran
c       calculate the smooth turbulent friction factor FWS1 and select the
c       larger value to calculate USW1 (the shear velocity based on the
c       principal shear stress. FLAGS is set to 1 or 0 for smooth or rough
c       turbulent regimes, respectively

        re1=(ub1**2.0)/(fre*vis)
        call smootht(re1,fws1)
        usws1=sqrt(fws1/2.0)*ub1
        usw1=max(uswr1,usws1)

        if(usws1.gt.uswr1) then
           print *,'smootht value used for w1'
           flags=1.0
        else
           flags=0.0
        end if
        fwc1=2.0*((usw1/ub1)**2.0)

c       calculate the shear velocity for the secondary wave component
c       if FLAGS = 0 the rough turbulent value is used while if FLAGS = 0
c       the smooth turbulent value is used

        if (ub2.eq.0.0) then

           usw2=0.0
           fwc2=0.0

        else

           if (flags.eq.0.0) then

              call finduswn(ze0,kap,alpha,ep,2.0,uswc,ub2,usw2,phib2,
     &        solu2)

              fwc2=2.0*((usw2/ub2)**2.0)

           else

              re2=(ub2**2.0)/(2.0*fre*vis)
              call smootht(re2,fwc2)
              usw2=sqrt(fwc2/2.0)*ub2

           end if

        end if

c       calculate the total wave shear velocity (i.e. an updated value of USW)
c       from Equation 119

        usw=sqrt(usw1**2.0+usw2**2.0)
```

```fortran
c       if the current shear velocity is not specified (i.e. FLAGC is not 1)
c       update USC by comparing the calculated and given current specifications

        if (flagc.eq.1.0) then
          usc1=usc
        else if (flagc.eq.2.0) then
          zecr=zcr/delta
          call velmean(usc,alpha,ep,kap,beta,zecr,ze0,ucr1)
          usc1=usc*(1.0+(0.5*(ucr-ucr1))/ucr)
        else if (flagc.eq.3.0) then
          fac=alpha*delta
          uave1=(usc/kap)*(alog(hei/(fac/ep))+ep*(alog(fac/z0)-
     &    1.0)+((ep*fac)/(2.0*hei))*(1.0/(ep**2.0)-1.0))
          usc1=usc*(1.0+(0.5*(uave-uave1))/uave)
        end if

        if(usc1.le.0.0) usc1=usc/2.0

c       calculate updated values of MU and EP using the new values USW
c       and USC1

        mu1=usc1/usw
        ep1=findep(mu1,phicw)

c       check for convergence of MU and EP. the criterion is that the
c       fractional change is less than 0.001. if the values converge go to the
c       end

        if (abs((mu1-mu)/mu).le.1.0e-3.and.abs((ep1-ep)/ep).
     &  le.1.0e-3) go to 20

c       if MU and EP do not converge update the values of MU, EP and USC and
c       repeat the calculation by going to statement 10

        mu=mu1
        ep=ep1
        usc=usc1
        nc=nc+1
        if (nc.gt.200) pause '200 iterations done for mu'
        go to 10

      end if

20    return
      end




c     FUNCTION FINDEP

      function findep(um,phicw)
```

```
c      calculates EP given MU (UM) and PHICW using Equation 120

       findep=um/((1.0+2.0*abs(cos(phicw))*(um**2.0)+(um**4.0))**0.25)

       return
       end




C      SUB-ROUTINE FINDUSWN

       subroutine finduswn(ze0,kap,alpha,ep,en,uswc,ub,usw,phib,solu)

c      calculates the solution for a periodic velocity component and the
c      bottom shear stress for that component. the output values are the shear
c      velocity USW, the phase of the bottom shear stress PHIB and the vector
c      SOLU which contains the five complex coefficients of Equations 67, 69
c      and 72. EN is the relative frequency defined by Equation 62

       complex*16 solu(5),term
       real*8 dber,dbei,dker,dkei,t1
       real*4 ze0,kap,alpha,ep,en,uswc,usw,ub,phib


c      call TCONCCOEFF to solve the 5 equations for the velocity problem
c      note that the value RHS in TCONCCOEFF is given as -1.0 to indicate
c      a velocity component.

       call tconccoeff(ze0,0.0,alpha,ep,solu,-1.0,en)

c      calculate the shear velocity and phase of the shear stress using
c      Equations 34 and 67.

       t1=2.0*sqrt(en*ze0)
       call dkelvinp(t1,0.0,dber,dbei,dker,dkei)
       term=0.5*t1*(solu(1)*dcmplx(dker,dkei)+
      &solu(2)*dcmplx(dber,dbei))

       usw=sqrt(kap*ub*uswc*abs(term))
       phib=datan2(dimag(term),dreal(term))

       return
       end




C      SUB-ROUTINES COEFF, MEAN, COS1 AND COS2 THAT CALCULATE THE REFERENCE
C      CONCENTRATION COMPONENTS

         subroutine coeff(um,phicw,ratpsi,rtau,delphi,valm,r1,r2)
```

```
c     integrates the instantaneous skin friction shear stress (Equation 100)
c     over a wave period to obtain the expansion in Equation 105.
c     the integration is done by the sub-routine CONTROL which integrates
c     the sub-routines MEAN, COS1 and COS2

      real*4 para(5)
      external mean,cos1,cos2

      pi=3.1415926
      hmin=0.001
      err=0.001

      para(1)=um
      para(2)=phicw
      para(3)=ratpsi
      para(4)=rtau
      para(5)=delphi

      call control(0.0,2.0*pi,valm,hmin,err,mean,5,para)
      call control(0.0,2.0*pi,valc1,hmin,err,cos1,5,para)
      call control(0.0,2.0*pi,valc2,hmin,err,cos2,5,para)

      valm=valm/(2.0*pi)
      valc1=valc1/pi
      valc2=valc2/pi
      r1=valc1/valm
      r2=valc2/valm

      return
      end




      function tau(phase,um,phicw,ratpsi,rtau,delphi)

c     calculates the instantaneous skin friction shear stress for the
c     sub-routines MEAN, COS1 and COS2

      tw=cos(phase)+rtau*cos(2.0*phase+delphi)

      t=tw**2.0+2.0*tw*(um**2.0)*cos(phicw)+um**4.0

      if(t.lt.0.0) t=0.0

      twc=sqrt(t)-ratpsi

      if(twc.lt.0.0) then
         tau=0.0
      else
         tau=twc
      end if

      return
      end
```

```fortran
      subroutine mean(phase,t,npara,para)

      real*4 para(npara)

      um=para(1)
      phicw=para(2)
      ratpsi=para(3)
      rtau=para(4)
      delphi=para(5)

      t=tau(phase,um,phicw,ratpsi,rtau,delphi)

      return
      end


      subroutine cos1(phase,t,npara,para)

      real*4 para(npara)

      um=para(1)
      phicw=para(2)
      ratpsi=para(3)
      rtau=para(4)
      delphi=para(5)

      t=tau(phase,um,phicw,ratpsi,rtau,delphi)*cos(phase)

      return
      end


      subroutine cos2(phase,t,npara,para)

      real*4 para(npara)

      um=para(1)
      phicw=para(2)
      ratpsi=para(3)
      rtau=para(4)
      delphi=para(5)

      t=tau(phase,um,phicw,ratpsi,rtau,delphi)*cos(2.0*phase)

      return
      end

C     SUB-ROUTINE TCONCCOEFF

      subroutine tconccoeff(zr,aa,alpha,ep,sol,rhs,en)
```

```
c         calculates the five coefficients of Equations 67, 69 and 72 for the
c         solution of a velocity or concentration component by solving the
c  ·      five simultaneous equations 74, 75, 76, 77 and 78.
c         EN is the relative frequency defined by Equation 62
c         for a velocity component the value RHS is given as -1.0 and the
c         non-dimensional reference level for the velocity (ZE0 in the main
c         program) is input to ZR .
c         for a concentration component the value RHS is given as 1.0 and the
c         non-dimensional reference level for the concentration (ZER in the main
c         program) is input to ZR .
c         the five coefficients are output in the vector SOL
c         if EP < 0.05 then the pure wave problem (bi-linear eddy viscosity)
c         is to be solved and SOL(4) and SOL(5) are zero.

          real*8 t1,t2,t3,t4,t5,t6,t7,t8,t9,t10,t11,t12,t13,a
          real*8 fber,fbei,fker,fkei,dber,dbei,dker,dkei
          complex*16 am(5,5),b(5),sol(5),am0(3,3),b0(3),sol0(3)
          complex*16 rplus,rminus,ti1,ti2,ti3,ti4,ti5,ti6,ti7
          real*4 en

          a=aa

          if (ep.lt.0.02) then

          n=3

          t1=(zr)**(-0.5*a)
          t2=2.0*sqrt(en*zr)
          t3=(alpha)**(-0.5*a)
          t4=2.0*sqrt(en*alpha)
          t5=t3*sqrt(en/alpha)
          t6=a*t3/(2.0*alpha)

          sr=a**2.0
          si=4.0*en*alpha
          ti1=cdsqrt(dcmplx(sr,si))
          rminus=(-1.0*a-ti1)/(2.0*alpha)
          ti3=alpha*rminus

          do 10 i=1,n
            do 20 j=1,n
             am0(i,j)=(0.0,0.0)
20          continue
           b0(i)=(0.0,0.0)
           sol0(i)=(0.0,0.0)
10        continue

          if (zr.le.alpha) then

          call kelvinp(t2,a,fber,fbei,fker,fkei)

          am0(1,1)=t1*dcmplx(fker,fkei)
          am0(1,2)=t1*dcmplx(fber,fbei)
```

```
        else

        ti7=zr*rminus

        am0(1,3)=cdexp(ti7)

        end if

        b0(1)=dcmplx(rhs,0.0)

        call kelvinp(t4,a,fber,fbei,fker,fkei)
        call dkelvinp(t4,a,dber,dbei,dker,dkei)

        am0(2,1)=t3*dcmplx(fker,fkei)
        am0(2,2)=t3*dcmplx(fber,fbei)
        am0(2,3)=-1.0*cdexp(ti3)

        am0(3,1)=t5*dcmplx(dker,dkei)-t6*dcmplx(fker,fkei)
        am0(3,2)=t5*dcmplx(dber,dbei)-t6*dcmplx(fber,fbei)
        am0(3,3)=-1.0*rminus*cdexp(ti3)

        call comsolve(am0,b0,sol0,n)

        do 30 i=1,n
            sol(i)=sol0(i)
30      continue
        sol(4)=(0.0,0.0)
        sol(5)=(0.0,0.0)

        else

        n=5

        t1=(zr)**(-0.5*a)
        t2=2.0*sqrt(en*zr)
        t3=(alpha)**(-0.5*a)
        t4=2.0*sqrt(en*alpha)
        t5=t3*sqrt(en/alpha)
        t6=a*t3/(2.0*alpha)
        t7=(alpha/ep)**(-0.5*(a/ep))
        t8=t4/ep
        t9=t7*sqrt(en/alpha)
        t10=a*t7/(2.0*alpha)
        t11=a/ep

        sr=a**2.0
        si=4.0*en*alpha
        ti1=cdsqrt(dcmplx(sr,si))
        rplus=(-1.0*a+ti1)/(2.0*alpha)
        rminus=(-1.0*a-ti1)/(2.0*alpha)
        ti2=alpha*rplus
        ti3=alpha*rminus
        ti4=ti2/ep
        ti5=ti3/ep
```

```fortran
      do 40 i=1,n
        do 50 j=1,n
        am(i,j)=(0.0,0.0)
50      continue
       b(i)=(0.0,0.0)
       sol(i)=(0.0,0.0)
40      continue

        if (zr.le.alpha) then

        call kelvinp(t2,a,fber,fbei,fker,fkei)

        am(1,1)=t1*dcmplx(fker,fkei)
        am(1,2)=t1*dcmplx(fber,fbei)

        else if (zr.gt.alpha.and.zr.le.(alpha/ep)) then

        ti6=zr*rplus
        ti7=zr*rminus

        am(1,3)=cdexp(ti6)
        am(1,4)=cdexp(ti7)

        else

        t12=(zr)**(-0.5*(a/ep))
        t13=2.0*sqrt((en*zr)/ep)

        call kelvinp(t13,t11,fber,fbei,fker,fkei)

        am(1,5)=t12*dcmplx(fker,fkei)

        end if

        b(1)=dcmplx(rhs,0.0)

        call kelvinp(t4,a,fber,fbei,fker,fkei)
        call dkelvinp(t4,a,dber,dbei,dker,dkei)

        am(2,1)=t3*dcmplx(fker,fkei)
        am(2,2)=t3*dcmplx(fber,fbei)
        am(2,3)=-1.0*cdexp(ti2)
        am(2,4)=-1.0*cdexp(ti3)

        am(3,1)=t5*dcmplx(dker,dkei)-t6*dcmplx(fker,fkei)
        am(3,2)=t5*dcmplx(dber,dbei)-t6*dcmplx(fber,fbei)
        am(3,3)=-1.0*rplus*cdexp(ti2)
        am(3,4)=-1.0*rminus*cdexp(ti3)
```

```
          call kelvinp(t8,t11,fber,fbei,fker,fkei)
          call dkelvinp(t8,t11,dber,dbei,dker,dkei)


          am(4,3)=cdexp(ti4)
          am(4,4)=cdexp(ti5)
          am(4,5)=-1.0*t7*dcmplx(fker,fkei)


          am(5,3)=rplus*cdexp(ti4)
          am(5,4)=rminus*cdexp(ti5)
          am(5,5)=-1.0*t9*dcmplx(dker,dkei)+t10*dcmplx(fker,fkei)


          call comsolve(am,b,sol,n)


          end if


          return
          end



C      SUB-ROUTINES TCONC, MCONC AND VELMEAN THAT CALCULATE THE SOLUTIONS
C      FOR THE PERIODIC COMPONENTS AND THE MEAN CONCENTRATION AND VELOCITY
C      RESPECTIVELY


          subroutine tconc(zr,aa,alpha,ep,sol,zz,ct,en)


C      calculates the complex value of the time-varying concentration or
C      velocity component at the non-dimensional height ZZ using Equations 67,
C      69 and 72.
C      EN is the relative frequency defined by Equation 62
C      the vector SOL contains the five complex constants in these equations
C      if EP < 0.05 then the pure wave (bi-linear) solution is calculated
C      using Equations 67 and 69 with the coefficient C set to zero.
C      CT is the calculated value.


          real*8 t1,t2,t3,a,z
          real*8 fber,fbei,fker,fkei
          real*4 en
          complex*16 sol(5),ct
          complex*16 rplus,rminus,ti1


          a=aa
          z=zz


          if(ep.lt.0.02) then


          if(z.lt.zr) then
           print*,'z is smaller than zr in tconc - returning zero'
          .ct=(0.0,0.0)
          else if(z.lt.alpha.and.z.ge.zr) then
           t1=(z)**(-0.5*a)
           t2=2.0*sqrt(en*z)
           call kelvinp(t2,a,fber,fbei,fker,fkei)
           ct=sol(1)*t1*dcmplx(fker,fkei)+sol(2)*t1*dcmplx(fber,fbei)
```

```
      else
       sr=a**2.0
       si=4.0*en*alpha
       til=cdsqrt(dcmplx(sr,si))
       rminus=(-1.0*a-til)/(2.0*alpha)
       ct=sol(3)*cdexp(rminus*z)
      end if


     else

      if(z.lt.zr) then
       print*,'z is smaller than zr in tconc'
       ct=(0.0,0.0)
      else if(z.lt.alpha.and.z.ge.zr) then
       t1=(z)**(-0.5*a)
       t2=2.0*sqrt(en*z)
       call kelvinp(t2,a,fber,fbei,fker,fkei)
       ct=sol(1)*t1*dcmplx(fker,fkei)+sol(2)*t1*dcmplx(fber,fbei)
      else if(z.ge.alpha.and.z.le.(alpha/ep)) then
       sr=a**2.0
       si=4.0*en*alpha
       til=cdsqrt(dcmplx(sr,si))
       rplus=(-1.0*a+til)/(2.0*alpha)
       rminus=(-1.0*a-til)/(2.0*alpha)
       ct=sol(3)*cdexp(rplus*z)+sol(4)*cdexp(rminus*z)
      else
       t1=(z)**(-0.5*(a/ep))
       t2=2.0*sqrt(en*z/ep)
       t3=a/ep
       call kelvinp(t2,t3,fber,fbei,fker,fkei)
       ct=sol(5)*t1*dcmplx(fker,fkei)
      end if

     end if

     return
     end




     subroutine mconc(zr,a,alpha,ep,beta,z,cm)

c    calculates the mean concentration (CM) from Equations 50, 52, 54 and
c    117 at a non-dimensional height Z

     e=exp(1.0)

     if(ep.eq.0.0) then
```

```fortran
       if(zr.lt.alpha) then
          b1=(zr)**a
          b2=b1*((e/alpha)**a)
       else
          b2=exp((a*zr)/alpha)
       end if

       if(z.lt.zr) then
          print*,'z is less than zrin mconc - returning zero'
          cm=0.0
       else if(z.ge.zr.and.z.lt.alpha) then
          cm=b1*(z**(-1.0*a))
       else
          cm=b2*exp(-1.0*((a*z)/alpha))
       end if

     else if((alpha/ep).gt.beta) then

       if(zr.lt.alpha) then
          b1=(zr)**a
          b2=b1*((e/alpha)**a)
       else
          b2=exp((a*zr)/alpha)
       end if

       if(z.lt.zr) then
          print*,'z is less than zrin mconc - returning zero'
          cm=0.0
       else if(z.ge.zr.and.z.lt.alpha) then
          cm=b1*(z**(-1.0*a))
       else
          cm=b2*exp(-1.0*((a*z)/alpha))
       end if

     else

       if(zr.lt.alpha) then
          b1=(zr)**a
          b2=b1*((e/alpha)**a)
          b3=b2*((alpha/(e*ep))**(a/ep))
          b4=b3*((e/beta)**(a/ep))
       else if(zr.ge.alpha.and.zr.le.(alpha/ep)) then
          b2=exp((a*zr)/alpha)
          b3=b2*((alpha/(e*ep))**(a/ep))
          b4=b3*((e/beta)**(a/ep))
       else if(zr.ge.(alpha/ep).and.zr.le.beta) then
          b3=(zr)**(a/ep)
          b4=b3*((e/beta)**(a/ep))
       else
          b4=exp((a*zr)/(ep*beta))
       end if
```

```fortran
      if(z.lt.zr) then
        print*,'z is less than zr in mconc - returning zero'
        cm=0.0
      else if(z.ge.zr.and.z.lt.alpha) then
        cm=b1*(z**(-1.0*a))
      else if (z.ge.alpha.and.z.lt.(alpha/ep)) then
        cm=b2*exp(-1.0*((a*z)/alpha))
      else if(z.ge.(alpha/ep).and.z.le.beta) then
        cm=b3*(z**(-1.0*(a/ep)))
      else
        cm=b4*exp(-1.0*((a*z)/(ep*beta)))
      end if

      end if


      return
      end






      subroutine velmean(uc,alpha,ep,ak,beta,zz,z0,v)

c     calculates the mean velocity (V) from Equations 10 and 116 at a
c     given non-dimensional height ZZ

      if(ep.eq.0.0) then

        u=0.0

      else if((alpha/ep).gt.beta) then

        if(zz.lt.z0) then
          print *,'z less than z0 in mvel - returning zero'
          u=0.0
        else if(zz.ge.z0.and.zz.lt.alpha) then
          u=ep*log(zz/z0)
        else
          u=ep*(zz/alpha+log(alpha/z0)-1.0)
        end if

      else

        if(zz.lt.z0) then
          print *,'z less than z0 in mvel - returning zero'
          u=0.0
        else if(zz.ge.z0.and.zz.lt.alpha) then
          u=ep*log(zz/z0)
        else if(zz.ge.alpha.and.zz.lt.(alpha/ep)) then
          u=ep*(zz/alpha+log(alpha/z0)-1.0)
```

```fortran
      else if(zz.ge.(alpha/ep).and.zz.lt.beta) then
        u=log(zz*ep/alpha)+1.0+ep*(log(alpha/z0)-1.0)
      else
        u=zz/beta+log((beta*ep)/alpha)+ep*(log(alpha/z0)-1.0)
      end if


    end if
    v=(uc/ak)*u
    return
    end
```

```fortran
C     SUBROUTINES FLUXMEAN, FLUXM, FLUXWAVE AND FLUXWV THAT CALCULATE THE
C     SUSPENDED SEDIMENT TRANSPORTS DUE TO THE MEAN AND PERIODIC COMPONENTS

      subroutine fluxmean(alpha,kap,ep,ze0,zer,a,usc,zet,zeb,delta,
     &beta,fm)

c     calculates the suspended sediment flux (FM) due to the mean velocity
c     by calling subroutines CONTROL to integrate the subroutine
c     FLUXM over the water depth from non-dimensional level ZEB to ZET.

      real*4 para(8),kap

      parameter (hmin=0.001,err=0.001)
      external fluxm

      para(1)=alpha
      para(2)=kap
      para(3)=ep
      para(4)=ze0
      para(5)=zer
      para(6)=a
      para(7)=usc
      para(8)=beta

      call control(zeb,zet,val,hmin,err,fluxm,8,para)

      fm=delta*val

      return
      end
```

```fortran
      subroutine fluxm(z,f,npara,para)

c     calculates the flux (F) due to the mean components at any
c     non-dimensional level Z

      real*4 para(npara),kap
```

```fortran
      alpha=para(1)
      kap=para(2)
      ep=para(3)
      ze0=para(4)
      zer=para(5)
      a=para(6)
      usc=para(7)
      beta=para(8)

      call mconc(zer,a,alpha,ep,beta,z,cm)
      call velmean(usc,alpha,ep,kap,beta,z,ze0,v)

      f=cm*v

      return
      end




      subroutine fluxwave(alpha,ep,ze0,zer,a,zet,zeb,delta,
     &r,ub,phib,en,solu,solc,fw)

c     calculates the suspended sediment flux (FM) due to the periodic
c     components of relative frequency (defined by Equation 62) EN
c     calls sub-routine CONTROL to integrate the subroutine FLUXWV
c     over the water depth from non-dimensional level ZEB to ZET.

      complex*16 solu(5),solc(5),solu1(5),solc1(5)
      real*4 para(9)

      parameter (hmin=0.001,err=0.001)
      external fluxwv

      common /wflux/solu1,solc1

      para(1)=alpha
      para(2)=ep
      para(3)=ze0
      para(4)=zer
      para(5)=a
      para(6)=r
      para(7)=ub
      para(8)=phib
      para(9)=en

      do 10 i=1,5
         solu1(i)=solu(i)
         solc1(i)=solc(i)
10    continue

      call control(zeb,zet,val,hmin,err,fluxwv,9,para)

      fw=delta*val
```

```fortran
      return
      end



      subroutine fluxwv(z,f,npara,para)

c     calculates the flux due to the periodic components (F) at any level Z

      complex*16 solu1(5),solc1(5),ct,uw
      real*4 para(npara)

      common /wflux/solu1,solc1


      alpha=para(1)
      ep=para(2)
      ze0=para(3)
      zer=para(4)
      a=para(5)
      r=para(6)
      ub=para(7)
      phib=para(8)
      en=para(9)

c     call TCONC to calculate the concentration

      call tconc(zer,a,alpha,ep,solc1,z,ct,en)

c     call TCONC to calculate the velocity

      call tconc(ze0,0.0,alpha,ep,solu1,z,uw,en)

      if (ct.eq.(0.0,0.0)) then
          phic=0.0
      else
          phic=atan2(dimag(ct),dreal(ct))
      end if

      phiu=atan2(dimag(uw),(1.0+dreal(uw)))
      u=ub*sqrt((1.0+dreal(uw))**2.0+dimag(uw)**2.0)

      f=0.5*r*u*abs(ct)*cos(phib+phic-phiu)

      return
      end
```

```
c       SUBROUTINES BEDLOAD, BLOADW AND BLOADN THAT CALCULATE THE BED LOAD
c       TRANSPORTS

        subroutine bedload(um,uswp1,rtau,delphi,phicwd,phiswd,betad,
       &diam,s,psic,phifd,qw,qn)

c       to calculate the bedload flux in the wave and wave normal
c       directions (QW and QN) in units of cm^3/cm/s.
c       integrates equation 85 over a wave cycle.
c       QW is positive in the wave direction
c       QN is positive in the anti-clockwise wave normal direction
c       USWP1 - wave skin friction shear velocities from ub1 (cm/s)
c       UM - ratio of current skin friction shear velocity to uswp1
c       RTAU - ratio of skin friction shear stresses from ub2 and ub1
c       DELPHI - difference in bottom phases of tauwp1 and tauwp2
c       PHICWD - anticlockwise angle between wave direction and current (deg)
c       PHISWD - anticlockwise angle between wave direction and
c                direction of increasing slope (rad)
c       BETAD - angle of slope (deg)
c       DIAM - sediment diameter (cm)
c       S - sediment specific gravity
c       PSIC - critical Shields' parameter for the initiation of motion
c       PHIFD - angle of repose of sediment (deg)
c       calls the integrating routine control
c       BLOADW and BLOADN are the subroutines that calculate the wave direction
c       and wave normal fluxes respectively.

        real*4 para(9)
        external bloadw,bloadn

        pi=3.1415926
        fac=pi/180.0
        gee=981.0

        hmin=0.001
        err=0.001

        phicw=phicwd*fac
        phisw=phiswd*fac
        phif=phifd*fac
        beta=betad*fac

        psiwp1=(uswp1**2.0)/((s-1.0)*gee*diam)

        para(1)=psiwp1
        para(2)=um
        para(3)=phicw
        para(4)=rtau
        para(5)=delphi
        para(6)=psic
        para(7)=phif
        para(8)=beta
        para(9)=phisw
```

```fortran
      fac1=(sqrt((s-1.0)*gee*diam)*diam)/(2.0*pi)

      call control(0.0,2.0*pi,valw,hmin,err,bloadw,10,para)

      qw=fac1*valw

      if(phicwd.ne.0.0.and.phicwd.ne.180.0) then

          call control(0.0,2.0*pi,valn,hmin,err,bloadn,10,para)

          qn=fac1*valn
      else
          qn=0.0
      end if


      return
      end




      subroutine bloadw(phase,q,npara,para)

c     calculates the non-dimensional bedload flux in the wave direction
c     Q for a given value of the phase of the bottom shear stress (PHASE)
c     para contains the parameters needed for the calculation

      real*4 para(npara)

      psiwp1=para(1)
      um=para(2)
      phicw=para(3)
      rtau=para(4)
      delphi=para(5)
      psic=para(6)
      phif=para(7)
      beta=para(8)
      phisw=para(9)

      ums=um**2.0
      tw=cos(phase)+rtau*cos(2.0*phase+delphi)
      e=tw**2.0+2.0*ums*tw*cos(phicw)+(ums**2.0)

c     calculate the magnitude of the bedload flux

      if(e.le.0.0) then
          psi=0.0
      else
          psi=psiwp1*sqrt(e)
      end if
```

```
c       calculate the angle PHIT made by the flux with the wave direction
c       TBT accounts for the effect of the slope in the direction of the flux
c       on both the critical shear stress and the flux

        phit=atan2(ums*sin(phicw),(cos(phase)+ums*cos(phicw)))
        tbt=(tan(beta)*cos(phit-phisw))/tan(phif)
        psicr=psic*(1.0+tbt)


c       and find Q as the component in the wave direction

        if (psi.le.psicr) then
           q=0.0
        else
           q=(8.0*((psi-psicr)**1.5)*cos(phit))/(1.0+tbt)
        end if


        return
        end




        subroutine bloadn(phase,q,npara,para)

c       calculates the non-dimensional bedload flux in the wave-normal
c       direction, Q for a given value of the phase of the bottom shear
c       stress (PHASE). para contains the parameters needed for the calculation

        real*4 para(npara)

        psiwp1=para(1)
        um=para(2)
        phicw=para(3)
        rtau=para(4)
        delphi=para(5)
        psic=para(6)
        phif=para(7)
        beta=para(8)
        phisw=para(9)

        ums=um**2.0
        tw=cos(phase)+rtau*cos(2.0*phase+delphi)
        e=tw**2.0+2.0*ums*tw*cos(phicw)+(ums**2.0)

c       calculate the magnitude of the bedload flux

        if(e.le.0.0) then
           psi=0.0
        else
           psi=psiwp1*sqrt(e)
        end if
```

```
c      calculate the angle PHIT made by the flux with the wave direction
c      TBT accounts for the effect of the slope in the direction of the flux
c      on both the critical shear stress and the flux

       phit=atan2(ums*sin(phicw),(cos(phase)+ums*cos(phicw)))
       tbt=(tan(beta)*cos(phit-phisw))/tan(phif)
       psicr=psic*(1.0+tbt)


c      and find Q as the component in the wave normal direction

       if (psi.le.psicr) then
          q=0.0
       else
          q=(8.0*((psi-psicr)**1.5)*sin(phit))/(1.0+tbt)
       end if


       return
       end




C      SUBROUTINES SHIELDS, FALLVEL, SMOOTHT, VISCOSITY AND FINDKB THAT
C      INCORPORATE THE RELATIONS FOR THE CRITICAL SHIELDS PARAMETER, THE FALL
C      VELOCITY, THE SMOOTH TURBULENT FRICTION FACTOR, THE VISCOSITY AND THE
C      EQUIVALENT ROUGHNESS

       subroutine shields(x,y)

c      calculates the critical Shields' parameter for the initiation of
c      motion from Shields curve. uses the modified Shields curve given
c      by Madsen and Grant(1976). X is the non-dimensional grain size
c      S* and Y the critical Shields parameter.

       real*4 sstar(58),psic(58),sstarr(58),psicr(58)
       logical first
       save first,nd,sstar,psic

       data first/ .true./

       data sstarr/0.9,0.938,1.04,1.14,1.28,
      &1.47,1.6,1.75,1.96,2.23,2.44,2.62,2.86,3.17,3.4,3.79,4.2,4.51,
      &4.99,5.46,5.93,6.51,7.03,7.6,8.24,9.24,9.83,10.6,11.6,12.9,14.2,
      &16.4,18.1,19.9,22.7,25.0,27.3,30.7,33.8,38.6,42.6,46.6,53.6,
      &60.8,68.0,77.0,90.7,107.0,127.2,147.6,172.6,194.0,218.0,242.0,
      &273.0,313.0,349.0,397.0/
```

```
      data psicr/0.103,0.0958,0.0898,0.0845,
&0.0788,0.0725,0.0687,0.0654,0.0614,0.0576,0.055,0.053,0.051,
&0.0484,0.0471,0.045,0.0431,0.0418,0.0403,0.0391,0.038,0.0368,
&0.0363,0.0356,0.0347,0.0341,0.0338,0.0334,0.033,0.0328,0.0327,
&0.0326,0.0325,0.0328,0.033,0.0333,0.0334,0.0339,0.0343,0.0349,
&0.0353,0.036,0.0368,0.038,0.0389,0.0403,0.042,0.0438,0.0459,
&0.0477,0.0499,0.0512,0.0523,0.0534,0.054,0.0543,0.0545,0.0546/


      if(first) then
        nd=58
        do 10 i=1,nd
           sstar(i)=alog(sstarr(i))
           psic(i)=alog(psicr(i))
10    continue
        first= .false.
      end if

      xl=alog(x)

      if(xl.lt.sstar(1)) then
        y=0.1/(x**0.25)
      else if (xl.ge.sstar(1).and.xl.le.sstar(nd)) then
         do 30 i=1,nd
           if(xl.ge.sstar(i).and.xl.le.sstar(i+1)) then
               yl=psic(i)+(xl-sstar(i))*(psic(i+1)-psic(i))/
&  (sstar(i+1)-sstar(i))
               y=exp(yl)
               go to 20
           end if
30    continue
      else
         y=0.0546
      end if
20    return
      end




      subroutine fallvel(x,y)

c     finds non-dimensional fall velocity (Y) given non-dimensional grain
c     size  S* (X)

      real*4 sstar(59),wstar(59),sl(59),wl(59)
      logical first
      save first,nd,sl,wl

      data first/ .true./
```

```
      data sstar/0.7,0.706,0.739,0.764,0.813,0.861,0.918,0.969,1.0,
     &1.05,1.13,1.26,1.39,1.52,1.70,1.88,2.08,2.32,2.61,
     &2.89,3.21,3.57,3.97,4.46,4.82,5.15,5.59,5.95,6.48,
     &6.95,7.59,8.24,8.94,9.43,10.3,11.6,12.7,14.2,15.8,
     &18.0,20.7,24.0,27.7,32.6,36.2,40.6,47.6,56.8,66.6,
     &80.2,98.1,117.5,139.6,166.1,212.6,260.5,307.4,393.4,400.6/

      data wstar/0.156,0.157,0.159,0.163,0.170,0.178,0.186,0.193,0.199,
     &0.205,0.216,0.232,0.249,0.264,0.286,0.306,0.327,0.351,0.380,
     &0.405,0.432,0.460,0.491,0.524,0.546,0.567,0.595,0.615,0.644,
     &0.670,0.699,0.729,0.754,0.777,0.811,0.849,0.879,0.919,0.954,
     &1.000,1.053,1.097,1.158,1.217,1.254,1.300,1.363,1.423,1.481,
     &1.544,1.615,1.666,1.714,1.753,1.790,1.792,1.795,1.797,1.799/

         if(first) then
           nd=59
           do 10 i=1,nd
              sl(i)=alog(sstar(i))
              wl(i)=alog(wstar(i))
10         continue
           first= .false.
         end if

         xl=alog(x)

         if (xl.lt.sl(1)) then
            y=0.22222*x
         else if(xl.ge.sl(1).and.xl.le.sl(nd)) then
            do 30 i=1,nd
               if(xl.ge.sl(i).and.xl.le.sl(i+1)) then
                  yl=wl(i)+(xl-sl(i))*(wl(i+1)-wl(i))/
     & (sl(i+1)-sl(i))
                  y=exp(yl)
                  go to 20
               end if
30          continue
         else
            y=1.8
         end if
20       return
         end




         subroutine smootht(x,y)

c        calculates the smooth turbulent friction factor (Y) for an input
c        value of the Reynolds number (X). uses the smooth turbulent curve of
c        Jonsson (1978)
```

```fortran
      real*4 rer(23),fwr(23),re(23),fw(23)
      logical first
      save first,nd,re,fw

      data first/ .true./

      data rer/2000.0,3008.0,4672.0,7426.0,9134.0,
     &11295.0,15650.0,19077.0,21718.0,28000.0,35800.0,48250.0,
     &61760.0,85830.0,114200.0,156000.0,198800.0,272000.0,
     &384500.0,558100.0,775300.0,1001360.0,10000000.0/

      data fwr/0.0447,0.0365,0.02922,0.02323,
     &0.02073,0.01898,0.01594,0.01481,0.01402,0.0127,0.01182,
     &0.01091,0.01029,0.009517,0.00884,0.008255,0.007726,0.007161,
     &0.006664,0.006078,0.005687,0.00539,0.003464/

      if(first) then
        nd=23
        do 10 i=1,nd
           re(i)=alog(rer(i))
           fw(i)=alog(fwr(i))
10      continue
        first= .false.
      end if

      xl=alog(x)

      if(xl.lt.re(1)) then
         y=2.0/sqrt(x)
      else if (xl.ge.re(1).and.xl.le.re(nd)) then
         do 30 i=1,nd
            if(xl.ge.re(i).and.xl.le.re(i+1)) then
               yl=fw(i)+(xl-re(i))*(fw(i+1)-fw(i))/
     & (re(i+1)-re(i))
               y=exp(yl)
               go to 20
            end if
30       continue
      else
         pause 're greater than 1e7 in smootht'
      end if
20    return
      end




      subroutine viscosity(x,y)
```

```fortran
c       calculates the kinematic viscosity of water when given the
c       temperature

        real*4 temp(12),vis(12)

        data temp/5.0,10.0,15.0,20.0,25.0,30.0,35.0,40.0,50.0,
     &60.0,70.0,80.0/

        data vis/0.0151,0.013,0.0114,0.01,0.00894,0.00802,0.00725,
     &0.00659,0.00554,0.00475,0.00414,0.00366/

        nd=12
        if(x.lt.temp(1).or.x.gt.temp(nd))
     & pause 'out of range viscosity'
        do 30 i=1,nd
        if(x.ge.temp(i).and.x.le.temp(i+1)) then
        y=vis(i)+(x-temp(i))*(vis(i+1)-vis(i))/
     & (temp(i+1)-temp(i))
        go to 20
        end if
30      continue
20      return
        end




        subroutine findkb(z,ab,diam,kb,flagz,ha,st)

        real*4 kb

c       calculates equivalent Nikuradse roughness of a sand bed.
c       uses Equations 35, 36 and 41.
c       Z - ripple parameter defined by Equation 37
c       AB - near bottom excursion amplitude (cm)
c       DIAM - mean grain diameter (cm)
c       KB - equivalent Nikuradse roughness
c       FLAGZ -flag that indicates the bed condition
c       FLAGZ = -1 for z < 0.0016 (i.e. less than the observed
c       range for field ripples)
c       FLAGZ = 0 for 0.0016 < z < 0.18 (z in the ripple range)
c       FLAGZ = 1 for z > 0.18 (z in flat bed range)
c       HA - ripple height (cm)
c       ST - ripple steepness
c      the bed condition and the ripple geometry are calculated by Equation
c       36 and the equivalent roughness by Equations 35 and 41.

       if (z.lt.0.0016) then
          flagz=-1.0
          ha=(ab*0.0181)/(z**0.5)
          st=0.147/(z**0.0105)
          kb=4.0*ha
```

```fortran
      else if (z.ge.0.0016.and.z.lt.0.012) then
        flagz=0.0
        ha=(ab*0.0181)/(z**0.5)
        st=0.147/(z**0.0105)
        kb=4.0*ha
       else if (z.ge.0.012.and.z.lt.0.18) then
        flagz=0.0
        ha=(0.0007*ab)/(z**1.23)
        st=0.0144/(z**0.552)
        kb=4.0*ha
      else
        flagz=1.0
        ha=0.0
        st=0.0
        kb=10.0*diam
      end if


      return
      end
```

```fortran
C     SUBROUTINES CONTROL AND INTEGRATE THAT PERFORM THE NUMERICAL
C     INTEGRATION OF A GIVEN FUNCTION

      subroutine control(tstart,tstop,val,hmin,err,grand,npara,para)
c
c     integrates a given function grand(X,Y,NPARA,PARA) with respect to
c     X from X = TSTART to X = TSTOP using a fourth order
c     runge-kutta method. HMIN is the minimum step length and
c     ERR is the permissible relative error per step. the result
c     is returned as VAL. calls subroutine integrate which performs
c     one step of the integration.
c
c     Based on a subroutine given in "Numerical Recipes" by Press et al.,
c     Cambridge University Press (1987).

      real*4 para(npara)
      external grand

      hnext=hmin
      hdid=0.0
      val=0.0
      x=tstart
      call grand(tstart,fx,npara,para)
10    x=x+hdid
      htry=hnext
      if ((tstop-x).le.0.1e-06) go to 20
      if ((tstop-x).le.hnext) htry=tstop-x
      call integrate(x,fx,add,htry,hdid,hnext,
     & hmin,err,f3,grand,npara,para)
      val=val+add
      fx=f3
      go to 10
```

```
20        return
          end




          subroutine integrate(x,fx,dely,htry,hdid,hnext
      &   ,hmin,err,f3,grand,npara,para)
c
c         performs one step of the integration. H = HTRY is the trial
c         step length. the step is performed as one step of H (result
c         DELY1) and as two of H/2 (result DELY2). PERR is the relative
c         error between the two results. if PERR > ERR the step length
c         is decreased and the process repeated with HMIN being the
c         minimum step length.if the step is successful the step length
c         is increased for the next step (HNEXT)
c         GRAND(X,Y,NPARA,PARA) is the function being integrated

          real*4 para(npara)
          external grand

10        h=htry
          call grand((x+h/2.0),f2,npara,para)
          call grand((x+h),f3,npara,para)
          call grand((x+h/4.0),f4,npara,para)
          call grand((x+0.75*h),f5,npara,para)
          dely1=h*(fx+4.0*f2+f3)/6.0
          dely2=dely1/2.0+h*(2.0*(f4+f5)-f2)/6.0
          if(dely2.eq.0.0) then
          hdid=h
          hnext=h
          dely=dely2
          go to 20
          else
          per=(dely2-dely1)/dely2
          perr=abs(per)/err
          end if
          if (h.le.hmin) then
          hdid=hmin
          hnext=2.0*hmin
          else
            if(perr.gt.1.001) then
            htry=h*(perr**-0.25)
              if (htry.le.hmin) then
              htry=hmin
              end if
            go to 10
            else
            hdid=h
              if(perr.gt.6.0e-04) then
              hnext=0.9*h*(perr**-0.2)
```

```fortran
              else
              hnext=4.0*h
              end if
             end if
            end if
            dely=dely2+(dely2-dely1)/15.0
20          return
            end
```

```fortran
C      SUBROUTINES LUDCMP, LUBKSB AND COMSOLVE THAT SOLVE A SET OF
C      SIMULTANEOUS EQUATIONS WITH COMPLEX COEFFICIENTS

       subroutine ludcmp(a,n,np,indx)

c      decomposes a matrix into upper and lower triangular form
c      code from "Numerical Recipes" by Press et al., Cambridge University
c      Press (1987).
c      the decomposed matrix is written over the original matrix A.
c      N is the logical dimension of A and NP the physical dimension
c      NMAX - the largest N that can be handled

       parameter (nmax=50)
       real*8 a(np,np),vv(nmax)
       dimension indx(n)

       do 10 i=1,n
       aamax=0.
       do 20 j=1,n
       if(abs(a(i,j)).gt.aamax) aamax=abs(a(i,j))
20     continue
       if(aamax.eq.0.0) pause ' singular matrix'
       vv(i)=1.0/aamax
10     continue
       do 30 j=1,n
       if(j.gt.1) then
       do 40 i=1,j-1
       sum=a(i,j)
       if(i.gt.1) then
       do 50 k=1,i-1
       sum=sum-a(i,k)*a(k,j)
50     continue
       a(i,j)=sum
       end if
40     continue
       end if
       aamax=0.
       do 60 i=j,n
       sum=a(i,j)
       if(j.gt.1) then
       do 70 k=1,j-1
       sum=sum-a(i,k)*a(k,j)
```

```
70       continue
         a(i,j)=sum
         end if
         dum=vv(i)*abs(sum)
         if(dum.ge.aamax) then
         imax=i
         aamax=dum
         end if
60       continue
         if(j.ne.imax) then
         do 80 k=1,n
         dum=a(imax,k)
         a(imax,k)=a(j,k)
         a(j,k)=dum
80       continue
         vv(imax)=vv(j)
         end if
         indx(j)=imax
         if(j.ne.n) then
         if(a(j,j).eq.0.0) then
         pause ' singular matrix 2'
         end if
         dum=1.0/a(j,j)
         do 90 i=j+1,n
         a(i,j)=a(i,j)*dum
90       continue
         end if
30       continue
         if(a(n,n).eq.0.0) pause 'singular matrix 3'
         return
         end




         subroutine lubksb(a,n,np,indx,b)

c        uses the decomposed matrix A from subroutine LUDCMP to solve
c        for a rhs vector B by back substitution
c        code from "Numerical Recipes" by Press et al., Cambridge University
c        Press (1987).
c        the solution vector is returned in B
c        N is the logical dimension of A and NP the physical dimension

         real*8 a(np,np),b(n)
         dimension indx(n)

         ii=0
         do 10 i=1,n
         ll=indx(i)
         sum=b(ll)
         b(ll)=b(i)
         if(ii.ne.0) then
         do 20 j=ii,i-1
```

```
              sum=sum-a(i,j)*b(j)
20            continue
              else if(sum.ne.0.0) then
              ii=i
              end if
              b(i)=sum
10            continue
              do 30 i=n,1,-1
              sum=b(i)
              if(i.lt.n) then
              do 40 j=i+1,n
              sum=sum-a(i,j)*b(j)
40            continue
              end if
              b(i)=sum/a(i,i)
30            continue
              return
              end




              subroutine comsolve(a,b,sol,n)

c        solves a system of simultaneous equations with complex coefficients
c        using the subroutines LUDCMP and LUBKSB.
c        the input complex coefficient matrix is first unpacked into
c        a real matrix of twice the size. the solution is returned
c        as a complex vector
c        can handle upto nmax/2 complex unknowns

              parameter (nmax=20)
              complex*16 a(n,n),b(n),sol(n)
              real*8 as(nmax,nmax),bs(nmax),ar,ai
              dimension indx(nmax)

c        unpack the complex matrix A and vector B into the real matrix AS
c        and real vector BS

              do 10 i=1,n
              n1=2*i-1
              n2=2*i
              do 20 j=1,n
              n3=2*j-1
              n4=2*j
              ar=dreal(a(i,j))
              ai=dimag(a(i,j))
              as(n1,n3)=ar
              as(n1,n4)=-1.0*ai
              as(n2,n3)=ai
              as(n2,n4)=ar
```

```
  20       continue
           bs(n1)=dreal(b(i))
           bs(n2)=dimag(b(i))
  10       continue

c     call LUDCMP to decompose the matrix as

           call ludcmp(as,2*n,nmax,indx)

c     call LUBKSB to obtain the solution vector bs

           call lubksb(as,2*n,nmax,indx,bs)

c     pack the real solution vector BS into the complex solution vector B

           do 30 i=1,n
           sol(i)=dcmplx(bs(2*i-1),bs(2*i))
  30       continue
           return
           end




c     SUBROUTINES KELVINP, BERBEI, DKELVINP, DBERBEI, ASKELVINP, ASDKELVINP,
c     AB AND GAMMA THAT CALCULATE THE FOUR KELVIN FUNCTIONS OF ARBITRARY
c     ORDER P AND THEIR DERIVATIVES

           subroutine kelvinp(x,p,fberx,fbeix,fkerx,fkeix)

c         calculates the 4 kelvin functions of order p
c         and argument x. (p and x both > 0 ).
c         the series used depends on whether p is an integer or not
c         if x > 5.0 the asymptotic form is used
c         calls the subroutines berbei, askelvinp and ab
c
c         based on the power series given in "Bessel Functions Part IV - Kelvin
c         Function" by A. Young and A. Kirk, Royal Society Mathematical Tables
c         Vol. 10, Cambridge University Press (1964)

           real*8 gamma,x,p,fberx,fbeix,fkerx,fkeix
           real*8 fbernx,fbeinx,rat1,rat2,one
           real*8 t,s,ss,fp,fac,aa,pi,gam,pp
           real*8 sumker,sumkei,sumkr1,sumkil,sp,cp,dgp,ch

           if(x.gt.5.0) then

           call askelvinp(x,p,fberx,fbeix,fkerx,fkeix)

           else
```

```fortran
      one=1.0
      pi=4.0*datan(one)
      gam=0.57721566490
      ch=1.0e-30
      fac=(0.25*(x**2.0))


      if(dabs(p-dnint(p)).lt.1.0e-3) then
       ip=nint(p)
       pp=dfloat(ip)
       fp=0.75*pp*pi
       call berbei(x,pp,fberx,fbeix)
       dgp=-1.0*gam
        if(ip.gt.0) then
          do 100 i=1,ip
            dgp=dgp+1.0/dfloat(i)
100       continue
        end if
       s=0.0
       ss=dgp-gam
       t=0.5*((0.5*x)**pp)/gamma(pp+1.0)
       sumker=t*ss*dcos(fp)
       sumkei=t*ss*dsin(fp)
10     s=s+1.0
       ss=ss+1.0/(pp+s)+1.0/s
       t=t*fac/(s*(s+pp))
       aa=fp+0.5*s*pi
       sumker=sumker+ss*t*dcos(aa)
       sumkei=sumkei+ss*t*dsin(aa)
       rat1=dabs(t/sumker)
       rat2=dabs(t/sumkei)
       if(rat1.lt.ch.and.rat2.lt.ch) go to 20
       go to 10
20     sumkr1=0.0
       sumki1=0.0
        if(ip.gt.0) then
         t=0.5*gamma(pp)/((0.5*x)**pp)
         sumkr1=t*dcos(fp)
         sumki1=t*dsin(fp)
          if(ip.gt.1) then
            do 200 i=1,ip-1
              t=t*fac/(i*(ip-i))
              aa=fp+0.5*i*pi
              sumkr1=sumkr1+t*dcos(aa)
              sumki1=sumki1+t*dsin(aa)
200         continue
          end if
        end if


      fkerx=-1.0*dlog(0.5*x)*fberx+0.25*pi*fbeix
     &      +sumker+sumkr1
      fkeix=-1.0*dlog(0.5*x)*fbeix-0.25*pi*fberx
     &      +sumkei-sumki1
```

```fortran
      else
       call berbei(x,p,fberx,fbeix)
       call berbei(x,-1.0*p,fbernx,fbeinx)
       cp=dcos(p*pi)
       sp=dsin(p*pi)
       t=0.5*pi/sp
       fkerx=t*(fbernx-cp*fberx-sp*fbeix)
       fkeix=t*(fbeinx-cp*fbeix+sp*fberx)
      end if

      end if

      return
      end




      subroutine berbei(x,p,fberx,fbeix)
      real*8 gamma,x,p,fberx,fbeix,fac,t,fp,aa,pi,sumber
      real*8 sumbei,ch,rat1,rat2,s,one

c     calculates the kelvin functions ber and bei of
c     order p (p is not an integer) and argument x where
c     x is greater than zero

      if(x.le.0.0) pause ' x is zero or less'
      one=1.0
      pi=4.0*datan(one)
      ch=1.0e-30
      s=0.0
      fac=(0.25*(x**2.0))
      t=((0.5*x)**p)/gamma(p+1.0)
      fp=0.75*p*pi
      sumber=t*dcos(fp)
      sumbei=t*dsin(fp)
10    s=s+1
      t=t*fac/(s*(s+p))
      aa=fp+0.5*s*pi
      sumber=sumber+t*dcos(aa)
      sumbei=sumbei+t*dsin(aa)
      rat1=dabs(t/sumber)
      rat2=dabs(t/sumbei)
      if(rat1.lt.ch.and.rat2.lt.ch) go to 20
      go to 10
```

```fortran
20      fberx=sumber
        fbeix=sumbei
        return
        end




        subroutine dkelvinp(x,p,dberx,dbeix,dkerx,dkeix)

c       calculates the derivatives with respect to the argument
c       of the 4 kelvin functions of order p
c       and argument x. (p and x both > 0 ).
c       if x > 5.0 the asymptotic form is used
c       calls the subroutines dberbei, asdkelvinp and ab
c
c       based on the power series given in "Bessel Functions Part IV - Kelvin
c       Function" by A. Young and A. Kirk, Royal Society Mathematical Tables
c       Vol. 10, Cambridge University Press (1964)

        real*8 gamma,x,p,dberx,dbeix,dkerx,dkeix,dbernx,dbeinx
        real*8 t,s,ss,fp,fac,aa,pi,gam,pp,sss,fberx,fbeix
        real*8 sumker,sumkei,sumkr1,sumki1,sp,cp,dgp,ch
        real*8 rat1,rat2,one

        if(x.gt.5.0) then

        call asdkelvinp(x,p,dberx,dbeix,dkerx,dkeix)

        else

        one=1.0
        pi=4.0*datan(one)
        gam=0.57721566490
        ch=1.0e-30
        fac=(0.25*(x**2.0))


        if(dabs(p-dnint(p)).lt.1.0e-3) then
         ip=nint(p)
         pp=dfloat(ip)
         fp=0.75*pp*pi
         call dberbei(x,pp,dberx,dbeix)
         dgp=-1.0*gam
          if(ip.gt.0) then
           do 100 i=1,ip
            dgp=dgp+1.0/dfloat(i)
```

```fortran
100         continue
       end if
       s=0.0
       ss=dgp-gam
       sss=p
       t=0.25*((0.5*x)**(pp-1.0))/gamma(pp+1.0)
       sumker=sss*t*ss*dcos(fp)
       sumkei=sss*t*ss*dsin(fp)
10     s=s+1.0
       ss=ss+1.0/(pp+s)+1.0/s
       sss=sss+2.0
       t=t*fac/(s*(s+pp))
       aa=fp+0.5*s*pi
       sumker=sumker+sss*ss*t*dcos(aa)
       sumkei=sumkei+sss*ss*t*dsin(aa)
       rat1=dabs(t/sumker)
       rat2=dabs(t/sumkei)
       if(rat1.lt.ch.and.rat2.lt.ch) go to 20
       go to 10
20     sumkr1=0.0
       sumki1=0.0
        if(ip.gt.0) then
         t=0.25*gamma(pp)/((0.5*x)**(pp+1.0))
         ss=-1.0*p
         sumkr1=ss*t*dcos(fp)
         sumki1=ss*t*dsin(fp)
          if(ip.gt.1) then
            do 200 i=1,ip-1
              ss=ss+2.0
              t=t*fac/(i*(ip-i))
              aa=fp+0.5*i*pi
              sumkr1=sumkr1+ss*t*dcos(aa)
              sumki1=sumki1+ss*t*dsin(aa)
200           continue
          end if
        end if
       call berbei(x,p,fberx,fbeix)

       dkerx=-1.0*dlog(0.5*x)*dberx+0.25*pi*dbeix
     &        -fberx/x
     &        +sumker+sumkr1
       dkeix=-1.0*dlog(0.5*x)*dbeix-0.25*pi*dberx
     &        -fbeix/x
     &        +sumkei-sumki1
      else
       call dberbei(x,p,dberx,dbeix)
       call dberbei(x,-1.0*p,dbernx,dbeinx)
       cp=dcos(p*pi)
       sp=dsin(p*pi)
       t=0.5*pi/sp
       dkerx=t*(dbernx-cp*dberx-sp*dbeix)
       dkeix=t*(dbeinx-cp*dbeix+sp*dberx)
      end if
```

```
            end if

            return
            end




            subroutine dberbei(x,p,dberx,dbeix)
            real*8 gamma,x,p,dberx,dbeix,fac,t,fp,aa,pi,sumber
            real*8 sumbei,ss,ch,one

c           calculates the derivatives with respect to the argument
c           of the kelvin functions ber and bei
c           order p and argument x where
c           x is greater than zero

            if(x.le.0.0) pause ' x is zero or less'
            one=1.0
            pi=4.0*datan(one)
            ch=1.0e-30
            s=0.0
            ss=p
            fac=(0.25*(x**2.0))
            t=0.5*((0.5*x)**(p-1.0))/gamma(p+1.0)
            fp=0.75*p*pi
            sumber=ss*t*dcos(fp)
            sumbei=ss*t*dsin(fp)
10          s=s+1
            ss=ss+2.0
            t=t*fac/(s*(s+p))
            aa=fp+0.5*s*pi
            sumber=sumber+ss*t*dcos(aa)
            sumbei=sumbei+ss*t*dsin(aa)
            rat1=abs(t/sumber)
            rat2=abs(t/sumbei)
            if(rat1.lt.ch.and.rat2.lt.ch) go to 20
            go to 10
20          dberx=sumber
            dbeix=sumbei
            return
            end




            subroutine askelvinp(x,p,fberx,fbeix,fkerx,fkeix)

c           calculates the asymptotic forms of the 4 kelvin functions
c           of argument x and order p
c           calls subroutine ab
```

```fortran
      real*8 x,p,fberx,fbeix,fkerx,fkeix
      real*8 pi,aa1,aa2,aa3,fac,fac1,fac2,two
      real*8 fa,fb,fan,fbn,one

      one=1.0
      pi=4.0*datan(one)
      two=2.0

      call ab(x,p,fa,fb)
      call ab(-1.0*x,p,fan,fbn)

      fac=x/dsqrt(two)
      fac1=dexp(fac)/dsqrt(2.0*pi*x)
      fac2=dexp(-1.0*fac)*dsqrt(pi/(2.0*x))
      aa1=fac-pi/8.0+p*pi/2.0
      aa2=fac+pi/8.0+p*pi/2.0
      aa3=2.0*p*pi

      fkerx=fac2*(fan*dcos(aa2)+fbn*dsin(aa2))

      fkeix=fac2*(-1.0*fan*dsin(aa2)+fbn*dcos(aa2))

      fberx=fac1*(fa*dcos(aa1)-fb*dsin(aa1))
     &  -(1.0/pi)*(fkerx*dsin(aa3)+fkeix*dcos(aa3))

      fbeix=fac1*(fa*dsin(aa1)+fb*dcos(aa1))
     &  +(1.0/pi)*(fkerx*dcos(aa3)-fkeix*dsin(aa3))

      return
      end




      subroutine asdkelvinp(x,p,dberx,dbeix,dkerx,dkeix)

c     calculates the asymptotic forms of the derivatives of the
c     4 kelvin functions of argument x and order p
c     calls subroutine ab

      real*8 x,p,dberx,dbeix,dkerx,dkeix
      real*8 pi,aa1,aa2,aa3,fac,fac1,fac2,two,one
      real*8 fap,fbp,fam,fbm,fapn,fbpn,famn,fbmn

      one=1.0
      pi=4.0*datan(one)
      two=2.0

      call ab(x,p+1.0,fap,fbp)
      call ab(x,p-1.0,fam,fbm)
      call ab(-1.0*x,p+1.0,fapn,fbpn)
      call ab(-1.0*x,p-1.0,famn,fbmn)
```

```fortran
      fac=x/dsqrt(two)
      fac1=dexp(fac)/dsqrt(2.0*pi*x)
      fac2=dexp(-1.0*fac)*dsqrt(pi/(2.0*x))
      aa1=fac-pi/8.0+p*pi/2.0
      aa2=fac+pi/8.0+p*pi/2.0
      aa3=2.0*p*pi

      dkerx=-0.5*fac2*((fapn+famn)*dcos(aa1)+(fbpn+fbmn)*dsin(aa1))

      dkeix=0.5*fac2*((fapn+famn)*dsin(aa1)-(fbpn+fbmn)*dcos(aa1))

      dberx=0.5*fac1*((fap+fam)*dcos(aa2)-(fbp+fbm)*dsin(aa2))
     & -(1.0/pi)*(dkerx*dsin(aa3)+dkeix*dcos(aa3))

      dbeix=0.5*fac1*((fap+fam)*dsin(aa2)+(fbp+fbm)*dcos(aa2))
     & +(1.0/pi)*(dkerx*dcos(aa3)-dkeix*dsin(aa3))

      return
      end




      subroutine ab(x,p,fa,fb)

c     calculates the two functions Ap(x) and Bp(x) needed for the
c     asymptotic forms of the kelvin functions
c     summation is continued until the smallest term is reached
c     and the sum neglecting that term is returned.

      real*8 x,p,fa,fb,told,tnew,pi,fac,aaold,aanew,pp,one

      one=1.0
      pi=4.0*datan(one)
      ch=1.0e-10

      pp=4.0*(p**2.0)
      fac=-1.0/(2.0*x)
      fa=1.0
      fb=0.0

      flag=0.0
      fac2=(pp-9.0)/16.0
      if(x.le.fac2) flag = 1.0

      r=1.0
      told=fac*(pp-((2.0*r-1.0)**2.0))/(4.0*r)
      aaold=(r*pi)/4.0

10    r=r+1.0

      tnew=told*fac*(pp-((2.0*r-1.0)**2.0))/(4.0*r)
      aanew=(r*pi)/4.0
```

```fortran
        if(flag.eq.0.0.and.abs(tnew).ge.abs(told)) go to 20
        if(flag.eq.1.0.and.abs(tnew).le.abs(told)) flag=0.0

        fa=fa+told*dcos(aaold)
        fb=fb-told*sin(aaold)

        told=tnew
        aaold=aanew
        go to 10

20      return
        end




        real*8 function gamma(x)

c       calculates the gamma function of argument x
c       x is not zero or a negative integer
c       polynomial approximation from "Handbook of Mathematical Functions" by
c       Abramowitz, M. and Stegun, I. A. (eds) Dover Press (1965)

        real*8 x,an,p

        nx=int(x)
        an=dint(x)

        if(x.gt.0.0) then
         p=x-an
        else if(x.lt.0.0) then
         if(an.eq.x) pause 'input to gamma function is a neg. int.'
         p=x-an+1.0
        else
         pause 'input to gamma function is zero'
        end if

c    calculate gamma(p) where 1<p<2

        gamma=1.0-0.577191652*p+0.988205891*(p**2.0)-0.897056937*(p**3.0)
     &  +0.918206857*(p**4.0)-0.756704078*(p**5.0)+0.482199394*(p**6.0)
     &  -0.193527818*(p**7.0)+0.035868343*(p**8.0)

c    calculate gamma(x) using the recursion relation

        if(an.eq.1.0) then
         go to 100
        else if(an.gt.1.0) then
         il=nx-1
          do 10 i=1,il
           gamma=(p+dfloat(i))*gamma
```

```
10         continue
           go to 100
         else if(an.lt.1.0) then
          if (x.gt.0.0) then
           il=nx+1
          else
           il=2-nx
          end if
           do 20 i=1,il
            gamma=gamma/(p+1.0-dfloat(i))
20          continue
         end if

100      return
         end
```

REPORT DOCUMENTATION PAGE

Public reporting burden for this collection of information is estimated to average 1 hour per response, including the time for reviewing instructions, searching existing data sources, gathering and maintining the data needed, and completing and reviewing the collection of information. Send comments regarding this burden estimate or any other aspect of this collection of information, including suggestions for reducing this burden, to Washington Headquarters Services, Directorate for Information Operations and Reports, 1215 Jefferson Davis Highway, Suite 1204, Arlington, VA 22202-4302, and to the Office of Management and Budget, Paperwork Reduction Project (0704-0188) Washington, DC 20503.

1. AGENCY USE ONLY (Leave blank)	2. REPORT DATE November 1994	3. REPORT TYPE AND DATES COVERED Final report

4. TITLE AND SUBTITLE
Calculation of Suspended Sediment Transport by Combined Wave-Current Flows

5. FUNDING NUMBERS
WU 32463

6. AUTHOR(S)
Palitha Nalin Wikramanayake, Ole Secher Madsen

7. PERFORMING ORGANIZATION NAME(S) AND ADDRESS(ES)
Ralph M. Parsons Laboratory
Massachusetts Institute of Technology
Cambridge, MA 02139

8. PERFORMING ORGANIZATION REPORT NUMBER
Contract Report DRP-94-7

9. SPONSORING/MONITORING AGENCY NAME(S) AND ADDRESS(ES)
USAE Waterways Experiment Station, Coastal Engineering Research Center, 3909 Halls Ferry Road, Vicksburg, MS 39180-6199

11. SUPPLEMENTARY NOTES

12a. DISTRIBUTION/AVAILABILITY STATEMENT
Approved for public release; distribution is unlimited.

12b. DISTRIBUTION CODE

13. ABSTRACT (Maximum 200 words)

The objective of this study was to investigate the application of simple eddy viscosity models, developed for wave-current interaction, to the problem of sediment suspension and transport. A review of exisiting models is given; however, it is pointed out that all models compute suspended sediment transport by interating the product of mean concentration and mean velocity. Because recent field experiments indicate that time-varying quantities may dominate the sediment flux due to mean components, the model described in this report calculates time-varying components of the concentration along with the mean flow component.

The report describes the governing equations and boundary conditions, the process used to select an eddy viscosity model for hydrodynamics of wave-current interaction, and the determination of a resuspension coefficient. Detailed summaries of model development and the solution scheme are provided, as well as example calculations using the computer program WCSTRANS. A source listing of the computer model is included.

14. SUBJECT TERMS
See reverse.

15. NUMBER OF PAGES
216

16. PRICE CODE

17. SECURITY CLASSIFICATION OF REPORT UNCLASSIFIED	18. SECURITY CLASSIFICATION OF THIS PAGE UNCLASSIFIED	19. SECURITY CLASSIFICATION OF ABSTRACT	20. LIMITATION OF ABSTRACT

NSN 7540-01-280-5500

14. (Concluded).

Eddy viscosity model
Non-cohesive sediment transport
Numerical model
Sediment resuspension

Sediment transport model
Suspended sediment concentration
Wave-current interaction